

Bio-active Ingredients during mini-bread Baking

?



Lu Zhang

Bioactive Ingredients during Mini-bread Baking

Lu Zhang

Thesis committee

Promotors

Prof. Dr Remko M. Boom
Professor of Food Process Engineering
Wageningen University & Research

Prof. Dr Xiao Dong Chen
Professor of School of Chemical and Environmental Engineering
Soochow University, China

Co-promotor

Dr Maarten A.I. Schutyser
Associate Professor, Laboratory of Food Process Engineering
Wageningen University & Research

Other members

Prof. Dr Martinus A.J.S. van Boekel, Wageningen University & Research
Dr Peter L. Weegels, European Bakery Innovation Centre, Papendrecht
Prof. Dr Reinhard Kohlus, University of Hohenheim, Germany
Dr Stefano Renzetti, Wageningen University & Research

This research was conducted under the auspices of the Graduate School VLAG (Advanced Studies in Food Technology, Agrobiotechnology, Nutrition and Health Sciences).

Bioactive Ingredients during Mini-bread Baking

Lu Zhang

Thesis

submitted in fulfilment of the requirements for the degree of doctor
at Wageningen University
by the authority of the Rector Magnificus,
Prof. Dr A.P.J. Mol,
in the presence of the
Thesis Committee appointed by the Academic Board
to be defended in public
on Monday 17 September 2018
at 4 p.m. in the Aula.

Lu Zhang

Bioactive Ingredients during Mini-bread Baking,

184 pages.

PhD thesis, Wageningen University, Wageningen, the Netherlands (2018)

With references, with summary in English

ISBN: 978-94-6343-309-9

DOI: <https://doi.org/10.18174/454331>

Table of contents

Chapter 1	General introduction	1
Chapter 2	Miniature bread baking as a timesaving research approach and mathematical modelling of browning kinetics	15
Chapter 3	Thermal inactivation kinetics of β -galactosidase during bread baking	35
Chapter 4	Effect of baking conditions and storage on the viability of <i>Lactobacillus plantarum</i> supplemented to bread	53
Chapter 5	Kinetic study of the thermal inactivation of <i>Lactobacillus plantarum</i> during bread baking	71
Chapter 6	Survival of encapsulated <i>Lactobacillus plantarum</i> during isothermal heating and bread baking	97
Chapter 7	Fortification of bread with arabinoxylan-enriched fractions obtained by dry fractionation	117
Chapter 8	General discussion	137
	References	149
	Summary	169

Chapter 1

General introduction



1.1 Functional bakery products

The father of modern medicine, Hippocrates, declared 2500 years ago that food and medicine are related: “*Let food be thy medicine and medicine be thy food.*” In the modern food industry, a new food category called “functional foods” emerged as a result of the increasing awareness of the link between personal health and well-being and diet. The term ‘functional foods’ was first used in Japan in the mid-1980s. To date, there is no universally accepted definition for functional foods, however three main concepts are involved in most of the proposed definitions in literature: (1) health benefits, (2) nutritional function and (3) technological processes (Bigliardi and Galati, 2013). Among these concepts, ‘technological processes’ refer to i) the development of functional foods by optimizing traditional food processing technologies, such as by fortification of foods with dietary fibre; ii) technologies designed to prevent the deterioration of active ingredients, such as by microencapsulation; iii) technologies aimed to design foods that are functionalized to the individual, for example by using the results from nutrigenomics, and creating foods by 3D printing. To simplify, functional foods can be defined here as modified food or food ingredients that can provide health benefits to consumers beyond its basic nutrients.

Functional foods introduced into the market have included beverages, dairy products, confectionery products, bakery products and breakfast cereals (Pinto et al., 2014). The category of functional bakery products is relatively new and has received increasing attention in scientific studies. Bakery products are not only nutritious plant-based foods containing important macronutrients (e.g. starch and dietary fibre) and micronutrients (e.g. antioxidants and minerals), but the logistics and storage of bakery products is also less demanding compared to liquid-form products such as yoghurt (Dewettinck et al., 2008), which have to remain refrigerated during the whole supply chain. In addition, the massive worldwide consumption of baked goods on a daily base makes them potential vehicles to deliver health-promoting ingredients at significant levels to the human diet.

Table 1-1 lists some recent studies of functional bakery products with a special focus on bread which is one of the most-consumed staple foods. The main active ingredients supplemented to bakery goods include probiotics and prebiotics (dietary fibre), antioxidants and phenolic compounds (Dziki, 2014). Other functional ingredients are oils and lipids, minerals and salts, and vitamins (Pinto et al., 2014). Among these ingredients, probiotics and prebiotics are important in human nutrition because of their influences on the gastrointestinal (GI) microbiota. Probiotics are defined as ‘live microorganisms which confer a health benefit on the

host when administered in adequate amounts' (FAO/WHO, 2002). Prebiotics are generally carbohydrates which are non-digestible by digestive enzymes in the upper GI tract of humans, but are 'consumed' selectively by some types of bacteria (typically bifidobacteria and/or lactobacilli). Prebiotics can therefore enhance the activity and prevalence of those beneficial bacteria (Al-Sheraji et al., 2013). The alleged health-promoting benefits of the aforementioned functional bakery products are diverse, e.g. reducing serum cholesterol and blood pressure, reducing the risk of coronary heart diseases, lowering the glycaemic response after food consumption, treating human intestinal barrier dysfunctions (Aleixandre and Miguel, 2016; Brownlee et al., 2016; Korem et al., 2017; Quirós-Sauceda et al., 2014; Zubillaga et al., 2001). Notwithstanding, research regarding these beneficial effects also reports contradictory results, indicating large interpersonal variation among consumers (Korem et al., 2017).

Table 1-1. An overview of scientific studies focusing on functional bakery products.

Functional ingredient	Product	Incorporation strategy	Baking condition	Functionality	Reference
Probiotics					
<i>Lactobacillus rhamnosus</i> R011	biscuit	mix microentrapped cells in whey protein isolate into dough	baked at 280 °C for 5 min	4.5×10 ⁵ CFU/g (initial viable counts in dough 1.3×10 ⁷ CFU/g)	(Reid et al., 2007)
<i>Lactobacillus</i> <i>acidophilus</i>	bread	apply edible coating layers onto the surface of part- baked bread before full baking	baked off at 180 °C for 16 min	~7 log CFU/70 g bread	(Altamirano- Fortoul et al., 2012)
<i>Lactobacillus reuteri</i> DSM 17938	chocolate Soufflé	supplement cells microcapsules into dough	dough weight 70 g; frozen at -18 °C for 2 h and baked at 180 °C for 10 min	~3-6 log CFU/g sample from core	(Malmo et al., 2013)
<i>Bifidobacterium lactis</i> Bb12	bread	mix cell suspension into dough	dough weight 60 g; baked at 165, 185 or 205 °C for 12 min	~2-3 log CFU/g (initial viable counts in dough 2.1×10 ⁶ CFU/g)	(Zhang, Huang, Ananingsih, Zhou, & Chen, 2014)
<i>Lactobacillus rhamnosus</i> GG	bread	apply probiotic containing film solution on the surface of prebaked pan bread	air dry the prebaked bread at 60 °C for 10 min or 180 °C for 2 min	7.6-9.0 log CFU/30-40 g bread slice	(Soukoulis et al., 2014)

<i>Bacillus coagulans</i> MTCC 5856	muffin	mix spray-dried bacteria powder into batter	baked at 205 °C for 20-25 min	6.99 log CFU/g (initial viable counts in batter 7.14 log CFU/g)	(Majeed et al., 2016)
Prebiotics					
carob fibre/inulin/pea fibre	bread	add 3% fibre to dough	dough weight 100 g; baked at 190 °C for 20 min	total dietary fibre in bread: carob fibre 5.06 %; inulin 5.14 %; pea fibre 5.38 %; control 2.96 %	(Wang, Rosell, & Benedito de Barber, 2002)
β-glucans & arabinoxylans	flat bread	substitute wheat flour with 20 % barley fibre-rich-fractions	diameter of circular dough sheet 20 cm; baked at 540 °C for 70 s	total β-glucans 3.0 g, arabinoxylans 4.2 g per flat bread	(Izydorczyk et al., 2008)
hemicellulose B	bread	add defatted rice bran	baked at 200 °C, baking time N/A	3.87 % dm dietary fibre in baked bread	(Hu et al., 2009)
bacterial nanocellulose (BNC)	bread	hemicellulose B to dough disperse BNC gel in water and mix with other ingredients	dough weight 70 g; baked at 195 °C for 23 min	N/A	(Corral et al., 2017)
inulin: Fibruline DS2	bread	mix inulin-type products into dough	dough weight around 350 g; baked at 230 °C for 30 min	N/A	(Sirbu and Arghire, 2017)
Others					
tea catechins	bread	mix green tea extract into dough	baked at 215 °C for 11 min	tea catechins content: 0.53 mg/g bread	(Wang & Zhou, 2004)

omega-3 fatty acids	sandwich	omega-3 fatty acids were	N/A	reduction in the content of	(Borneo et al.,
(eicosapentaenoic acid and docosahexaenoic acid)	cookie	encapsulated in a matrix of starch and gelatin and incorporated into the cream		EPA and DHA was 4.48 % and 5.87 %, respectively after 28-day storage	2007)
omega-3 fatty acids	bread	encapsulate omega-3 fatty acids in high amylose corn starch and then add the capsules into dough	dough weight 150 g; baked at 220 °C for 24 min	N/A	(Gökmen et al., 2011)
phenolic antioxidants	bread	substitute wheat flour with fruit phenolic extracts (apple, kiwifruit and blackcurrant)	baked at 155 °C for 60 min	phenolic recovery ranged from 9 % to 39 %; the total antioxidant activity of fortified breads was higher than the control	(Sivam et al., 2011)
polyphenols (rutin and gallic acid)	bread	substitute wheat flour with quinoa leaves powder	dough weight 300 g; baked at 230 °C for 30 min	rutin content 209.89 µg/g dm after baking; gallic acid content 2214.6 µg/g dm after in vitro digestion	(Gawlik-Dziki et al., 2015)
anthocyanin	bread	mix anthocyanin-rich black rice extract powder into dough	dough weight 50 g; baked at 200 °C for 8 min	79 % of cyanidin-3-glucoside was retained in bread crumb after baking	(Sui et al., 2016)
chia mucilage	pita bread	substitute 2 % of wheat flour with chia mucilage	dough weight 10 g; baked at 530 °C for 30 s	N/A	(Cruz et al., 2017)

1.2 Bread baking process

Bread is one of the most-consumed staple foods worldwide. Bread making is a complex process involving dough mixing, proofing (i.e., fermentation), baking and cooling. Among these steps, baking is of great importance because a series of physical and chemical changes occurs during baking, e.g. water evaporation, gas cell expansion, starch gelatinization, protein coagulation, dough-crumb transition and crust formation (Lucas, 2014). These changes are dominated by heat and mass transfer mechanisms inside the oven chamber as well as in the product, and interact in a complex manner, which significantly influence the product quality.

During baking, heat transport in the dough is dominated by the classic ‘evaporation-condensation’ mechanism (De Vries et al., 1989). Hence, the temperature in the crumb reaches a plateau of 100 °C while the moisture content remains similar to that of the dough; the temperature in the crust keeps increasing towards the oven temperature (if the baking time is long enough) and the moisture content reduces more significantly compared to the crumb. These distinct temperature and moisture content histories in the inner part and the outer layer of the dough result in a matrix with unique macroscopic features: a soft and porous crumb and a crispy and dense crust. In addition, the brown colour of the crust and the flavour/aroma of the bread are formed during baking due to the Maillard reactions.

Several physical models have been developed to better understand the baking process (Mondal & Datta, 2008; Papasidero, Manenti, & Pierucci, 2015; Putranto, Chen, & Zhou, 2015; Zhang, Datta, & Mukherjee, 2005). In previous research, full-sized bread is used which usually requires long baking times, e.g. 35 min for the dough with an initial weight of 380 g. This implies that research into baking is time and resource consuming. Small scale bread-baking under adjusted conditions generates larger data sets in a shorter time (Figure 1-1), and hence could lead to faster research using much less resources. Small scale processes in general use much less raw materials, which is especially useful when the tested functional ingredients are expensive or where the available amount of these ingredients is still limited (Garzón and Rosell, 2014; Trinh et al., 2016).

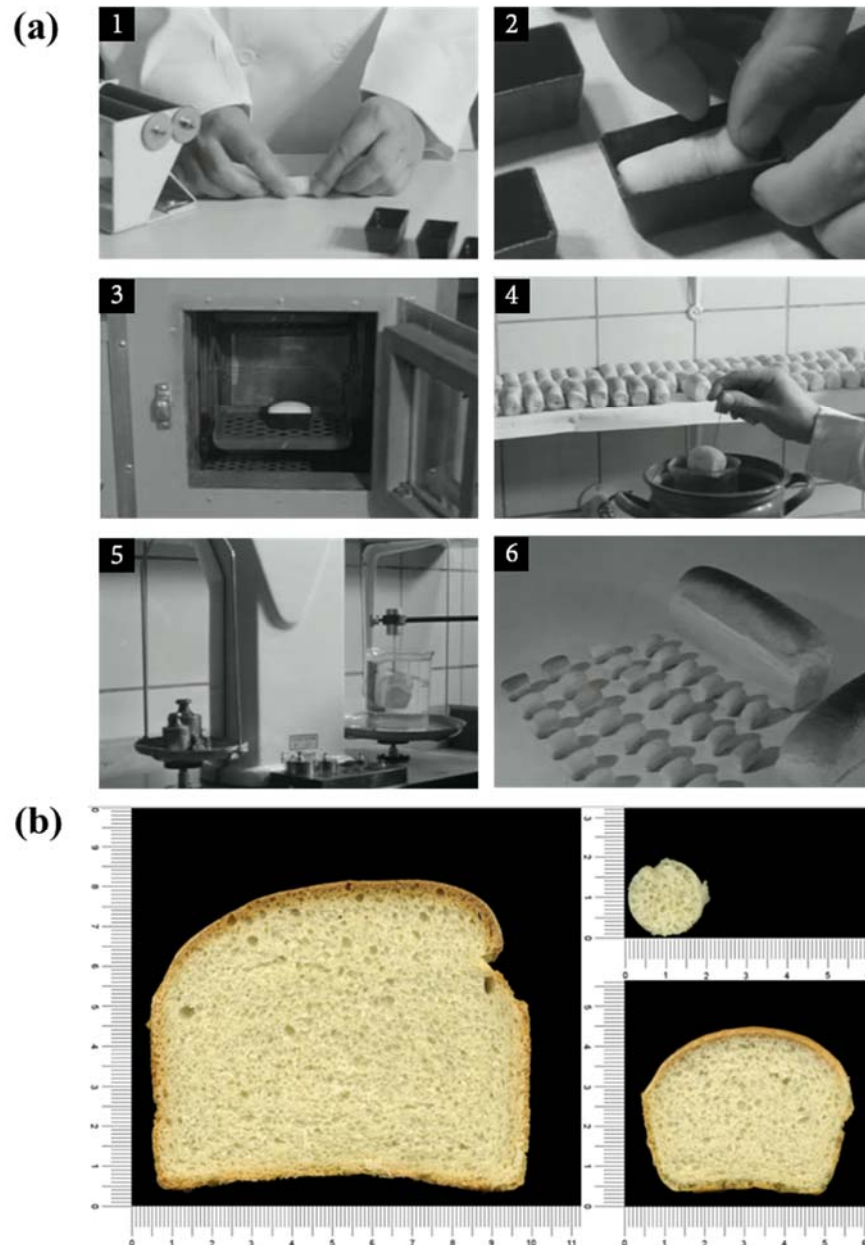


Figure 1-1. Small scale bread-baking experiments: (a) “Speelgoedbroodjes” mini-loaf baking experiment (IGMB, 1959): a small piece of dough was divided, put into a mould and baked in a customized oven; baked loaf was coated with paraffin and its volume was determined; (b) the crumb structure of bread with different initial dough weight, i.e. 500 g, 50 g and 4 g, respectively (Garzón and Rosell, 2014).

1.3 Factors influence the functionality of bioactive ingredients

The demand for functional foods worldwide is increasing and a large range of innovative products is expected to be launched in the coming years (Arbolea et al., 2010). However, the development of functional bread is challenging because the baking process may partially or

completely destroy the bioactivity or bioavailability of the active ingredients, due to either the high baking temperature or their interaction with other ingredients. For example, the formation of ferulic acid-protein cross-links will decrease the bioavailability of water-extractable arabinoxylan in bread (Hartmann et al., 2005). Therefore, it is important to investigate the interaction between the bread making process and the fate of the active ingredients.

On the one hand, the baking process influences the bioactivity of heat-sensitive ingredients supplemented to bread such as probiotics (Zhang, Huang, Ananingsih, Zhou, & Chen, 2014). Although certain probiotic strains (i.e., *Bacillus coagulans*) may show high heat resistance due to their ability to form spores (see Table 1-1) (Majeed et al., 2016), several strategies have been explored to preserve other probiotic strains (i.e., lactic acid bacteria) under stressful conditions, such as micro-entrapment or encapsulation into edible films, coatings, and micro-beads (Champagne et al., 2005; Lakkis, 2016; De Vos et al., 2010). However, the available information for wide application of microencapsulation of active compounds in thermal-processed foods is still scarce (Pitigraisorn et al., 2017).

On the other hand, incorporation of active ingredients into bread can influence the product quality in either a positive or a negative manner. For example, sourdough fermentation can produce bread with increased specific volume and softer crumb. Some of the added lactic acid bacteria (LAB) produce metabolites with antimicrobial activity, which along with the lactic acid, prolong the shelf-life of bread (Black et al., 2013; Cizeikiene et al., 2013; Moore et al., 2007). However, the addition of active ingredients may also compromise the organoleptic properties of the products (Patel and Velikov, 2011). For example, supplementation of starch based coatings containing probiotics changed the crispness of the bread crust (Altamirano-Fortoul et al., 2012). The substitution of wheat flour with fibre-rich-fractions also negatively influences the aesthetic properties of the bread (e.g. dark discolouration, harder crumb with lower loaf volume) (Curti et al., 2013), which consequently makes the fortified bread less acceptable for consumers (Izydorczyk and Dexter, 2008). Specific techniques may amend the problems caused by the addition of bioactives. For instance, enzymatic pre-treatment on the fibre-rich-fractions ameliorates their baking properties (Laurikainen et al., 1998; Messia et al., 2016). Encapsulation can be employed to reduce the off-flavours caused by the incorporation of omega-3 fatty acids (Gökmen et al., 2011).

In summary, in order to develop functional bread that contains sufficient active ingredients without compromising product quality, systematic study on the impact of baking on the functionality/bioavailability of those active ingredients and the interaction between the

functional ingredients and other ingredients of bread (e.g. starch, protein, salt, yeast) is of great importance.

1.4 Research objective and thesis outline

The overall objective of this thesis is to provide deeper understanding of the interaction between the bread making process and active ingredients, gain insights on the inactivation mechanisms of active ingredients during baking and explore possible strategies to better retain their bioactivity. A mini-bread baking approach is proposed, validated and employed to access experimental data and kinetic modelling is conducted to obtain mechanistic insights. The knowledge gained in this thesis provides guidance for process optimization and product design to develop functional bread.

Figure 1-2 sketches the conceptual network of this thesis, and the positioning of each chapter.

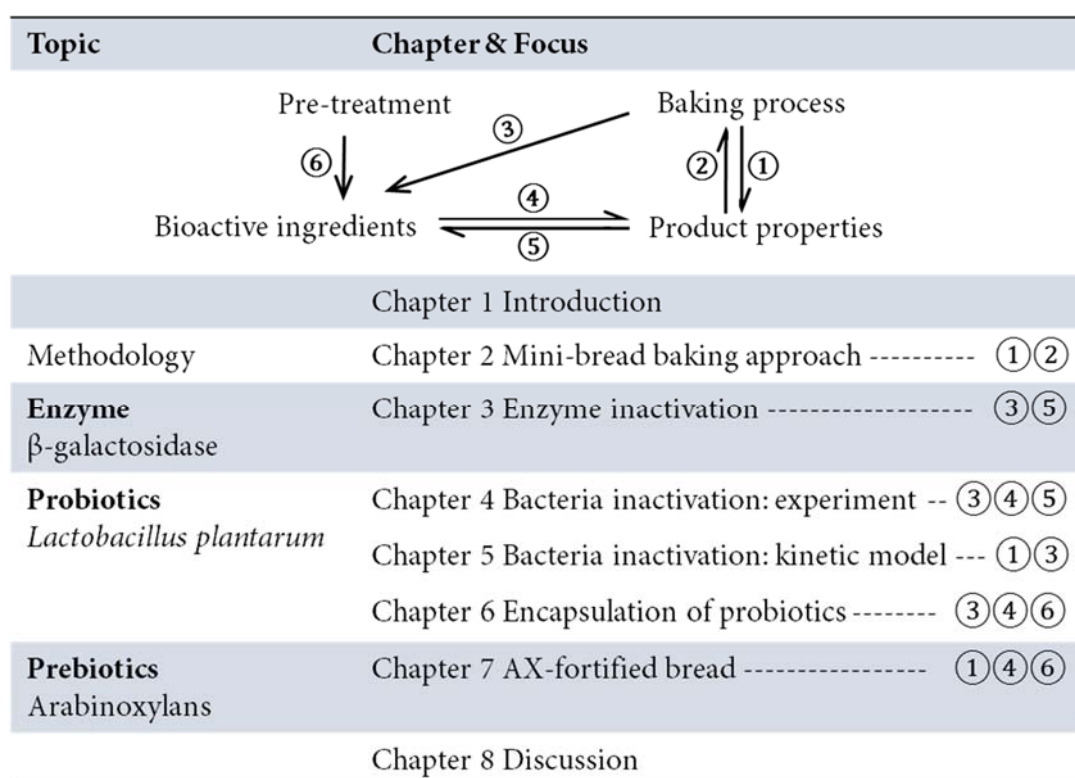


Figure 1-2. Schematic overview of the concepts and their relations, plus the focus of each chapter in this thesis. The numerals refer to different research questions: (1&2) how the baking process and product properties development (e.g. crust formation) affect each other; (3) how the baking process influences the functionality of active ingredients; (4&5) how the addition of active ingredients and quality attributes of the product interact; (6) how pre-treatment (encapsulation or enzymatic treatment) changes the functionality of active ingredients.

Chapter 2 proposes the method of miniature bread baking as an economical laboratory approach to study the baking process. The physicochemical properties of the mini-breads are compared with those of regular-sized breads. The spatial reaction engineering approach (S-REA) is used to model the temperature and moisture content profiles during baking which are then used to describe the browning kinetics.

Chapter 3 reports on the mechanism of enzyme inactivation during bread baking. Thermal inactivation of β -galactosidase is studied in a wheat flour/water model system by varying the temperature and the moisture content of the mixtures. A kinetic model describes the inactivation of β -galactosidase as influenced by temperature and moisture content and is subsequently used to predict the residual enzyme activity in bread during baking.

Chapter 4 demonstrates the effect of baking and subsequent storage on the viability of a probiotic strain *Lactobacillus plantarum* P8 in bread crust and crumb. The effects of initial dough weight and baking temperature on the inactivation kinetics of the bacteria are investigated systematically. The microstructure of the bread matrix is hypothesized to affect the heat resistance the embedded bacteria.

The kinetic study presented in **chapter 5** was done to obtain more quantitative understanding of the thermal inactivation of probiotics during baking. Rate-dependent models are developed to describe the dependence of inactivation kinetics on parameters such as temperature, moisture content, temperature variation rate and drying rate. The obtained models are mechanistically interpreted and validated against independent experimental data.

Chapter 6 explores the effect of encapsulation on the survival of probiotics during baking. The heat resistance of probiotics in different carriers (i.e., reconstituted skim milk, gum arabic, maltodextrin and inulin) is compared during isothermal heating and bread baking at various conditions. The residual viability of probiotics is predicted using kinetic models when the dried powders are applied onto the surface of the dough.

The application of dry-fractionated arabinoxylan-enriched fraction (AXF) from wheat bran as a novel ingredient for bread making is reported in **chapter 7**. The AXF was modified by enzymatic treatment using feruloyl esterase. Several quality-related properties of bread fortified with AXF or modified AXF are characterised. Bread with a high fibre content and acceptable quality can be obtained by AX-supplementation.

Chapter 8 concludes the thesis with a general discussion. Based on the main findings in this thesis, several strategies to improve the retention of active ingredients during baking are proposed. Subsequently, the remaining research questions related to the development of functional bakery products are discussed, followed by an outlook for future research.

Chapter 2

Miniature bread baking as a timesaving research approach and mathematical modelling of browning kinetics



This chapter has been published as:

Zhang, L., Putranto, A., Zhou, W., Boom, R.M., Schutyser, M.A.I., Chen, X.D. (2016). Miniature bread baking as a timesaving research approach and mathematical modelling of browning kinetics. Food and Bioprocess Processing, 100, 401–411

Link: <https://doi.org/10.1016/j.fbp.2016.08.007>

Abstract

Miniature bread baking is presented as an economical and timesaving laboratory approach to study the baking process in the present work. Results indicate that the miniature bread baking is essentially analogical to the baking process of regular-sized bread: quality-related properties of miniature breads, such as crumb formation, crust thickness, crust colour and moisture content, behaved similarly to regular-sized breads (380 g) during baking, albeit at a different time scale. This was explained as analogous for large breads, initially baking is externally limited and only later internal limitations play a dominant role with the crust being formed. After initial development of the crust, the lightness and the total colour difference were found linearly correlated with the crust thickness. Moreover, the S-REA (spatial reaction engineering approach) was used here to model the moisture content and temperature during miniature bread baking whose results were implemented to describe the browning kinetics. The results indicate that the S-REA accurately models the browning kinetics during miniature bread baking.

2.1 Introduction

Bread making is a complex process involving dough mixing, proofing, baking and cooling. Among these processes, baking is of great importance. During baking, many quality-related properties of bread, such as colour, texture and flavour, are developed by transformations that depend on the development of the temperature and moisture content. Those transformations are due to simultaneous heat and mass transfer phenomena and mechanical deformation of the bread (Therdthai and Zhou, 2003; Thorvaldsson and Janestad, 1999; Zhang and Datta, 2006). However, prediction of the bread quality properties according to baking conditions is relatively difficult since the mechanisms of the baking process are not fully understood (Mondal and Datta, 2008). For instance, the colour change on the crust of bread, which is a result of Maillard reactions and caramelization, is complicated to predict due to the influence of water activity, heat transfer mode, temperature and air velocity (Mundt and Wedzicha, 2007). Therefore, more detailed understanding of the baking process is necessary, especially when the quality of the final products need to be optimized or when bread recipes need to be modified.

In previous studies on the quality prediction of bread in terms of crust formation, crust browning, moisture content of the final products, regular-sized bread were used. Mohd Josoh et al. (2009) presented a strong positive correlation between crust thickness and the total crust colour difference (ΔE) which allows prediction of crust thickness from the brown surface colour of baked bread. The original weight of the dough used in this study before baking was 380 g and the baking time was up to 35 min. Purlis and Salvadori (2007) explained that the browning at bread surface during baking depends on weight loss and oven temperature: linear trend was found between total colour change and weight loss of 100 g breads. Moreover, a strong positive correlation between crust thickness and the bread moisture ratio was found by Soleimani Pour-Damanab, et al. (2012), which allows prediction of bread quality. However, the influence of the sample size on the baking behaviour of bread has rarely been addressed. To gain insight into the possible effects of dough size on the bread baking process, we propose here a miniature bread baking approach, which was inspired by a kind of Chinese biscuit (Figure 2-1a). This approach offers the opportunity to easily generate larger data sets in a shorter baking time (Figure 2-1b) which may be used to study physical and chemical reactions during baking and validate mathematical models of baking processes.

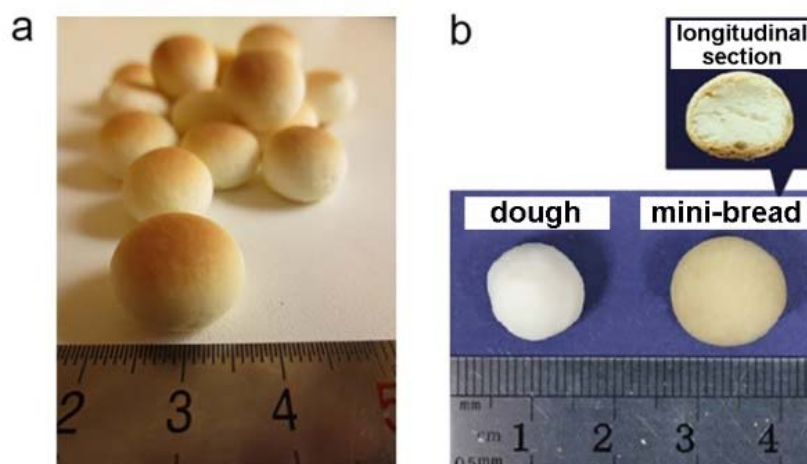


Figure 2-1. a: A popular snack food among children in China - Want-Want[®] Mantou, which is made from edible potato starch, sugar, egg, skim milk powder and honey. b: Schematic diagram of 1.0 g dough before and after baking at 205 °C for 8 min. The vertical section of the baked miniature bread is also shown. The crispy crust with a brown colour and the soft crumb with porous structure can be observed.

The aim of this work is therefore to study the bread baking process by using a miniature bread making approach and to model the browning kinetics of miniature bread during baking using S-REA. For this, miniature breads (0.5 g and 1.0 g dough) were made according to a traditional process of bread baking at three different baking temperatures (175, 205 and 235 °C) with a baking time of 8 min. Physical properties of miniature breads, such as temperature profiles, moisture content, crust colour, and crust thickness, were monitored to gain insight into the baking behaviour of miniature breads. To make sure that miniature bread baking is essentially analogical to larger bread baking process, a comparison between the data gained from the miniature baking experiment and the data of regular-sized bread from the literature was made. In addition, the applicability of S-REA to model the temperature and moisture content profiles during miniature bread baking was evaluated. The accuracy of the S-REA to describe the colour change of the crust was assessed.

2.2 Materials and methods

2.2.1 Preparation of miniature bread

Bread dough was made following a recipe in Wang and Zhou (2004) with slight modification: bread flour (75 g), sugar (7.5 g), fine salt (1.25 g), butter (2.25 g), instant yeast (0.75 g), and UHT skim milk (50 g). Dough was first made in a mixer (Twinbird, Japan) and then leavened for 45 min at ambient temperature. After proofing, small pieces of dough (0.5 g and 1.0 g) were shaped

into a ball before proceeding to baking at 175, 205 and 235 °C in an electric oven (Changdi, China) for 8 min. The baking dish was placed in the central zone of the oven (Figure 2-2).

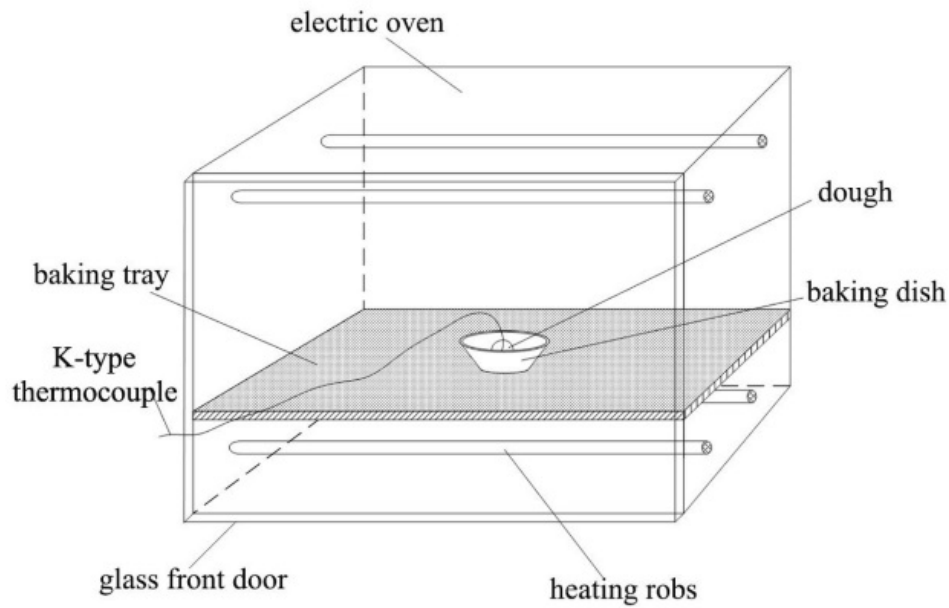


Figure 2-2. Schematic diagram of experimental setup: the electric oven was pre-heated to a certain temperature before use; the weighted dough was placed inside an aluminium baking dish which was put in the centre area of a baking tray; a K-type thermocouple connected to a data logger was inserted into the dough, and the temperature inside the dough during baking was automatically recorded by a computer program.

2.2.2 Physical properties

Weight loss and moisture content

Weight loss and moisture content analyses were carried out immediately after each sampling, and were calculated according to Eqns. 2-1 and 2-2, respectively.

$$\text{Weight loss} = \frac{W_1 - W_2}{W_1} \times 100 \% \quad (2-1)$$

$$\text{Moisture content} = \frac{W_2 - W_3}{W_2} \times 100 \% \quad (2-2)$$

where, W_1 and W_2 are the weights of the dough prior and after baking for a certain time; and W_3 is the weight of the baked bread after dehydration at 105 °C for 24 h.

Crust colour and crust thickness

Crust colour and crust thickness analyses were conducted after cooling down the baked breads to room temperature. The crust colour was measured by a spectrophotometer (Konica Minolta sensing, Japan). The crust thickness was determined according to the method described in Mohd Jusoh et al. (2009) with little differences in implementation. Several measures of each sample were recorded and an average value was obtained for each baking time. All tests were done by triplicate at least with the oven under steady condition. All data were presented as mean values of at least three replicates, and error bars represent standard error (SE) except where noted.

2.3 Results and discussion**2.3.1 Coupled heat and mass transfer**

Weight and moisture content of the miniature breads continuously decreased during baking (Figure 2-3). The initial rates of weight loss could be well described by a simple model (Eqn. 2-3) assuming a bread temperature of 100 °C and external heat transfer to be limited during the initial part of the baking. The external heat transfer coefficients were obtained by fitting Eqn. 2-3 to the experimental data from this study and data from Purlis and Salvadori (2009) for larger breads obtained at different oven temperatures.

$$R_{WL} = \frac{h \cdot A \cdot (T_{oven} - 100^{\circ}\text{C})}{M \cdot \Delta H_{ev}} \quad (2-3)$$

in which, R_{WL} is the rate of total weight loss (1/s); h is the heat transfer coefficient, W/(m²·K); A is the surface area, m²; M is the initial weight of dough, kg; T_o is oven temperature, °C; ΔH_{ev} the latent heat of evaporation at 100 °C (2256 kJ/kg).

The coefficients were determined 31.2 W/(m²·K) for the miniaturized breads and 20.2 W/(m²·K) for the regular bread (Figure 2-4). These values are in the range of common values found for free convective heat transfer 10~100 W/(m²·K). The difference between the heat transfer coefficients can probably be explained by the different baking oven used.

The agreement between model and experimental data confirms that the heat transfer is externally heat transfer limited both for small and larger breads at the initial stage of baking. At

a later stage during baking, internal limitations start to dominate when the evaporation front moves inward and the crust being formed. The result is that the temperature of the bread starts to increase as the heat transferred is not compensated by water evaporation. Both for miniature and for larger breads baking, the two stages of external limitation and internal limitation occur, although they appear at a different time scale.

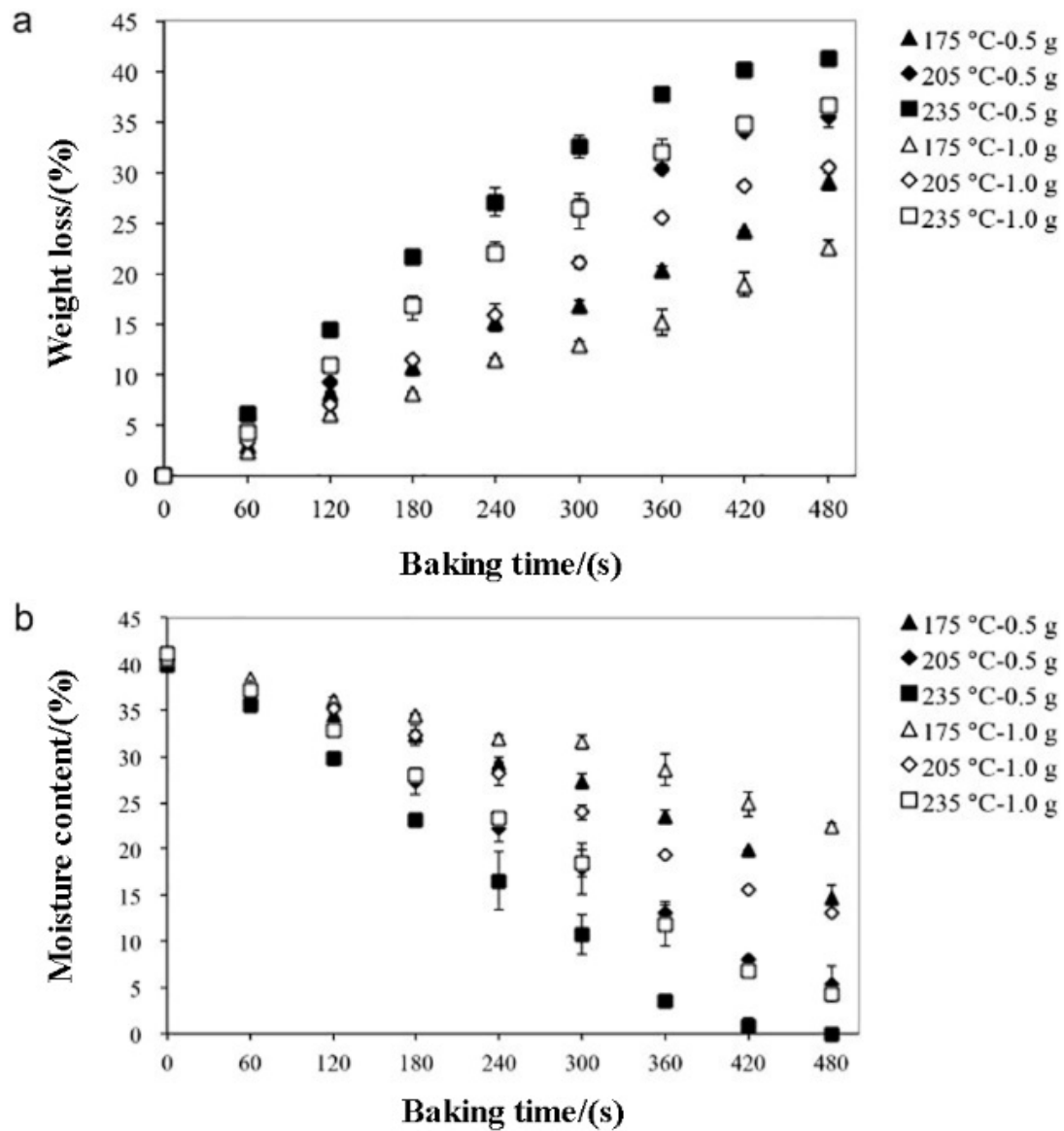


Figure 2-3. Total weight loss (a) and wet-based moisture content (b) of the whole miniature bread baked at different baking temperature as a function of baking time.

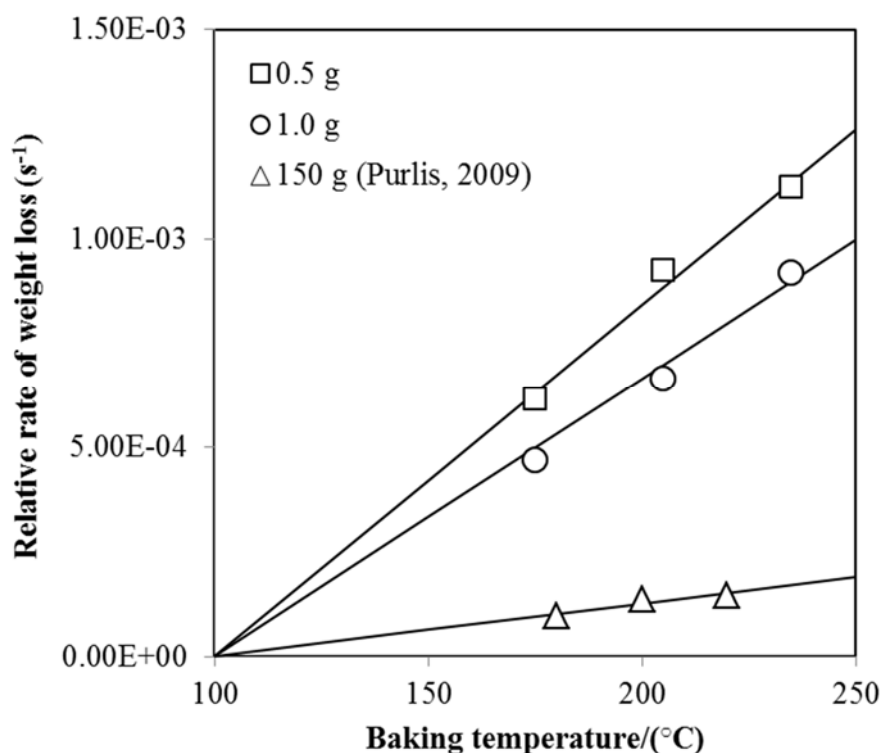


Figure 2-4. Weight loss rate of the 0.5 g (\square), 1.0 g (\circ) and 150 g (Δ) breads during baking as a function of baking temperature. Solid lines represent the fitted data.

2.3.2 Crust chromaticity

Bread crust colour is an important quality indicator for bread, which is affected by non-enzymatic browning reactions including Maillard reaction and caramelization of sugars (Purlis, 2010). These reactions are activated by the higher temperature and lower water content in bread crust during bread baking (Zhou and Therdthai, 2007). In this work, we observed that the crust colour of miniature breads baked at 175 °C remained almost the same during baking, and there was also no crust browning at the early stage of baking at 205 °C and 235 °C (Figure 2-5). However, after baking for a certain time, the bread surface is expected to reach a critical browning temperature (110~120 °C) (Mundt and Wedzicha, 2007; Purlis and Salvadori, 2009a), initiating the discoloration and thus formation of a brown crust in the end. Browning only occurred when the moisture content of the bread was lower than 25 % (Figures 2-3 & 2-5) in this study.

The CIELab colour model was used to quantitatively describe the colour change of the bread during baking (Yam and Papadakis, 2004). The total colour change (ΔE) of the crust during baking was calculated according to (Eqn. 2-4):

$$\Delta E = [(L^* - L_{ref}^*)^2 + (a^* - a_{ref}^*)^2 + (b^* - b_{ref}^*)^2]^{1/2} \quad (2-4)$$

where L_{ref}^* , a_{ref}^* , and b_{ref}^* are the reference values taken from dough before baking.

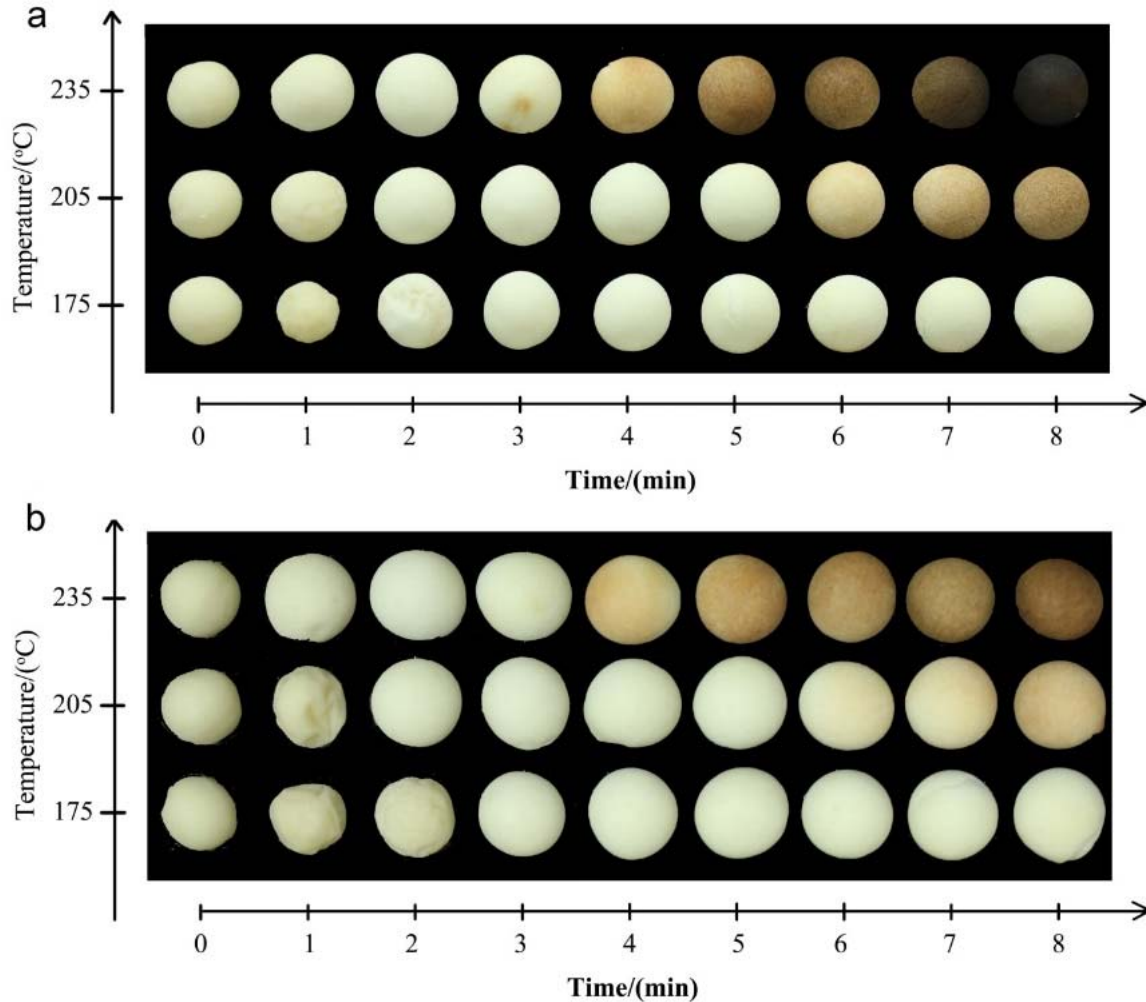


Figure 2-5. Browning of miniature breads (initial weight of dough, a: 0.5 g; b: 1.0 g) baked at different temperatures. Bread surface wrinkling and carving deformation occurred during cooling at room temperature after baking at 175 °C and 205 °C for 1 min and 2 min. This happened because the gluten network of the crumb was not solidified, so the dough contracted after exposure to cold air.

The total colour difference (ΔE) of miniature bread depended mostly on the applied oven temperature and increased with baking time (Figure 2-6a), as can be expected. However, at the same oven temperature and residence time, 0.5 g miniature breads were slightly browner than 1.0 g breads, which is related to the faster temperature rise of the crust of the smaller breads. In agreement with the study of Purlis and Salvadori (2007) on regular-sized bread (toast), the total colour difference is mainly correlated to the change in lightness (L^*) during baking, because the

total colour differences calculated from Eqn. 2-4 are very similar to the change of lightness with respect to the raw dough (Figure 2-6b). This prominent role of lightness may be explained by the definition of the CIELab colour model: the purity and the hue of a certain colour are defined by the red-green and yellow-blue opponent channels, i.e., a^* and b^* , and the lightness (L^*) further defines the exact colour in a three-dimensional space (León et al., 2006). The chromaticity of the crust is more or less brown after baking for 5 minutes, so the difference of colour mainly comes from the lightness variation afterwards.

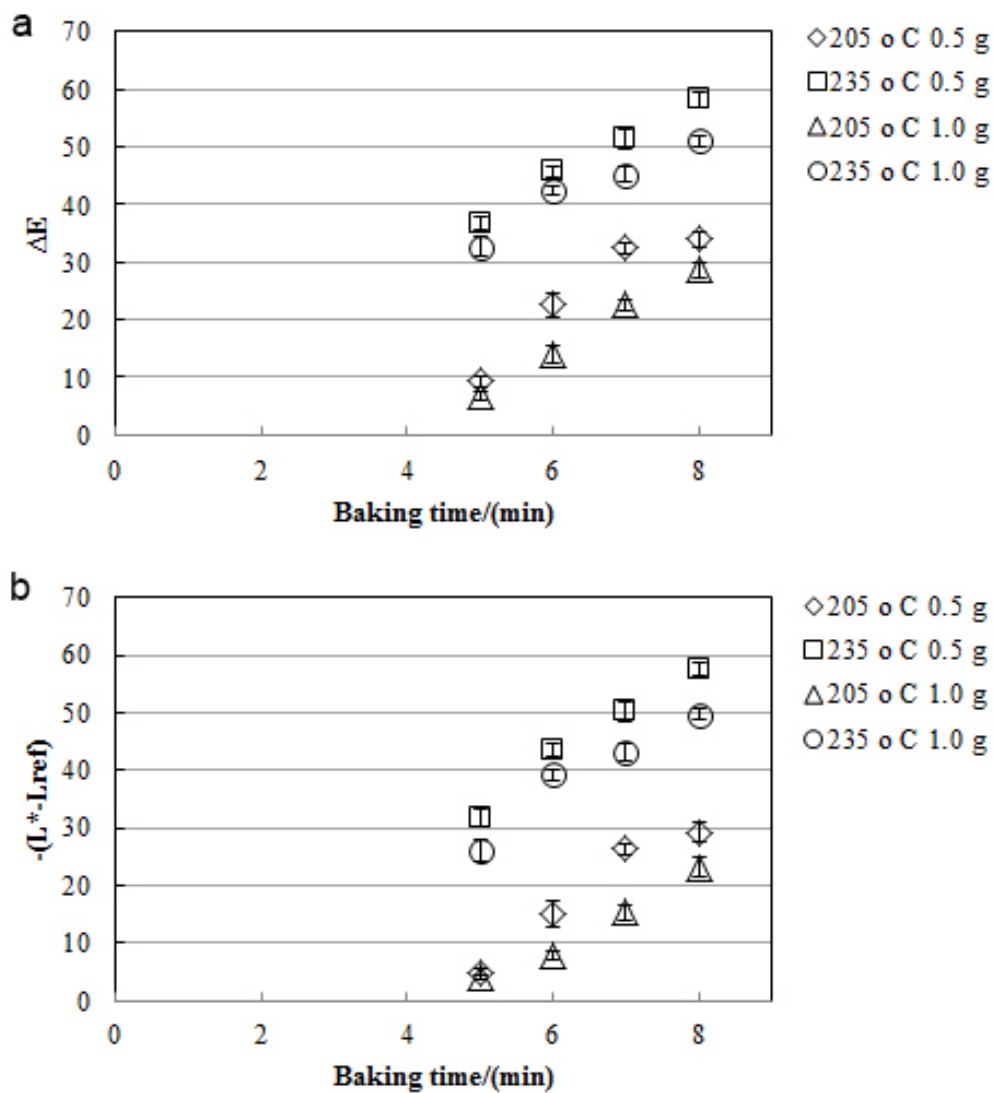


Figure 2-6. a: Total colour difference (ΔE) of miniature bread crust during baking; b: Variation of miniature bread crust lightness (L^*) during baking, in comparison to unbaked dough (L_{ref}^*). Here, data of miniature breads (0.5 g and 1.0 g) baked at 205 °C and 235 °C for 5, 6, 7 and 8 min are shown because they are more representative than others.

2.3.3 Crumb formation and crust thickness

Figure 2-7 illustrates the cross section of miniature breads as function of baking time and temperature. It can be observed that the transition of dough into crumb occurred already within 120 to 180 second for all conditions. Purlis (2012) introduced a critical time defined as the time necessary to achieve a complete transition of dough into crumb given by a complete starch gelatinization. It is obvious that both the characteristic length of the bread and the external heat transfer rate affect the critical time. With miniature breads, the critical time is much shorter and crust formation starts only after reaching the critical time, which is an advantage compared to larger breads, which may be non-baked inside while a crust is already formed.

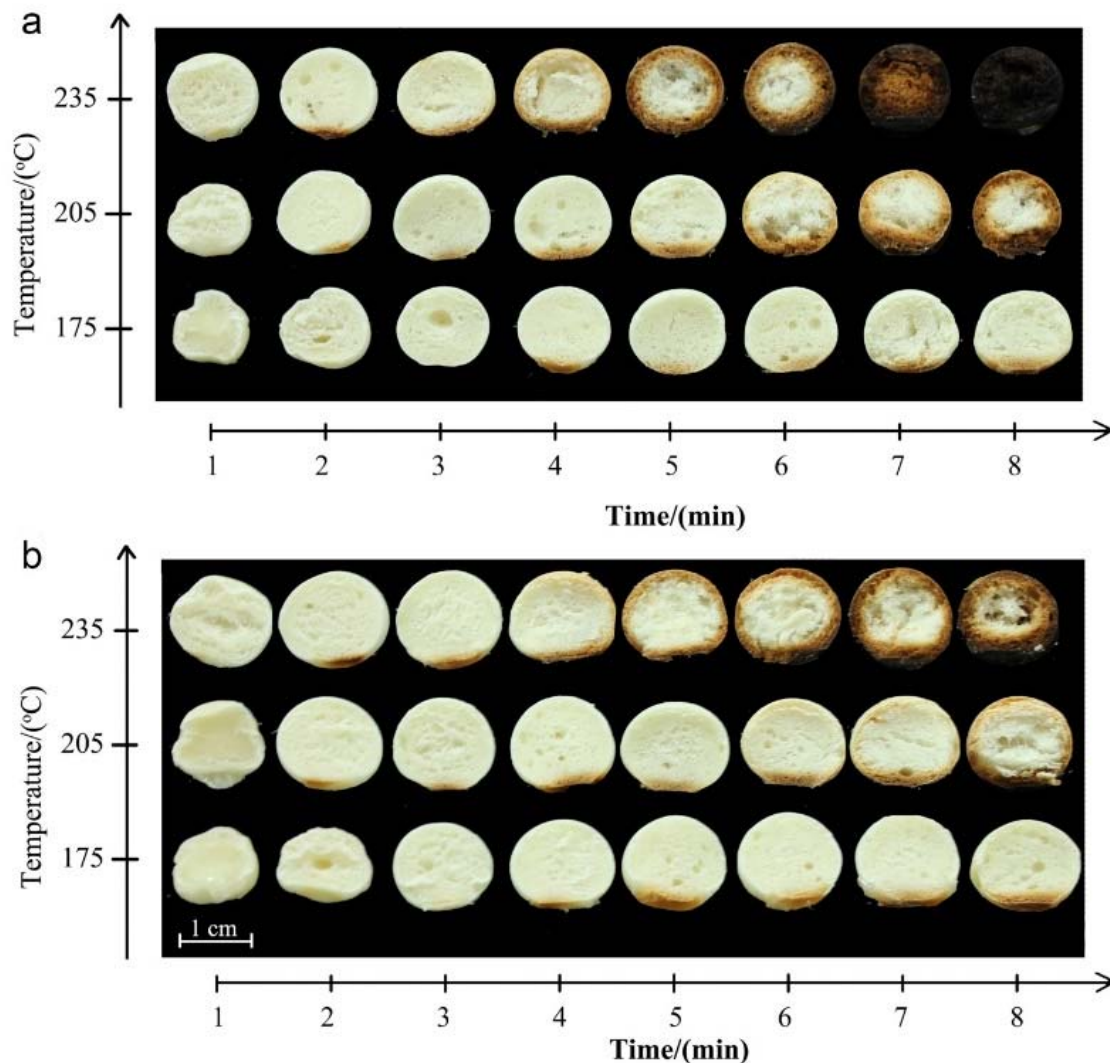


Figure 2-7. Crust formation and crumb development of miniature bread (Initial weight of dough, a: 0.5 g; b: 1.0 g) baked at different temperatures. The 0.5 g dough “burned” after baking at 235 °C for 8 min.

It can also be observed in Figure 2-7 that the crust of miniature breads baked at 175 °C is absent or at most unmeasurable thin. For miniature breads baked at 205 °C and 235 °C, the crust thickness remained stable during the first 4 minutes of baking and increased afterwards, and a firm crust was only formed at the end of the baking.

It is important to observe that a clear difference between crust and crumb could be obtained at 205 °C and 235 °C. This indicates that the internal and external transfer limitations are similar to those during baking of larger breads. While Figure 2-4 showed that the baking process initially is limited by external heat transfer, external limitation during the whole baking process would result in a homogeneous crumb, which is a poor thermal conductor compared with the wet dough (Clark, 2009). Therefore the crust formation indicates that later in the baking process internal limitation dominates, as is the case with larger breads.

Figure 2-8a shows the relationship between the crust colour (lightness, L^*) and the crust thickness of miniature breads baked at 205 and 235 °C for 5, 6, 7, 8 min, respectively. The crust thickness value of 0.5 g miniature bread baked at 235 °C for 8 min are not shown here because the crumb structure did not exist anymore, which makes it meaningless to define the crust (Figure 2-7). It can be concluded that L^* is linearly related to crust thickness, with a high coefficient of determination ($R^2=0.95$), i.e., the crust colour darkened while the crust thickened. This correlation is consistent with previous results on regular-sized bread (380 g), in which the colour component L^* could be used to predict the crust thickness (Mohd Jusoh et al., 2009). In contrast, this linear relationship is not observed for colour values a^* and b^* . Possibly, the reported a^* and b^* values vary due to the difference of ingredients used. Moreover, this also may be related to the definition of the CIELab colour space as discussed in the previous section.

Similarly, the total colour difference (ΔE) of miniature bread can be linearly correlated to crust thickness that develops in a later stage of the baking process when the evaporation front moves inward, which was also found in regular bread (Mohd Jusoh et al., 2009). The correlation was not valid for the very initial period, which may be explained by other physical changes occurring at the product surface that lead to slight colour changes (Figure 2-8b). It can be concluded that the relationship between crust colour and thickness is not influenced by the variation of dough weight, baking time, and baking temperature used in this study. Therefore, although the time needed to bake the bread may vary due to the changes in dough weight and baking temperature, the browning is not limited by baking time but only by temperature and moisture content of the crust (Mohd Jusoh et al., 2009). This is important when we want to use the miniature breads as a model for larger breads.

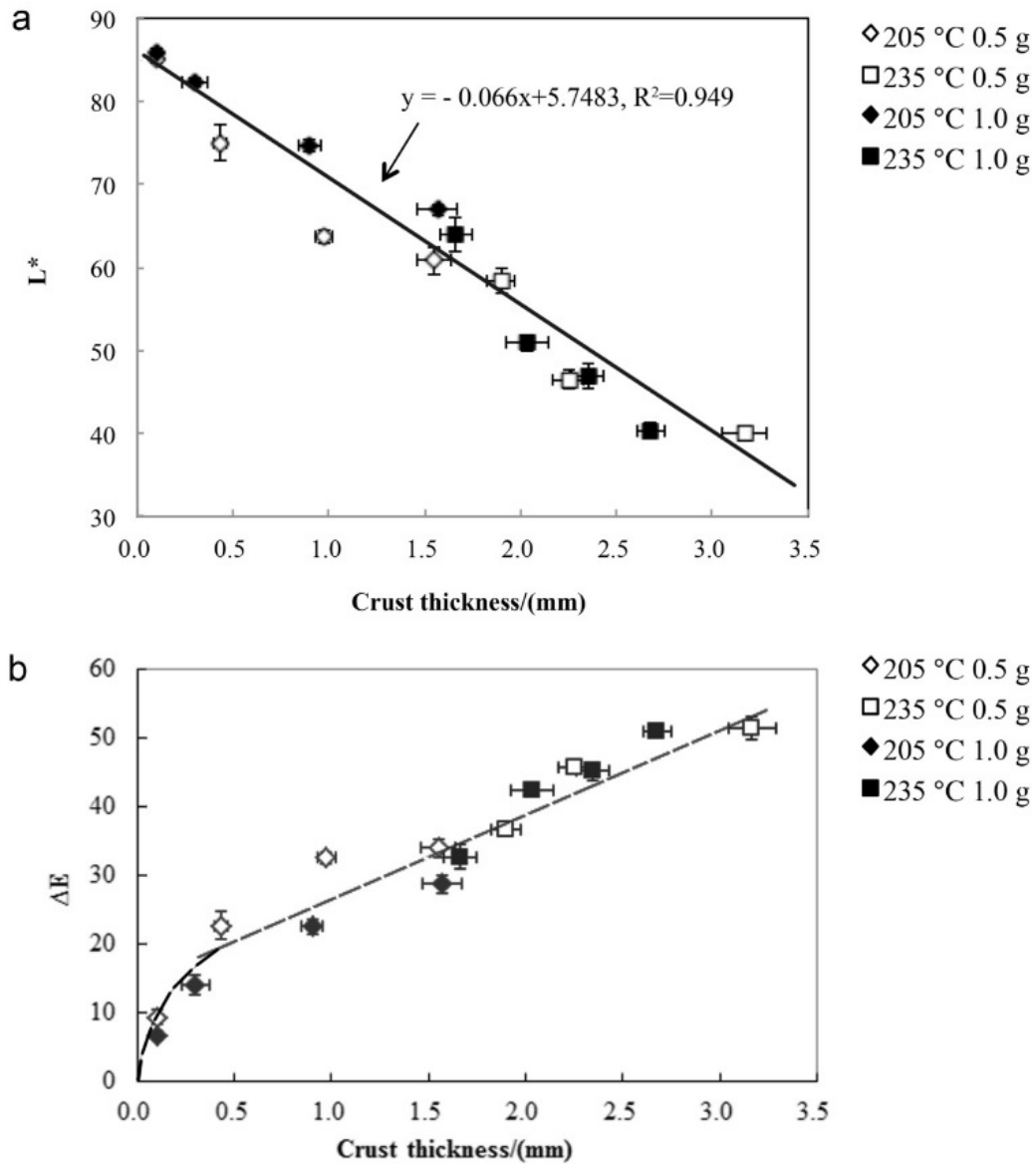


Figure 2-8. a: linear correlation between outer crust colour reported as L^* value (lightness) with crust thickness; b: variation of total colour difference (ΔE) against crust thickness. The dot line in the second graph is added to guide the eye.

2.4 Modeling of browning kinetics during mini-bread baking

2.4.1 Mathematical modelling of browning kinetics

In order to describe the colour change during miniature bread baking, the spatial reaction engineering approach (S-REA) (Chen and Putranto, 2013; Putranto and Chen, 2015) is implemented. The S-REA is essentially a multiphase model which consists of a set of equations of heat and mass transfer in which the reaction engineering approach (REA) is used to describe

the local evaporation/condensation rate. Although it is represented in the format of partial differential equations, it is not similar to the commonly employed diffusion models. In these classical models, no local evaporation/condensation rate is implemented. However, in the spatial reaction engineering approach (S-REA), the reaction engineering approach (REA) is developed and used to describe the local evaporation/condensation rate inside the porous materials as affected by local structure. The REA is the first approach which is proposed and published to describe the phenomena. This makes the S-REA the first non-equilibrium multiphase approach. The S-REA has been implemented to model several challenging drying cases and in this paper, the S-REA is employed to model the baking of small bread sample (Chen and Putranto, 2013).

The S-REA framework for modelling miniature bread baking is shown in Appendix 2-A and detailed explanation of the S-REA is presented in Chen and Putranto (2013). The modelling using the REA yields the spatial profiles of moisture content, concentration of water vapour and temperature of the bread miniature. For yielding the profiles of total colour changes (ΔE) during baking, the S-REA is combined with a model that relates the total colour changes and surface moisture content and temperature (Tan and Zhou, 2003, 2008) which can be written as:

$$\Delta E = \Delta E_{\infty} [1 - \exp(-\sum_{i=1}^n k(X_s(t), T_s(t)) \Delta t_i)] \quad (2-5)$$

where X_s is the surface moisture content (kg water.kg dry solids⁻¹), T_s is the surface temperature (K), ΔE is the surface colour at particular time, ΔE_{∞} is the surface colour at infinite time, k is the first order kinetic constant (s⁻¹) dependent on surface temperature and surface moisture content and Δt_i is the small time interval during which the surface temperature and moisture content is assumed to be constant (s). The dependency of k on surface moisture content and temperature can be written as (Tan and Zhou, 2003; 2008):

$$k = (k_1 + k_2 X_s + k_3 X_s^2 + k_4 X_s^3) \exp\left(\frac{-E_a}{RT_s(t)}\right) \quad (2-6)$$

where k_1 , k_2 , k_3 and k_4 are model parameters. It was found that cubic polynomial equations gave better agreement to experimental data than the second order polynomial while the forth order polynomial did not result in any significant improvement (Tan and Zhou, 2008). Upon solving the S-REA shown in Eqns. 2-A1 to 2-A3, the predicted surface moisture content and surface temperature are used in Eqns. 2-5 and 2-6. Equations 2-A1 to 2-A3 are solved by method of

lines. By implementing this method, the partial differential equation is transformed into a set of ordinary differential equations by discretizing the spatial parts. The set of ordinary differential equations is then solved using the 'ode' solver available in Matlab®.

The constants ΔE_∞ , k_1 , k_2 , k_3 , k_4 and E_a are determined by least-square method implemented in MS Excel® based on the experimental data of baking of 1 g miniature bread at temperature of 205 and 235 °C. The criteria of RMSE below 1×10^{-4} and R^2 higher than 0.99 were employed for the fitting. The results of modelling are validated towards the experimental data of baking of 0.5 g bread at these temperatures.

2.4.2 Profiles of browning kinetics during miniature bread baking

Figures 2-9 and 2-10 show the results of modelling of browning kinetics using the S-REA and Eqns. 2-5 to 2-6. Based on the experimental data of baking of 1 g of bread, the values of E_0 , k_1 , E_a are 104.82, 21576.61 and 60670.38 J·mol⁻¹, respectively while k_2 , k_3 and k_4 are 0. Therefore, Eqn. 2-6 can be simplified into:

$$k = k_1 \exp\left(\frac{-E_a}{RT_s(t)}\right) \quad (2-7)$$

The reasonable agreement of the predicted and experimental total colour changes during baking is shown in Figure 2-9 and indicated by R^2 of 0.95. Putranto et al. (2015) implemented the similar model to describe baking of flat bread with initial weight of 250 g and initial thickness of 0.2 cm and yielded relatively similar activation energy i.e. 58708.26 J·mol⁻¹. The zero values of k_2 , k_3 and k_4 shown in this modelling may indicate that the surface moisture content does not play significant role in determining the browning kinetics during baking. The results are indeed in agreement with Putranto et al. (2015) which showed that the effects of temperature are more dominant than moisture content on the browning kinetics.

When validated towards the experimental data of baking of 0.5 g of bread at temperature of 205 and 235 °C, the modelling shows a good agreement as shown in Figure 2-10 and confirmed by R^2 of 0.99. The combination of the S-REA and Eqns. 2-5 to 2-6 is able to accurately describe the colour changes during baking. It is shown here that the S-REA is also able to model miniature bread baking following its accuracy to model relatively large flat bread (initial thickness of 0.2 cm and initial weight of 250 g). The S-REA can model not only the browning kinetics in relatively large samples but also in miniature bread.

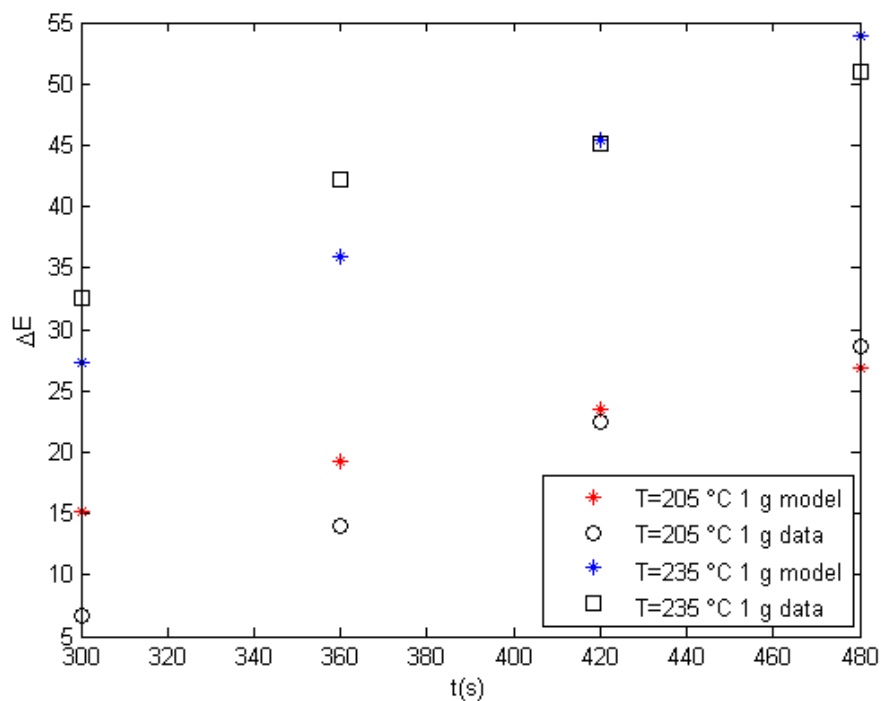


Figure 2-9. Profiles of total colour changes during baking of 1 g bread at temperatures of 205 and 235 °C.

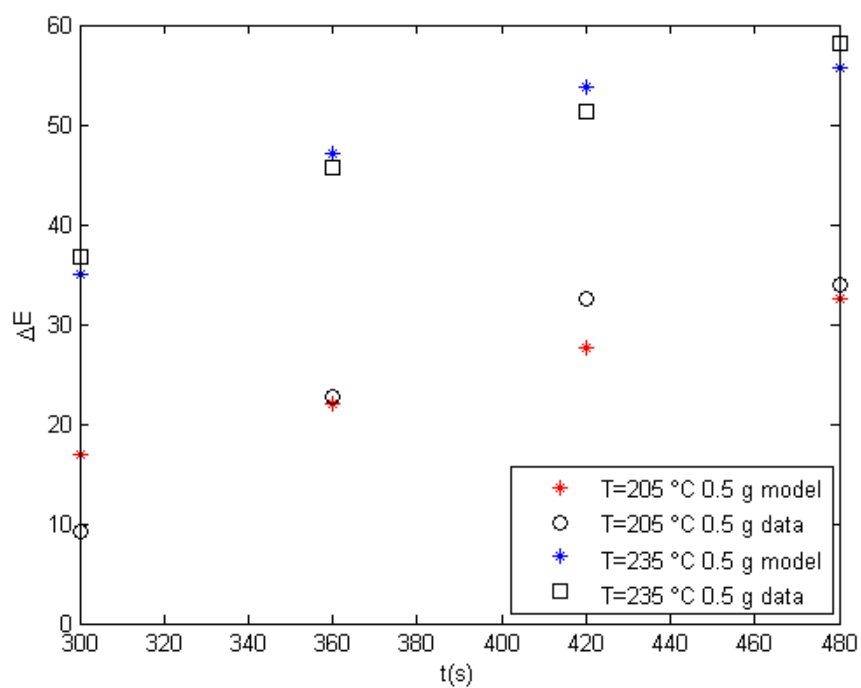


Figure 2-10. Profiles of total colour changes during baking of 0.5 g bread at temperatures of 205 and 235 °C.

2.5 Conclusions

A miniature bread baking approach is described, which can be used as small scale models for larger bread baking. The baking behaviour of miniature breads in terms of weight loss and crust formation is initially limited by external heat transfer; later this shifts to internal limitation. This is also observed for larger bread. Crust formation and browning start during a later stage where internal limitations dominate and the temperature of the bread starts to rise with the evaporation front moving inwards. Browning of crust is especially dependent on the temperature and moisture content history of the crust at this stage. As the baking of miniature bread can be characterized in a similar way as for larger breads, it is implied that indeed the miniature breads can be utilized as models for regular-sized bread. Moreover, in this study, the browning kinetics during miniature bread baking is described using the S-REA. The combination of the S-REA and equations that relate surface moisture content and temperature with total colour changes models well the browning kinetics.

Appendix 2-A. S-REA model

Based on the experimental details summarized above, the S-REA is set up. It consists of a set of equations of conservation of mass and heat transfer (in spherical coordinate system) in which the REA is used to describe the local evaporation/condensation rate. The mass balance of water in the liquid phase (liquid water) is written as (Putranto and Chen, 2013a, 2013b, 2013c):

$$\frac{\partial(C_s X)}{\partial t} = \frac{1}{r^2} \frac{\partial}{\partial r} \left(r^2 D_w \frac{\partial(C_s X)}{\partial r} \right) - \dot{I} \quad (2-A1)$$

where D_w is the local effective liquid water diffusivity ($\text{m}^2 \cdot \text{s}^{-1}$), X is the concentration of liquid water ($\text{kg H}_2\text{O} \cdot \text{kg dry solids}^{-1}$), C_s is the solids concentration ($\text{kg dry solids} \cdot \text{m}^{-3}$) which can change if the structure changes, \dot{I} is the evaporation or condensation rate ($\text{kg H}_2\text{O} \cdot \text{m}^{-3} \cdot \text{s}^{-1}$) and \dot{I} is positive when evaporation occurs locally.

The mass balance of water in the vapour phase (water vapour) in spherical coordinate system is expressed as (Putranto and Chen, 2013a, 2013b, 2013c):

$$\frac{\partial C_v}{\partial t} = \frac{1}{r^2} \frac{\partial}{\partial r} \left(r^2 D_v \frac{\partial C_v}{\partial r} \right) + \dot{I} \quad (2-A2)$$

where D_v is the local effective vapour diffusivity ($\text{m}^2 \cdot \text{s}^{-1}$) and C_v is the concentration of liquid water ($\text{kg H}_2\text{O} \cdot \text{m}^{-3}$).

The heat balance is represented by the following equation (Putranto and Chen, 2013a, 2013b, 2013c):

$$\rho C_p \frac{\partial T}{\partial t} = \frac{1}{r^2} \frac{\partial}{\partial r} \left(r^2 k \frac{\partial T}{\partial r} \right) - \dot{I} \Delta H_v \quad (2-A3)$$

where T is the sample temperature (K), k is the local thermal conductivity of sample ($\text{W} \cdot \text{m}^{-1} \cdot \text{K}^{-1}$), ΔH_v ($\text{J} \cdot \text{kg}^{-1}$), C_p is the local specific heat of sample ($\text{W} \cdot \text{m}^{-1} \cdot \text{K}^{-1}$) and ρ is the sample local density ($\text{kg} \cdot \text{m}^{-3}$).

The initial and boundary conditions for Eqns. 2-A1 to 2-A3 are:

$$t = 0, X = X_0, C_v = C_{v0}, T = T_0 \quad (2-A4)$$

$$r = 0, \frac{dX}{dr} = 0, \frac{dC_v}{dr} = 0, \frac{dT}{dr} = 0 \quad (2-A5)$$

$$r = R_s, -C_s D_w \frac{dX}{dr} = h_m \varepsilon_w \left(\frac{C_{v,s}}{\varepsilon} - \rho_{v,b} \right) \quad (2-A6)$$

$$-D_v \frac{dC_v}{dr} = h_m \varepsilon_v \left(\frac{C_{v,s}}{\varepsilon} - \rho_{v,b} \right) \quad (2-A7)$$

$$k \frac{dT}{dr} = h(T_b - T) \quad (2-A8)$$

where R_s is the sample radius (m), h is the heat transfer coefficient ($\text{W} \cdot \text{m}^{-2} \cdot \text{K}^{-1}$), ε_w and ε_v are fraction of surface area influenced by liquid water and water vapour respectively.

\dot{I} is the local evaporation/condensation rate within the solid structure described as (Kar and Chen, 2011, 2010):

$$\dot{I} = h_{m,in} A_{in} (C_{v,s} - C_v) \quad (2-A9)$$

where $h_{m,in}$ is the internal mass transfer coefficient ($\text{m} \cdot \text{s}^{-1}$), A_{in} is the total internal surface area available for phase change (m^2), $C_{v,s}$ is the internal-solid-surface water vapour concentration ($\text{kg} \cdot \text{m}^{-3}$).

By implementing the REA, the internal-surface water vapour concentration can be written as (Kar and Chen, 2010; 2011; Putranto and Chen, 2013^{a-c}):

$$C_{v,s} = \exp\left(\frac{-\Delta E_v}{RT}\right) C_{v,sat} \quad (2-A10)$$

where $C_{v,sat}$ is the internal-saturated water vapour concentration ($\text{kg} \cdot \text{m}^{-3}$).

Therefore, the local evaporation rate can be expressed as (Putranto and Chen, 2013a, 2013b, 2013c):

$$\dot{I} = h_{m,in} A_{in} \left[\exp\left(\frac{-\Delta E_v}{RT}\right) C_{v,sat} - C_v \right] \quad (2-A11)$$

The relative activation energy for baking of bread is generated from one accurate baking run i.e. baking of 0.5 g of bread at baking temperature of 205 °C. It is found to be suitably fitted as:

$$\frac{\Delta E_v}{\Delta E_{v,b}} = -55.754(\bar{X} - X_b)^5 + 113.95(\bar{X} - X_b)^4 - 96.768(\bar{X} - X_b)^3 + 40.609(\bar{X} - X_b)^2 - 8.385(\bar{X} - X_b) + 1.006 \quad (2-A12)$$

The good agreement between the fitted and experimental relative activation energy is shown by R^2 of 0.995.

Nomenclatures

A	surface area of samples	(m ²)
A_{in}	internal surface area	(m ²)
C_p	specific heat of sample	(J·kg ⁻¹ ·K ⁻¹)
C_s	solid concentration	(kg·m ⁻³)
C_v	water vapour concentration	(kg·m ⁻³)
$C_{v,s}$	internal–surface vapour concentration	(kg·m ⁻³)
$C_{v,sat}$	internal–saturated vapour concentration	(kg·m ⁻³)
D_v	effective water vapour diffusivity	(m ² ·s ⁻¹)
$D_{v,o}$	water vapour diffusivity	(m ² ·s ⁻¹)
D_w	liquid diffusivity	(m ² ·s ⁻¹)
h	heat transfer coefficient	(W·m ⁻² ·K ⁻¹)
h_m	mass transfer coefficient	(m·s ⁻¹)
$h_{m,in}$	internal mass transfer coefficient	(m·s ⁻¹)
\dot{i}	local evaporation rate	(kg·m ⁻³ ·s ⁻¹)
k	first order kinetic constant	(s ⁻¹)
k	thermal conductivity of sample	(W·m ⁻¹ ·K ⁻¹)
M	initial weight of dough	(kg)
n	constant	
r	radial position	(m)
RH_b	relative humidity of drying air	
R_s	sample radius	(m)
R_{WL}	rate of total weight loss	(s ⁻¹)
T	sample temperature	(K)
T_{oven}	oven temperature	(K)
T_s	surface sample temperature	(K)
t	time	(s)
T_b	drying air temperature	(K)
W	weight of sample	(kg)
X	moisture content on dry basis	(kg·kg ⁻¹)
\bar{X}	average moisture content on dry basis	(kg·kg ⁻¹)
X_b	equilibrium moisture content on dry basis	(kg·kg ⁻¹)
X_o	initial moisture content	(kg·kg ⁻¹)
X_s	moisture content at the surface of sample	(kg·kg ⁻¹)
ΔE_v	apparent activation energy	(J·mol ⁻¹)
$\Delta E_{v,b}$	‘equilibrium’ activation energy	(J·mol ⁻¹)
ΔE	surface colour at particular time	
ΔE_∞	surface colour at infinite time	
Δt	time interval	(s ⁻¹)
ΔH_{ev}	latent heat of evaporation	(kJ·kg ⁻¹)

ΔH_v	vaporization heat of water	(J·kg ⁻¹)
ε_w	fraction by liquid water	
ε_v	fraction by water vapour	
ρ	sample density	(kg·m ⁻³)
ρ_s	density of solids	(kg·m ⁻³)
$\rho_{v,b}$	vapour concentration in drying medium	(kg·m ⁻³)
$\rho_{v,s}$	surface vapour concentration	(kg·m ⁻³)
$\rho_{v,sat}$	saturated vapour concentration	(kg·m ⁻³)
ρ_w	density of water	(kg·m ⁻³)

Chapter 3

Thermal inactivation kinetics of β -galactosidase during bread baking



This chapter has been published as:

Zhang, L., Chen, X.D., Boom, R.M., Schutyser, M.A.I. (2017). Thermal inactivation kinetics of β -galactosidase during bread baking. Food Chemistry. 225, 107–113.

Link: <http://dx.doi.org/10.1016/j.foodchem.2017.01.010>

Abstract

In this study, β -galactosidase was utilized as a model enzyme to investigate the mechanism of enzyme inactivation during bread baking. Thermal inactivation of β -galactosidase was investigated in a wheat flour/water system at varying temperature-moisture content combinations, and in bread during baking at 175 or 205 °C. In the wheat flour/water system, the thermostability of β -galactosidase increased with decreased moisture content, and a kinetic model was accurately fitted to the corresponding inactivation data ($R^2=0.99$). Interestingly, the residual enzyme activity in the bread crust (about 30 %) was hundredfold higher than that in the crumb (about 0.3 %) after baking, despite the higher temperature in the crust throughout baking. This result suggested that the reduced moisture content in the crust increased the thermostability of the enzyme. Subsequently, the kinetic model reasonably predicted the enzyme inactivation in the crumb using the same parameters derived from the wheat flour/water system. However, the model predicted a lower residual enzyme activity in the crust compared with the experimental result, which indicated that the structure of the crust may influence the enzyme inactivation mechanism during baking. The results reported can provide a quantitative understanding of the thermal inactivation kinetics of enzyme during baking, which is essential to better retain enzymatic activity in bakery products supplemented with heat-sensitive enzymes.

3.1 Introduction

Enzymes are naturally present or deliberately added in foods as processing-aids. During processing at elevated temperatures the activity of enzymes is generally affected strongly. For many foods, it is desired to have low residual enzyme activity to stabilize the quality of the product. Examples where high residual enzyme activity detrimentally affects food quality are enzymatic browning in vegetables and fruits, starch degradation in grain products, and enzymatic reactions causing rancidity and off-flavours, etc. (Doblado-Maldonado et al., 2013; Kalita et al., 2017; Lante et al., 2016; Luyben et al., 1982). In some other cases, one strives to retain high residual activity of the enzyme after processing, for example when the enzyme is used as a food ingredient or a processing-aid to achieve a specific transformation (Guidini et al., 2011; Ramos and Malcata, 2011; Wu et al., 2010). To control the degree of enzyme inactivation, especially during thermal processing, it is therefore of importance to have quantitative understanding of the enzyme inactivation kinetics (Illanes, Wilson, & Tomasello, 2000; Illanes, Wilson, & Tomasello, 2001; Ladero, Ferrero, Vian, & Santos, 2005; Ladero, Santos, & García-Ochoa, 2006).

In this study, the well-characterized enzyme β -galactosidase (β -D-galactoside galactohydrolase EC 3.2.1.23) was selected as the model enzyme. The activity of β -galactosidase is affected by many factors, such as the temperature, moisture content, substrate binding, pH and the presence of salts (Adams, 1991). These effects can be quantitatively described with kinetic models, which can then be used to optimize the residual activity after processing (Ladero et al., 2006). Previous studies showed that the thermal inactivation mechanism of β -galactosidase consists of a reversible unfolding step and a second irreversible reaction step following the widely accepted Lumry-Eyring approach (Ladero, Ferrero, Vian, & Santos, 2005; Lumry & Eyring, 1954; Perdana, Fox, Schutyser, & Boom, 2012; van Boekel, 2009).

Several studies investigated the thermal inactivation kinetics of β -galactosidase in dilute solutions, and first order kinetics are generally used to describe the reactions involved in the inactivation of β -galactosidase in solutions (Ladero et al., 2005; Yoshioka et al., 1994). However, relatively few studies have addressed enzyme inactivation in systems with very low moisture content, which is relevant for processes such as drying, baking or other processes involving changes in moisture content. It is also known that presence of other components such as carbohydrates affects the thermal inactivation of β -galactosidase during drying (Ladero et al., 2006). A mechanistic model was developed to describe the inactivation of β -galactosidase in maltodextrin as a function of temperature and moisture content in relation to optimal spray

drying (Perdana, Fox, Schutyser, & Boom, 2012), which is however very different from the environment and conditions relevant to bread baking.

The objective of this study is therefore to develop quantitative understanding of the influence of baking on the inactivation of β -galactosidase. First, the inactivation of β -galactosidase in a wheat flour/water mixture is investigated at varying heating times, temperatures and moisture contents. A kinetic model is then fitted to the experimental inactivation data. Subsequently, the inactivation of β -galactosidase during baking is studied experimentally, where the temperature, moisture content and residual enzyme activity in the bread crust and crumb during baking are monitored as function of baking time. Finally, the kinetic model and the experimentally measured temperature and moisture profiles during baking are combined to describe the enzyme inactivation during baking.

3.2 Materials and methods

3.2.1 Enzyme solution preparation

β -galactosidase from *Aspergillus oryzae* (≥ 8 units/mg solid, Sigma-Aldrich, Germany) was stored at $-20\text{ }^{\circ}\text{C}$ and remained fully active throughout the work. The enzyme solution (1 % w/w) was prepared by dissolving β -galactosidase in McIlvaine's buffer solution. The enzyme solution was stored in the fridge overnight and filtered with a $0.22\text{ }\mu\text{m}$ filter (Sartorius Stedim Biotech GmbH, Germany) before use. The McIlvaine's buffer solution was prepared by mixing 0.2 M Na_2HPO_4 (Sigma-Aldrich, Germany) and 0.1 M citric acid solutions ($\text{C}_6\text{H}_8\text{O}_7$, Sigma-Aldrich, Germany), and the pH was adjusted to 6.00 ± 0.01 .

3.2.2 Isothermal heating experiments at different moisture contents

Isothermal heating experiments were carried out following two different procedures depending on the moisture content of the flour/water mixtures.

1. For high moisture contents (70 %, 80 %, 90 % w/w), flour suspensions were prepared by mixing wheat flour (C1000[®], The Netherlands) into McIlvaine's buffer solution. For heat treatment, 400 μL of flour suspensions was transferred into 2 mL centrifuge tubes (Eppendorf, Germany) and pre-heated to a desired temperature ($60\text{ }^{\circ}\text{C} \sim 70\text{ }^{\circ}\text{C}$) in a Thermomixer (Eppendorf, Germany) with a rotation speed of 900 rpm. After pre-heating, 100 μL enzyme solution was added and heated for the designated time. In one centrifuge tube, 100 μL buffer solution instead of enzyme solution was added as blank. After heating, 1500 μL cold buffer (4

°C) was added and the centrifuge tubes were transferred to an ice bath to prevent any further inactivation of β -galactosidase.

2. For the moisture contents 20 % and 40 % w/w, a different procedure was applied. In this case, a flour paste (40 % w/w) was made by mixing wheat flour and the 1 % w/w enzyme solution. To obtain 20 % w/w moisture content, 0.100 g flour paste (40 % w/w) was transferred into a 200 μ L centrifuge tube and dried at 25 °C in a vacuum oven to a final weight of 0.075 g. Subsequently, the dough mixtures were heated in a PCR machine (DongSheng[®], China) at 65 °C, 70 °C, 75 °C, 80 °C, and 90 °C, respectively, for a certain time. The influence of heating-up time on the experiment can be ignored compared to the total heating time. After heating, the sample was dispersed into 1000 μ L cold buffer solution (4 °C) in a 1.5 mL centrifuge tube with two stainless steel balls inside (diameter=3.0 mm). The suspension was re-suspended in a tissuelyser (JingXin Industrial Development Co., Ltd, China) at 60 Hz for 1 min to extract β -galactosidase from the dried matrix.

3.2.3 Bread baking experiment

Bread samples were prepared following a no-time bread-baking procedure. In brief, wheat flour (50 g), instant yeast (0.5 g), and 1 % w/w enzyme solution (30 mL) were mixed manually, and then the dough was divided into balls of 5.0 g. After 45-min proofing at 40 °C and 85 % relative humidity in a climate chamber (Mettler, Germany), the small breads were baked at two different temperatures (175 °C and 205 °C) for 8 minutes. The bread was cut open immediately after baking and transferred to a fridge to avoid further β -galactosidase inactivation. The residual enzyme activity was measured on the following day. Temperature profiles in the bread crust and crumb during baking were measured using K-type thermocouples (Omega, USA). Moisture contents of the bread crust and crumb were determined according to the AACC method 925.10 (2002).

3.2.4 Enzyme activity analysis

Before the measurement of the enzyme activity, all the treated samples were stored at 7 °C overnight to allow for refolding of reversibly unfolded enzyme. The residual activity of β -galactosidase was measured using the o-nitrophenyl- β -D-galactopyranoside (ONPG) assay (Sigma-Aldrich, Germany). For enzyme activity in the model system, 980 μ L ONPG solution was heated to 40 °C, and 20 μ L sample solution was then added. For the enzyme activity in bread (Figure 3-1), 0.05 g of the bread crumb or the bread crust was first divided into small pieces and added to the ONPG solution. The residual active β -galactosidase cleaves ONPG into

galactose and o-nitrophenol (ONP) at 40 °C. The reaction was terminated by adding 1000 µL 10 % w/w Na₂CO₃ solution (Sigma-Aldrich, Germany) after 10 min. The suspension was centrifuged at 5000 rpm for 5 min. Subsequently, the light absorbance of the clear supernatant was measured at 420 nm using a spectrophotometer (Beckmann Coulter Inc, USA). Residual enzyme activity was expressed as the ratio between A_{420nm} after a certain time of baking (A) and the initial value (A₀). The change of the moisture content in the crust during baking was taken into account when doing the calculation, to exclude the influence of the changing concentration of enzyme in the crust due to water evaporation.

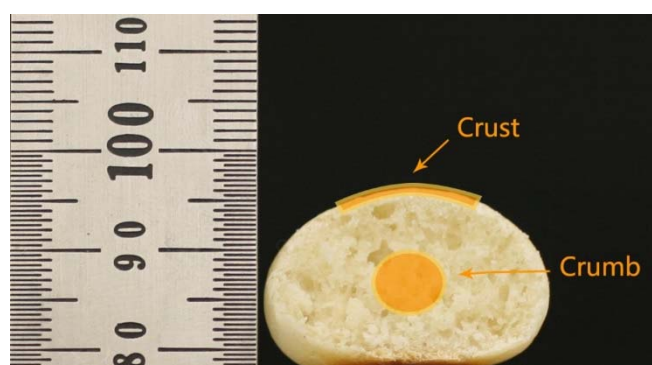
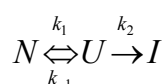


Figure 3-1. A schematic diagram shows the sampling areas of the bread (length unit: mm).

3.2.5 Kinetic modelling

Inactivation of β-galactosidase can be described with a reversible unfolding reaction followed by an irreversible inactivation:



where N is the native enzyme, U is the unfolded enzyme, and I is the inactivated enzyme. The observed inactivation kinetic rate constant, k_{obs} , was calculated from the experimental data of residual activity (A/A_0) and heating time using linear regression (Eqn. 3-1), by assuming the unfolded enzyme can completely refold to its native form after cooling, as describe by Perdana et al. (2012).

$$\ln \frac{A}{A_0} = -k_{obs} \cdot t \quad (3-1)$$

$$k_{obs} = \left(\frac{K_1}{1 + K_1} \right) k_2; K_1 = \frac{k_1}{k_{-1}} \quad (3-2)$$

in which K_1 is the unfolding equilibrium constant, and k_1 and k_{-1} are the unfolding and refolding kinetic rate constants, respectively, and k_2 is the kinetic rate constant of the irreversible inactivation. Finally, the observed inactivation kinetic rate constants were estimated at specific temperature-moisture content (T - x_w) combinations in the kinetic model (Eqns. 3-2 to 3-4) as also reported in a previous study (Perdana, Fox, Schutyser, & Boom, 2012):

$$K_1 = \exp\left(\frac{\Delta\Delta S_{1,w}^\ddagger}{R} - \frac{\Delta\Delta H_{1,w}^\ddagger}{RT_{ref}}\right) \exp\left(-\frac{\Delta\Delta H_{1,w}^\ddagger}{R}\left(\frac{1}{T} - \frac{1}{T_{ref}}\right)\right) \\ \times \exp\left(-\frac{m \cdot (1 - x_w)}{RT}\right) \quad (3-3)$$

and

$$k_2 = \frac{k_B T}{h} \exp\left(\frac{\Delta S_{2,w}^\ddagger}{R} - \frac{\Delta H_{2,w}^\ddagger}{RT_{ref}}\right) \exp\left(-\frac{\Delta H_{2,w}^\ddagger}{R}\left(\frac{1}{T} - \frac{1}{T_{ref}}\right)\right) \\ \times \exp\left[-\frac{\Delta H_{2,s}^\ddagger - \Delta H_{2,w}^\ddagger}{R}\left(\frac{1}{T} - \frac{1}{T_{int}}\right) \exp\left(-p \cdot \frac{x_w}{1 - x_w}\right)\right] \quad (3-4)$$

The symbols are described in the Nomenclature.

The parameters were optimized via nonlinear least-squares regression using the Solver option in Excel (Microsoft®, USA). The parameters that describe the rate constants at infinite dilution ($x_w = 1$), are $\Delta\Delta S_{1,w}^\ddagger$, $\Delta\Delta H_{1,w}^\ddagger$, m in Eqn. 3-3, and $\Delta S_{2,w}^\ddagger$, $\Delta H_{2,w}^\ddagger$, T_{ref} in Eqn. 3-4 were kept the same as in Perdana, et al, (2012). The parameters $\Delta H_{2,s}^\ddagger$, p , and T_{int} were optimized using the whole dataset (number of data points, $n = 48$).

3.2.6 Statistical analysis

All experimental data are presented as mean values of at least three replicates, and error bars represent standard deviation (Mean \pm SD) except where noted. Statistical analysis of the results was performed using Microsoft Excel (Microsoft®, USA).

3.3 Results and discussion

3.3.1 Enzyme inactivation kinetics in the flour/water mixture model system

The residual enzyme activity of β -galactosidase in flour/water mixtures after isothermal heat treatment was investigated for different temperatures and moisture contents. The heating temperature ranged between 60 °C and 90 °C, while the moisture content of the mixtures varied from 20 % w/w to 99.8 % w/w (pure buffer). Figure 3-2 shows the observed inactivation kinetic rate constants (k_{obs}) as a function of different T - x_w combinations. The k_{obs} increases strongly with increasing temperature showing that the enzyme is much less stable at higher temperatures (Figure 3-2a). For example, the half-life of the β -galactosidase activity in buffer solution ($x_w = 0.998$) decreases from 31 min to 34 s when the temperature increases from 60 °C to 70 °C.

In addition, the decrease of the moisture content in the mixtures positively affected the thermal stability of the enzyme. For example, at a heating temperature of 65 °C, the half-life of the enzyme activity increased from 3.2 min in pure buffer solution to 71.2 min in the mixture with a moisture content of 20 % w/w (Figure 3-2a). The k_{obs} decreases strongly when the moisture content is reduced from 70 % w/w to 20 % w/w at 65 °C and 70 °C (Figure 3-2b), indicating the enzyme is more heat stable at reduced moisture contents. The conformational flexibility of the enzyme decreases at lower moisture content due to the absence of water or other hydrogen-bond-forming solutes, which can enhance the thermal stability of the enzyme (Adams, 1991; Klibanov, 1989; van Boekel, 2009). Eventually, this can lead to conformational modification of the protein. It is noted that for matrixes with high moisture contents (i.e., $x_w \geq 0.70$), k_{obs} was observed dependent only on temperature and not on moisture content (Figure 3-2a).

The sudden change in the slope in Figure 3-2a, especially visible at lower moisture content ($x_w = 0.20$ and 0.40) can be explained by a kinetic shift indicating that at lower temperatures the reversible unfolding reaction is limiting and at higher temperatures the irreversible reaction is limiting (Jakób et al., 2010; Perdana, Fox, Schutyser, & Boom, 2012).

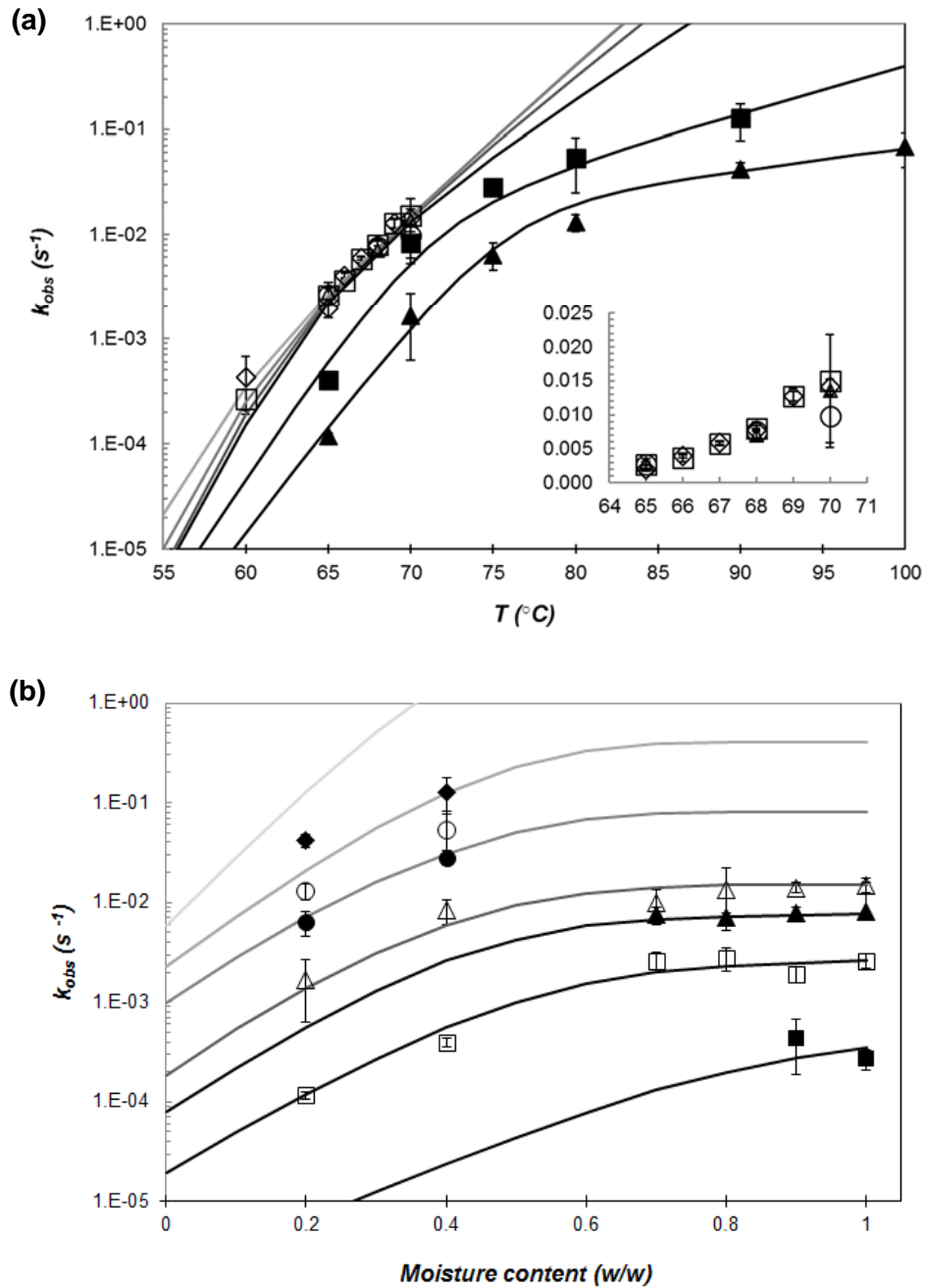


Figure 3-2. Inactivation kinetic constants of β -galactosidase at different T - x_w conditions: (a) $x_w = 0.998$ (□ Pure buffer), 0.90 (◇), 0.80 (Δ), 0.70 (○), 0.40 (■), and 0.20 (▲); (b) $T = 60$ °C (■), 65 °C (□), 68 °C (▲), 70 °C (Δ), 75 °C (●), 80 °C (○) and 90 °C (◆). Solid lines represent the fitted kinetic model. The error bars show the standard deviation of the experimental data.

3.3.2 Optimization of kinetic parameters

The kinetic parameters were optimized based on the data of the inactivation data of β -galactosidase in the model system using the method described in section 3.2.5. As mentioned

above, the parameters that describe the rate constants at infinite dilution (in pure water) were kept the same as reported before (Table 3-1). Among the three optimized parameters (Table 3-1), $\Delta H_{2,s}^\ddagger$ is the activation enthalpy of the reversible enzyme inactivation in pure solid form ($x_w = 0$), p is the parameter that describes the effect of the moisture content on k_2 , and T_{int} is the temperature at which k_2 remains constant at all moisture contents. These three parameters were optimized on purpose in this study because their values are expected to be dependent on the food matrix (Adams, 1991).

In general, the experimental inactivation data and the kinetic model are in good agreement ($R^2 = 0.989$) (Figure 3-3). The model slightly overestimated the inactivation kinetic rate constant at higher temperatures (80 °C and 90 °C) and lower moisture contents ($x_w = 0.20$ and $x_w = 0.40$) as shown in Figure 3-2b. This may be explained by the relatively sparse experimental data at high T and low x_w (only 4 data points) and the higher degree of complexity of the irreversible inactivation of β -galactosidase at higher temperature due to protein aggregation or coagulation (Lencki et al., 1992).

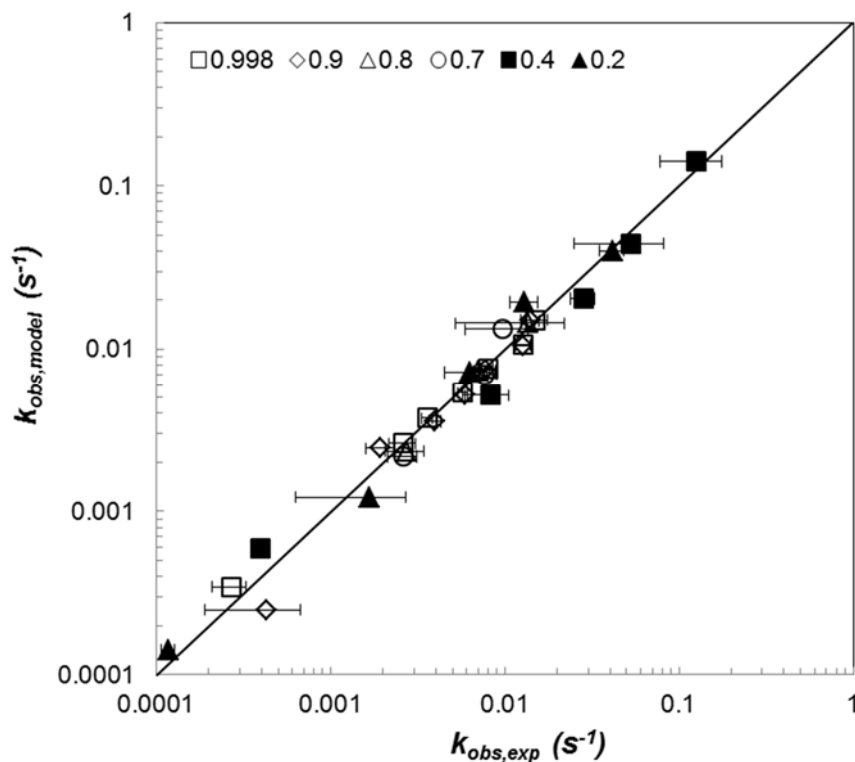


Figure 3-3. Parity plot of the experimental and the predicted values for k_{obs} in the model system for different moisture contents.

The different used food matrices explain why the parameters in this study and our earlier study on maltodextrin are different (Perdana, Fox, Schutyser, & Boom, 2012). Specifically, the $\Delta S_{2,s}^\ddagger$, which is the activation entropy of the reversible enzyme inactivation in pure solid form ($x_w = 0$), can be calculated by realizing that at T_{int} the k_2 value is similar for $x_w = 1$ and $x_w = 0$ (Eqn. 3-5):

$$\frac{\Delta S_{2,w}^\ddagger}{R} - \frac{\Delta H_{2,w}^\ddagger}{RT_{int}} = \frac{\Delta S_{2,s}^\ddagger}{R} - \frac{\Delta H_{2,s}^\ddagger}{RT_{int}} \quad (3-5)$$

The value of $\Delta S_{2,s}^\ddagger$ in the flour/water system was found to be $268 \text{ J}\cdot\text{mol}^{-1}\cdot\text{K}^{-1}$, which is much larger than that determined in maltodextrin ($24 \text{ J}\cdot\text{mol}^{-1}\cdot\text{K}^{-1}$). Moreover, the activation enthalpy $\Delta H_{2,s}^\ddagger$ in the flour/water system ($4.6 \times 10^3 \text{ J}\cdot\text{mol}^{-1}$) was also lower than the value found in maltodextrin ($1.28 \times 10^5 \text{ J}\cdot\text{mol}^{-1}$, Table 3-1). A smaller positive activation enthalpy and a larger positive activation entropy indicates a smaller overall Gibbs' activation energy ($\Delta G = \Delta H - T\Delta S$) (van Boekel, 2009), indicating that the irreversible inactivation reaction of β -galactosidase in the wheat flour-based dried matrix is easier and thus faster than in maltodextrin. The latter is also in agreement with the experimental observations of different k_{obs} in maltodextrin and wheat flour at specific moisture content and heating temperature (Perdana, Fox, Schutyser, & Boom, 2012). This difference can be explained by the high glass transition temperature of maltodextrin which protects the native enzyme (Burin et al., 2004; Mazzobre et al., 1997).

Table 3-1. Estimated parameter values of the inactivation kinetic model

Parameter	Unit	Value for flour/water system	Value for maltodextrin solution (Perdana, Fox, Schutyser, & Boom, 2012)
$\Delta\Delta S_{1,w}^\ddagger$	$\text{J}\cdot\text{mol}^{-1}\cdot\text{K}^{-1}$	1.08×10^3	1.08×10^3
$\Delta\Delta H_{1,w}^\ddagger$	$\text{J}\cdot\text{mol}^{-1}$	3.57×10^5	3.57×10^5
m	-	2.60×10^4	2.60×10^4
$\Delta S_{2,w}^\ddagger$	$\text{J}\cdot\text{mol}^{-1}\cdot\text{K}^{-1}$	6.75×10^2	6.75×10^2
$\Delta H_{2,w}^\ddagger$	$\text{J}\cdot\text{mol}^{-1}$	3.28×10^5	3.28×10^5
$\Delta H_{2,s}^\ddagger$ *	$\text{J}\cdot\text{mol}^{-1}$	4.60×10^3	1.28×10^5
p^*	-	0.63	1.16
T_{int} *	K	343	307
T_{ref}	K	334	334

*optimized parameters

3.3.3 Enzyme activity in bread during baking

Bread samples with enzyme were baked at different baking temperatures (175 °C and 205 °C). The temperature profiles in both crust and crumb of the breads were monitored. In the crumb, a sigmoid-shape profile was observed: temperature increased asymptotically after a lag stage until 100 °C was reached, while the temperature of the crust gradually increased throughout baking (Figure 3-4a). The moisture content in the crust decreased due to water evaporation from the surface of the dough, while the crumb remained at the same moisture content as the dough (Figure 3-4b). These observations are similar to those reported in other studies (Purlis, 2011; Purlis and Salvadori, 2009a; Zhang et al., 2005).

β -galactosidase in the bread crumb remained active during the initial phase of baking, but gradually inactivated after 4 minutes of baking at 205 °C and after 6 minutes at 175 °C, respectively (Figure 3-4c). Interestingly, different inactivation behaviour of β -galactosidase was observed in the crust. At 175 °C, the enzyme inactivated progressively during the initial phase (0~5 min), while the inactivation slowed down after this phase (5~8 min). At 205 °C, the activity of the enzyme in the crust was more strongly affected, but decreased to a plateau value with a final residual enzyme activity of 0.3. For both temperatures, higher residual enzyme activities were observed in the crust than in the crumb, although the local temperatures reached in the crust were much higher than in the crumb (Figure 3-4a).

The reduced inactivation of the enzyme in the crust may be explained by the strong local decrease in moisture content. A similar phenomenon is also observed for other enzymes. Samborska et al. (2005) reported that *Aspergillus oryzae* α -amylase is more heat stable in maltodextrin systems at reduced moisture content than in aqueous solutions. The heat stability of lipoxygenase in a glucose calcium-alginate gel also increases strongly with decreasing moisture content (from 80 % w/w to 40 % w/w) (Liou, 1982). At reduced moisture content levels, the enzyme unfolding becomes slower because of the lower conformational flexibility, which implies that the thermostability of enzymes is higher in dried foods than in an aqueous environment (van Boekel, 2009). In this study, the thermostability of β -galactosidase may thus have improved by the dense structure of the dehydrated crust. However, further research is needed to verify this effect.

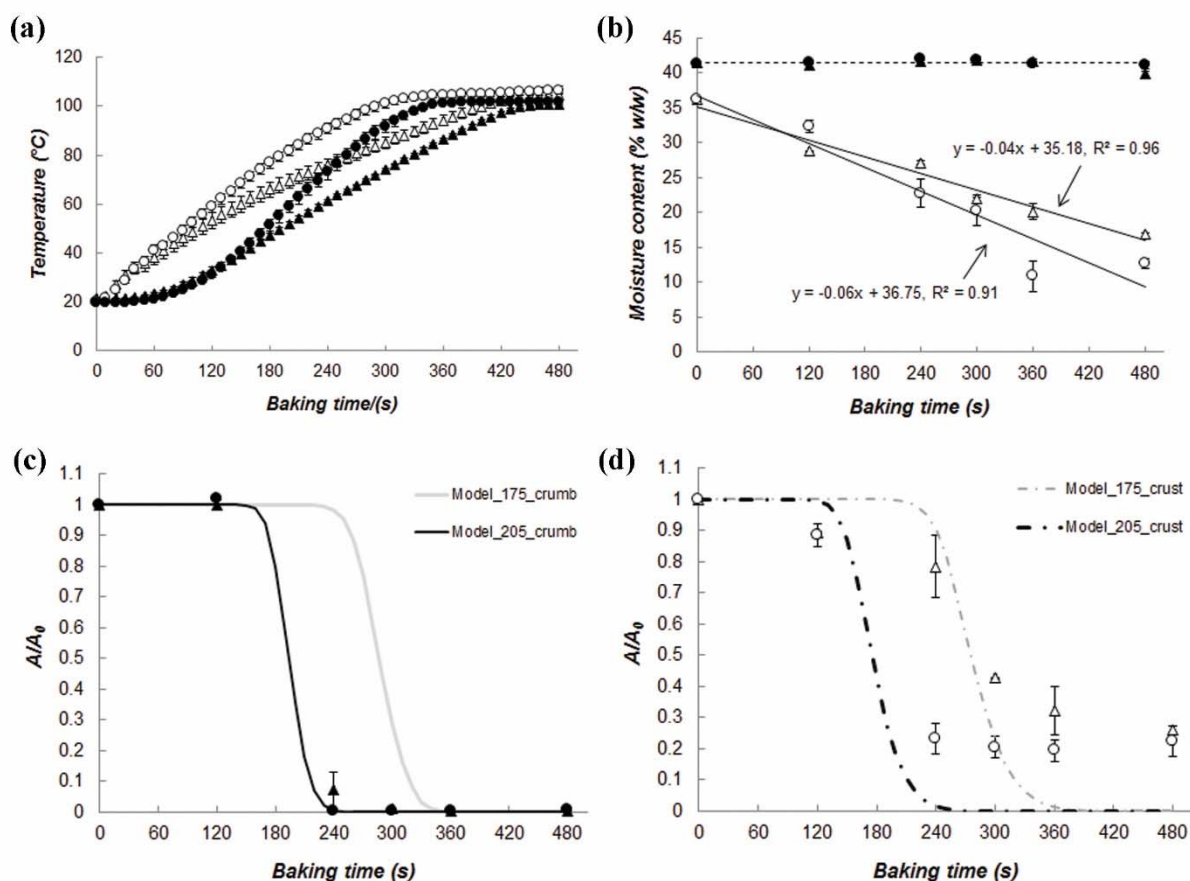


Figure 3-4. Temperature profiles of bread during baking (a); Moisture content histories of bread during baking (b); Residual enzyme activity in the crumb (c) and in the crust (d) as a function of baking time. Symbols represent different baking temperatures and sampling positions: \blacktriangle 175 °C, crumb; \triangle 175 °C, crust; \bullet 205 °C, crumb; \circ 205 °C, crust. Solid lines and dotted lines represent calculated residual enzyme activity based on the kinetic model.

Another explanation may be related to the specific structure of the relatively dry bread crust as well. The crust structure can be defined as a composite of granular starch in a matrix of gelatinized starch blended with a continuous gluten network (Della Valle et al., 2012; Primo-Martín et al., 2006) (see Appendix 3-A, Figure 3-A1). In contrast, the bread crumb contains fully-gelatinized starch after baking. The native wheat starch has a higher glass transition temperature compared to the gelatinized wheat starch (van Nieuwenhuijzen et al., 2010). The non-gelatinized fraction of starch in the crust region probably showed a similar protective mechanism of the enzyme upon heat treatment as the maltodextrin matrix (high T_g): the glassy structure of the crust formed in the later stage of baking lead to a smaller $\Delta S_{2,s}^\ddagger$ and a larger $\Delta H_{2,s}^\ddagger$, resulting in a larger overall Gibbs' activation energy to trigger the enzyme inactivation reaction, as explained before. Consequently, this may explain the higher residual enzyme activity of β -galactosidase in the crust than in the crumb (Figure 3-4).

3.3.4 Prediction of enzyme retention in bread

The residual enzyme activity of β -galactosidase in the bread crust and crumb was estimated with the previously established kinetic inactivation models and the measured temperature-time and moisture content-time profiles. The k_{obs} was described before as a function of T - x_w combinations (Eqns. 3-2 to 3-4), i.e., $k_{obs} = f(T, x_w)$. The residual enzyme activity in the bread was expressed as A/A_0 and was calculated using Eqns. 3-1 to 3-4, in which $A_0 = 1$ and the time interval Δt was 10 s. The temperatures used for the calculations were obtained from the experiments. A linear equation ($R^2 > 0.9$) was used to describe the relation between moisture content in the crust and the baking time, while the moisture content in the crumb was set to 0.41 (Figure 3-4b).

Figure 3-4c shows that the kinetic model can reasonably describe the experimentally observed inactivation in the bread crumb, especially during the first two minutes and the last two minutes of baking. The enzyme in the crumb is predicted to be fully inactivated after 4-min baking at 175 °C and 6-min baking at 205 °C, while our experiments indicated 4 minutes at 175 °C and 5 minutes at 205 °C, respectively. According to the experiment, after baking for 4 minutes, the residual enzyme activity in the crumb of bread baked at 175 °C was slightly higher (about 0.1) than that of bread baked at 205 °C. However, the difference predicted by the model was more significant (about 1).

However, the kinetic model was not able to describe the inactivation data in the crust, especially during the late phase of baking (from 4 to 8 min). One of the explanations is that the kinetic model tends to overestimate the k_{obs} at higher heating temperatures as mentioned in section 3.3.2, subsequently it predicted lower enzyme retention in the crust compared to the experimental data. Another possible explanation could be the difference in the structure/composite of the dry crust compared to the wheat flour/water mixture with a low moisture content (i.e., $x_w = 0.20$) despite of their similar moisture content. In the real baking experiment, the crust region is a dense, glassy and continuous structure, while the wheat flour/water system ($x_w = 0.20$) exhibited a strongly porous and irregular structure caused by vacuum drying (see section 3.2.2). This porous structure was created by the large pressure difference between the wheat flour/water mixture ($x_w = 0.40$) and atmosphere leading to rapid moisture evaporation and subsequent channel and pore formation (Tian et al., 2016). This difference in structure may lead to different inactivation kinetics in the crust during the real baking experiment and in the model system during the isothermal experiment. In addition, it is technically difficult to obtain the experimental data of k_{obs} at high temperatures ($>90^\circ\text{C}$)

during separate isothermal experiment, because the enzyme will be completely inactivated in a short time. The lack of the inactivation data in this temperature range (90~100 °C) might also reduce the accuracy of the prediction by applying the kinetic model.

3.4 Conclusions

This study has illustrated explicitly the thermal inactivation kinetics of *A. oryzae* β -galactosidase through separate isothermal heating experiments and bread baking experiments. Thermostability of the enzyme in the wheat flour/water system increased at reduced moisture content, which can be accurately described by a kinetic model. The parameters of the kinetic model depended on the matrix in which the enzyme is embedded. After bread baking, the residual enzyme activity in the crust was found around 30 %, while the enzyme in the crumb was almost fully inactivated. This is explained by the lower local moisture content in the crust which significantly improved the thermostability of the enzyme. In addition, the dense and glassy microstructure of the crust may have an additional protective effect on β -galactosidase upon heat treatment.

This study also showed that it is possible to simulate enzyme inactivation in a real food system once sufficient data on inactivation kinetics and corresponding temperature and moisture content histories during processing are available. In this study, the thermal inactivation of β -galactosidase in the bread crumb during baking was reasonably well predicted by kinetic modelling using the same parameters derived from the isothermal heating experiments. However, the final residual enzyme activity in the bread crust was underestimated by the prediction, which suggests that the specific characteristics of the crust structure may influence the mechanism of enzyme inactivation during the actual baking process, which may be different from the separate isothermal heating experiments.

Nomenclatures

A	enzyme activity	-
E_a	activation energy	(J·mol ⁻¹)
ΔG	Gibbs' free energy	(J·mol ⁻¹)
h	Planck's constant (6.626×10^{-34})	(J·s ⁻¹)
ΔH^\ddagger	activation enthalpy	(J·mol ⁻¹)
$\Delta\Delta H^\ddagger$	activation enthalpy difference between unfolding and	(J·mol ⁻¹)
I	inactivated enzyme	(-)
k	inactivation kinetic constant	(s ⁻¹)
k_B	Boltzmann's constant (1.381×10^{-23})	(J·K ⁻¹)
K_I	reversible unfolding Equilibrium constant	(mol·mol ⁻¹)
m	parameter to describe the effect of moisture content on the	(-)
N	native enzyme	(-)
p	parameter to describe the effect of moisture content on	(-)
R	ideal gas constant (8.314)	(J·mol ⁻¹ ·K ⁻¹)
ΔS^\ddagger	activation entropy	(J·mol ⁻¹ ·K ⁻¹)
$\Delta\Delta S^\ddagger$	activation entropy difference between unfolding and	(J·mol ⁻¹ ·K ⁻¹)
t	time	(s)
Δt	increment of time	(s)
T	temperature	(K)
U	unfolded enzyme	(-)
x	mass fraction	(kg·kg total ⁻¹)
n	number of data points (48)	(-)
<i>Subscript:</i>		
0	initial condition	
1	unfolding reaction	
-1	refolding reaction	
2	irreversible inactivation	
int	intercept	
obs	observed	
ref	reference	
s	in pure solid form ($x_w = 0$)	
w	in a solution with infinite dilution ($x_w = 1$)	
g	glass transition	

Appendix 3-A. Microstructure of the crust

The microstructure of the crust was observed using scanning electric microscopy (SEM), and abundant intact starch granules can be found (Figure 3-A1).

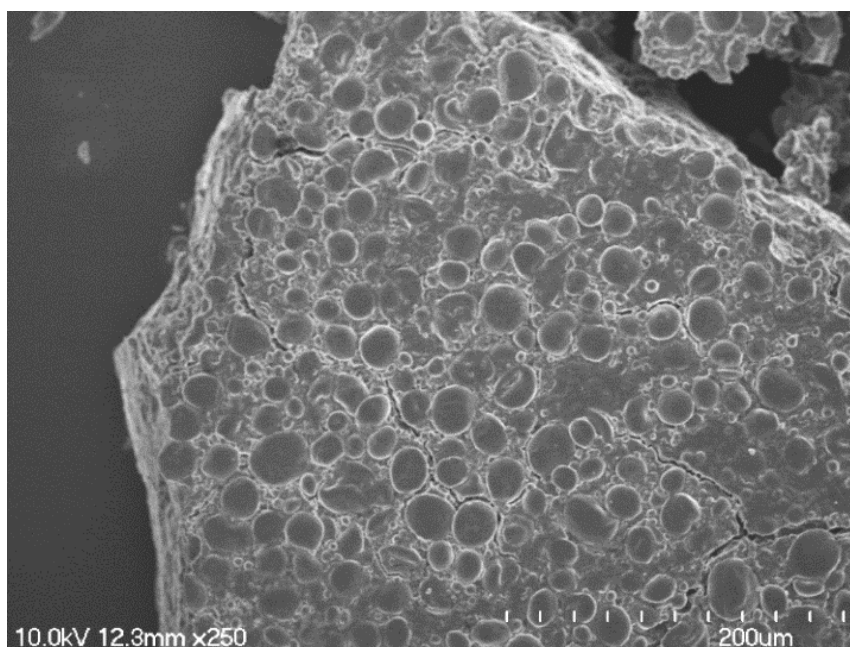


Figure 3-A1. SEM image of the bread crust: abundant intact starch granules can be observed (scale bar represents 200 μm and the bread sample was freeze-dried for SEM analysis after baking at 175 $^{\circ}\text{C}$ for 8 min).

Chapter 4

Effect of baking conditions and storage on the viability of *Lactobacillus plantarum* supplemented to bread



This chapter has been published as:

Zhang, L., Taal, M.A., Boom, R.M., Chen, X.D., Schutyser, M.A.I. (2018). Effect of baking conditions and storage on the viability of *Lactobacillus plantarum* supplemented to bread. LWT - Food Science & Technology. 87, 318–325.

Link: <https://doi.org/10.1016/j.lwt.2017.09.005>

Abstract

Bread is an interesting non-dairy-based vehicle for probiotics delivery given its daily consumption worldwide. The incorporation of probiotics in bread is challenging due to the high baking temperatures. In this study the influence of various baking conditions and subsequent storage on survival of a model strain *Lactobacillus plantarum* P8 is systematically investigated. Bread samples with varying dough weight (5, 30, and 60 g) were baked at different temperatures (175, 205, and 235 °C) for 8 min, and the residual viability of bacteria was determined every 2 min. Under all baking conditions, the viability of probiotics decreased from 10^9 CFU/g to 10^{4-5} CFU/g after baking. For specific conditions a difference in bacterial viability between bread crust and crumb was observed, which was explained by the different temperature-moisture history and developed microstructure during baking. Remarkably, during storage bacterial viability increased by 2~3 log to 10^8 CFU/g in crust and 10^6 CFU/g in crumb, respectively. The re-growth of probiotics was accompanied by a decrease in pH of the bread and an increase of the total titratable acidity. The results of this work provide valuable experimental data for further modelling and optimization studies, which then could contribute to the development of probiotic bakery products.

4.1 Introduction

Probiotics are defined as live microorganisms that confer health benefits on the hosts when administered in adequate amounts (FAO/WHO, 2002). Most probiotic food available on the market are dairy fermented foods such as yoghurt, korut and kefir (De Prisco and Mauriello, 2016). However, there is an increasing consumer demand for non-dairy-based probiotic products, given the drawbacks of dairy products, such as the prevalence of allergy and lactose intolerance (Kumar et al., 2015).

Bread is a nutritious non-dairy based food containing carbohydrates, minerals, vitamins and dietary fibres (Pinto et al., 2014). Non-digestible carbohydrates like oligosaccharides present in whole-wheat bread have been suggested to promote growth of probiotic bacteria (Charalampopoulos et al., 2002). Moreover, inoculation of lactic acid bacteria in dough can lead to high quality sourdough bread (Corsetti et al., 2008). Based on these perspectives, we identified bread as a potential food that can be enriched with probiotics.

Preservation of cell viability during baking and storage are essential as the minimum amount of live bacteria in the probiotic foods should be 10^6 ~ 10^7 CFU/g to confer beneficial influence on consumer health (Ross et al., 2005). However, incorporation of probiotics in bread is challenging because of the high temperatures during baking that negatively affect survival of the bacteria and additional loss of bacterial viability during subsequent storage at ambient temperatures (Soukoulis et al., 2014). Only few studies investigated strategies to improve bacterial survival in bread. Altamirano-Fortoul et al. (2012) micro-encapsulated *Lactobacillus acidophilus* in starch, applied it to the dough and obtained reasonably high viable counts after baking (about 10^6 CFU/bread). However, drawback of this approach was that the probiotic coating negatively affected the physicochemical properties of the bread crust, leading to different color and crispness. Soukoulis et al. (2014) applied sodium alginate solutions with *Lactobacillus rhamnosus* GG (LGG) as a coating on the surface of pre-baked pan bread, and dried the crust at mild conditions. The viability of LGG was found approx. 7.6 - 9.0 log CFU in 30 - 40 g of bread slice. As stated above, only few studies have reported on the application of probiotics in bread or other bakery products (Espitia, Batista, Azeredo, & Otoni, 2016; Malmo, La Storia, & Mauriello, 2013; Reid, Champagne, Gardner, Fustier, & Vuilleumard, 2007; Zhang et al., 2014). However, none of these previous studies systematically evaluated the survival of bacteria during baking and storage conditions.

Therefore, the aim of this study is to better understand the impact of different bread sizes, baking conditions and subsequent storage on the survival of probiotic bacteria (*Lactobacillus plantarum* P8). The viability of bacteria was evaluated for both bread crust and crumb as they have a distinct temperature-moisture history during baking with corresponding microstructural properties.

4.2 Materials and methods

4.2.1 Probiotic strain and bacteria culture

The model probiotic strain *Lactobacillus plantarum* P8 (ATCC 14917) was provided by Inner Mongolia Agricultural University. The *L. plantarum* culture was routinely prepared using MRS broth (OXOID, United Kingdom) as the growth medium. A single colony of *L. plantarum* was inoculated in 10 mL sterile MRS broth and pre-cultured at 37 °C for 12 h. Subsequently, 1 % v/v inoculum of *L. plantarum* was sub-cultured in 100 mL MRS broth at 37 °C for 24 h without agitation. Thirty millilitres of cell suspension were transferred into a centrifuge tube (50 mL), and the cell pellets were harvested by centrifugation (Thermo Fisher Scientific, USA) at 8000 ×g and 4 °C for 15 min, and were aseptically re-suspended in UHT skim milk for the baking experiment.

4.2.2 Bread samples preparation

Bread samples were made following a recipe from Zhang et al. (2016): wheat flour (100 g), sugar (4 g), salt (1.5 g), instant yeast (1 g), butter (3 g), and UHT skim milk (65 g) with *L. plantarum* added. Bread without bacteria addition was made as the control. Dough was prepared in a stand mixer (Hauswirt® HM730, China) by mixing the dry ingredients at speed 1 for 1 min and mixing at speed 3 for 7 min after milk was added. After resting for 5 min, dough was divided into balls of 5, 30 and 60 g, respectively. The dough was proofed at 40 °C, 85 % RH in a climate chamber (Yiheng Scientific Instruments Co., Ltd., China) for 1 hour (or 45 min for 5 g dough). Subsequently, bread samples were baked for 8 min in an electric oven (Changdi® CRTF30W, China) at 175 °C, 205 °C and 235 °C, respectively.

After baking at 175 °C for 8 min, bread samples with an initial weight of 30 g were sealed in polyethylene bags and stored at 25 °C, 55 % RH in the climate chamber for 5 days, to investigate the impact of storage on the viability of *L. plantarum* in bread. Some properties, i.e. viability of bacteria in bread, moisture content of bread matrix, pH of crumb, etc. were determined according to the methods described in the following section.

4.2.3 Physicochemical properties analysis

Temperature profiles of the bread crust and crumb during baking were monitored by inserting K-type thermocouples (Omega[®], USA) into the top surface and core sections of the dough. The thermocouples were connected to a computer via a Picometer TC-08 (Pico Technology, UK), and the sampling interval was 1 second.

Moisture contents (% kg/kg wet base) of the bread crust (top surface) and crumb (centre) during baking and storage were determined according to Eqn. 4-1.

$$\text{Moisture content (\%)} = \frac{W_1 - W_2}{W_1} \quad (4-1)$$

in which, W_1 (kg) is the weight of the sample after sampling and W_2 (kg) the weight after dehydration at 105 °C for 24 h in an oven.

The pH and total titratable acidity (TTA) of the bread crumb were measured before and after baking, as well as during storage (Palacios et al., 2006). Bread dough or crumb (10 g) was mixed with 100 mL acetone/water (5/95, v/v) in a stomacher (iMix[®], Interlab, France), and the pH of the suspension was determined using a pH meter (Thermo Scientific, USA). The same suspension was titrated against 0.1 N NaOH to a final pH value of 8.5 to determine the TTA. The TTA was expressed as the amount (mL) of NaOH used for titrating 10 g of sample.

4.2.4 Microbiological analysis

Viable cell counts of *L. plantarum* in bread were determined after baking for 0, 2, 4, 6, 8 min and after storage for 1, 2, 3, 4, 5 days. Samples of bread crust and crumb were obtained from the top surface and the core section of the bread, respectively. For bread samples with an initial weight of 30 g or 60 g, samples of bread crust or crumb (5.0 g) aseptically homogenized with 95 mL sterile peptone water (0.1 % w/w, Solarbio[®], China) in a stomacher (iMix[®], Interlab, France) for 1 min, while 1.0 g of crust or crumb were homogenized in 49 mL peptone water for those 5 g bread samples. Subsequently, serial dilutions of the cell suspension were made in 9 mL sterile peptone water (0.1 % w/w), and 100 µL suspension was spread onto a modified MRS agar plate.

To inhibit the growth of *Bacillus* strains and yeast on the MRS agar plate, vancomycin (20 ppm, Shyuanye[®], China) and natamycin (200 ppm, Antai[®], China) were added into the MRS agar broth (MRS: Oxoid, UK; agar powder: Solarbio, China) through a 0.22 µm polyethylene sulfone

filter (Millipore®, USA) (Hartemink et al., 1997; Liu and Tsao, 2009). The growth of *L. plantarum* was not affected by the addition of vancomycin and natamycin (Zhang et al., 2014). The agar plates were statically incubated at 37 °C for 48 h. *L. plantarum* colonies were counted and the viability (N) was expressed as colonies forming units per gram of sample (CFU/g). The semi-logarithmic survival curves of *L. plantarum* were presented by plotting the residual viability, i.e. $\log(N/N_0)$, against baking time for each baking condition, in which N_0 was the initial viable count (CFU/g) of *L. plantarum* in the dough before baking.

4.2.5 Microstructure analysis

Microstructure of the bread with or without (control) *L. plantarum* addition was monitored using scanning electron microscopy (SEM). Samples from the crust and crumb of the 30 g bread baked at 175 °C were stored at - 80 °C overnight, and were dried in a lyophilizer (Sihuan Scientific Instruments Co., Ltd., China). The dried samples were cut into small pieces with a knife blade and fixed on an aluminium stub using a conducting carbon tape, and then coated with gold using a sputter. SEM images were recorded using a JEOL 7001 F (Jeol Ltd, Tokyo, Japan).

4.2.6 Statistical analysis

All the experiments were done independently at least in duplicate and all the data are presented as mean \pm standard deviation (SD). One-way analysis of variance (ANOVA) and Student's *t*-test were performed using Microsoft Excel 2010, and a *p*-value smaller than 0.05 meant the difference between groups was statistically significant.

4.3 Results and discussion

4.3.1 Minimum baking time

To investigate the influence of different baking conditions (dough weight and baking temperature) and subsequent storage on the survival of probiotic bacteria, it is important to establish a minimum baking time that provides bread of acceptable quality. Therefore, we first determined the minimum baking time according to the extent of starch gelatinization in dough (Purlis, 2011). Bread is considered properly baked when the extent of starch gelatinization in the coldest point of the dough (i.e., the core area) reaches 98 % ($\alpha \geq 0.98$) (Purlis, 2011; Purlis and Salvadori, 2009b). The starch gelatinization can be described by a first-order kinetic model

as a function of temperature and time (Eqns. 4-2 and 4-3, Therdthai et al., 2002; Zannoni et al., 1995).

$$\frac{d(1 - \alpha)}{dt} = -K(1 - \alpha) \quad (4-2)$$

$$K = K_0 \exp\left(\frac{-E_a}{RT}\right) \quad (4-3)$$

in which α is the mass fraction of gelatinized starch (-), t is time (s), K is the rate constant (s^{-1}) which depends on the temperature according to the Arrhenius equation (pre-exponential factor, $k_0 = 2.8 \times 10^{18} s^{-1}$; activation energy, $E_a = 138$ kJ/mol, in Eqn. 4-3). The extent of starch gelatinization (α) for a time interval ($\Delta t = 1$ s) was calculated based on the temperature profiles of the crumb measured experimentally by inserting a K-type thermocouple in the core zone of the dough. The temperature measurements were performed in triplicate for each baking condition.

Figure 4-1 shows the minimum baking time for bread with different initial weights (5 g, 30 g, and 60 g) which were baked at different oven temperatures (175 °C, 205 °C and 235 °C). The time required for complete starch gelatinization in the bread decreased as the baking temperature increased from 175 °C to 235 °C and as the dough weight (or size) decreased from 60 g to 5 g. These results are in agreement with Purlis (2011) showing baking time decreases when oven temperature is increased and bread radius is decreased. It is noted that surface colour could be considered as well to establish baking time (Zhang et al., 2016). However, because the evaluation of the optimum surface browning may be considered more subjective, complete starch gelatinization was used as the indicator of minimum baking time in this study.

The viability of bacteria is affected by the exposure time to heat and dehydration stresses (Hansen and Riemann, 1963; Peleg, 2000). If the baking time is shortened by increasing the baking temperature or reducing the bread size, higher residual viability of *L. plantarum* may be obtained after baking (see section 4.3.3). To facilitate data collection, it was chosen to use one baking time (8 minutes) for all conditions tested, and a sampling interval of 2 minute was applied.

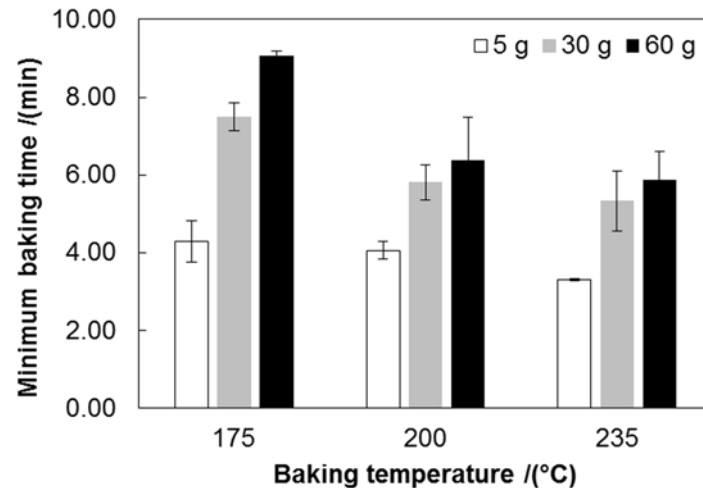


Figure 4-1. Minimum baking time determined by the 98 % completion of starch gelatinization in the crumb of bread with different initial dough weights and baked at different baking temperatures (175, 205 or 235 °C). Dough weight: white bar, 5 g; grey bar, 30 g; black bar, 60 g. Error bars indicate the standard deviation.

4.3.2 Bread baking kinetics

The bread crust is a continuous envelope and a compact layer developed around a bread during baking, while the crumb is characterized by its cellular structure (Della Valle et al., 2012). The bread crust and crumb exhibit different textural properties due to their distinct temperature-moisture histories during baking (Vanin et al., 2009). As shown in Figure 4-2, for all baking conditions, the temperature profiles of bread crust or crumb show a similar trend, which is in agreement with other studies (Besbes et al., 2014; Purlis and Salvadori, 2009a; Sui et al., 2015). Specifically, the crust temperature continuously increased during baking to 140~180 °C for 5 g bread, 120~150 °C for 30 g bread and 110~140 °C for 60 g bread at the end of baking, respectively. In the crumb of 30 g and 60 g dough, the temperature remained more or less constant in the beginning, after which it increased to 100 °C and remained at 100 °C due to water evaporation and condensation (Wong et al., 2007). However, the crumb temperature of 5 g bread gradually increased from the beginning until a plateau of 100 °C was reached.

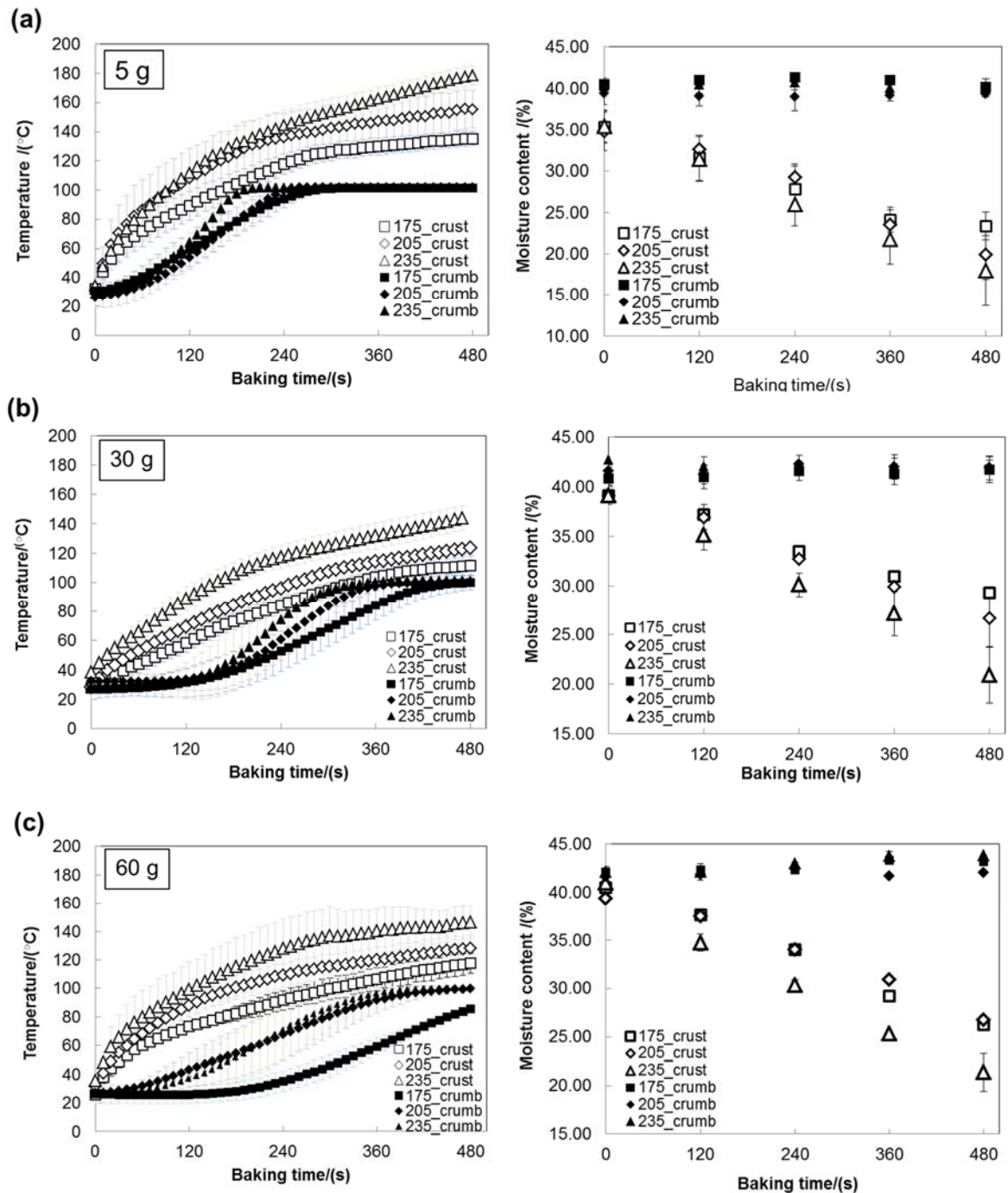


Figure 4-2. Temperature profiles (left) and moisture content profiles (right) of bread with different initial dough weights (a: 5 g, b: 30 g, c: 60 g) during baking at different temperatures: 175 °C (□ crust, ■ crumb); 200 °C (◇ crust, ◆ crumb); 235 °C (△ crust, ▲ crumb). Error bars indicate the standard deviation.

In addition, the moisture content records for crust and crumb were determined in this study (Figure 4-2). Moisture contents of the crumb remained at the same level (t-test, $p > 0.05$) during baking whatever initial dough weight or baking temperature used. This can be explained by the

evaporation-condensation phenomena inside the bread during baking (De Vries et al., 1989; Purlis and Salvadori, 2009c). In contrast, water from the crust is quickly removed by the high evaporation rate near the surface, which resulted in a strong decrease in the moisture content (Figure 4-2). Similar moisture content profiles have been reported in other studies for larger breads (Vanin et al., 2009; Wagner et al., 2007).

4.3.3 Effect of baking conditions on *L. plantarum* viability

Figure 4-3 shows approx. 4~5 log reduction of viable counts of *L. plantarum* in both the crust and crumb of 5, 30 or 60 g bread after baking at 175, 205 or 235 °C for 8 min, while the initial viable count (N_0) in dough was 8.8 ± 0.1 log CFU/g. As mentioned in section 4.3.1, the residual viability of *L. plantarum* may increase if the baking time is shortened. The minimum baking time is marked (grey line) for each baking condition (Figure 4-3). The survival of *L. plantarum* in 5 g bread increased by about 2 log if the minimum baking time is considered instead of the whole 8 minutes (Figures. 4-3a~c), with a final viability of 10^7 CFU/g. However, this improvement for 30 g and 60 g dough was not significant (Figures 4-3d~i).

As shown in Figure 4-3, in the first 2 minutes of baking, the bacteria were just slightly inactivated (< 0.5 log reduction) in the crumb of 30 g and 60 g bread. This can be explained by the limited thermal inactivation as the temperature in the crumb was still low ($T < 45$ °C, Figures 4-2b & c) (Fu and Chen, 2011). However, the bacterial viability in the crumb of 5 g bread decreased by 1~2 log during the first 2-min of baking (Figures 4-3a~c). This is probably because the crumb temperature of 5 g bread increased rapidly at a rate of about 20 °C/min to above 45 °C in 2-min baking (Figure 4-2a). Additionally, we expected that thermally-induced inactivation of *L. plantarum* was the dominant mechanism of bacterial inactivation during bread baking. Whereas the dehydration inactivation of bacteria via osmotic stress was assumed to be minor because the moisture content in the crumb remained constant (Bustos and Bórquez, 2013; Fu and Chen, 2011). The viability of *L. plantarum* in the bread crust eventually may be expected to decrease for all baking conditions due to the high temperature during baking (Figure 4-3).

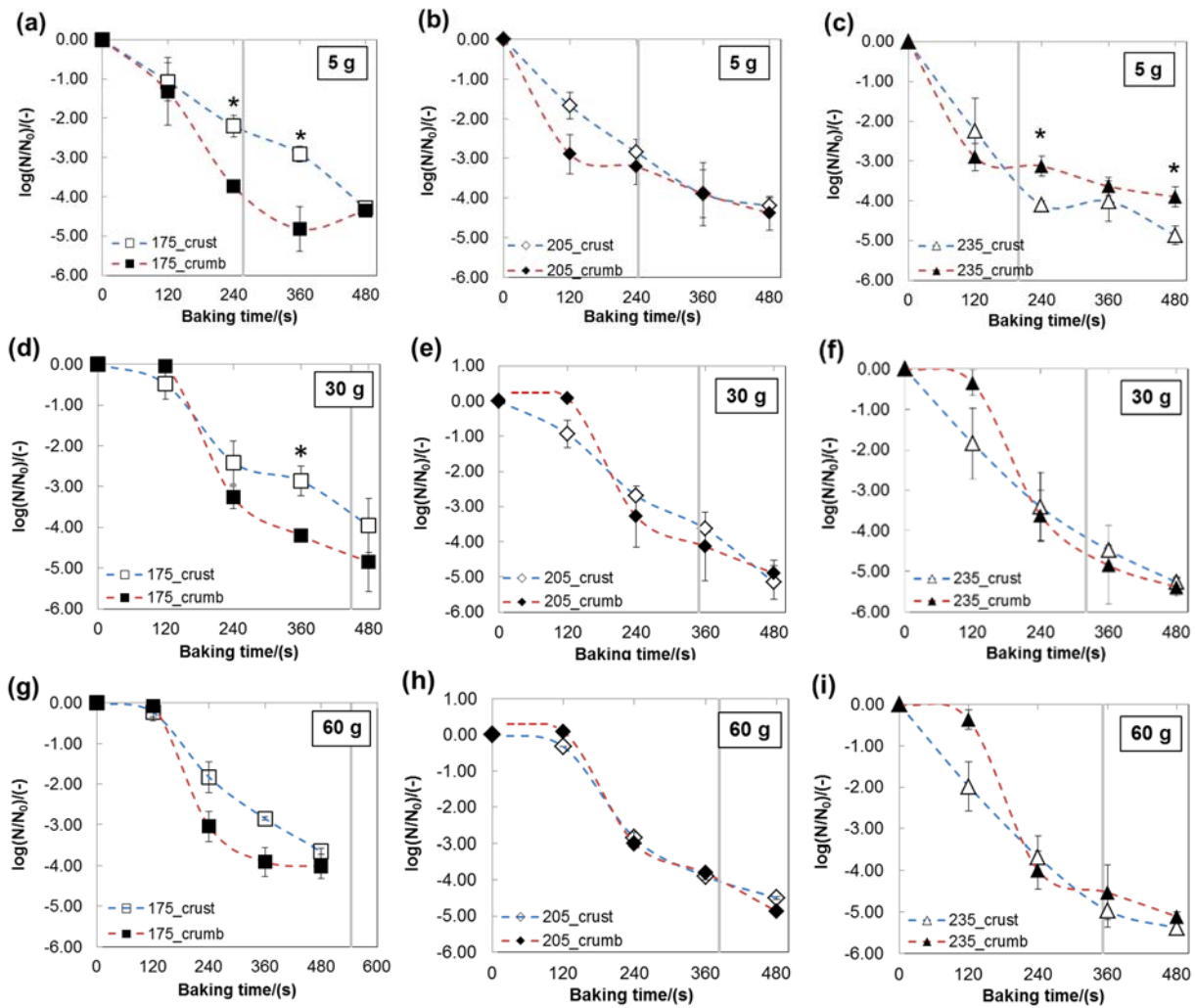


Figure 4-3. Semi-logarithmic survival curves of *L. plantarum* in the crust and crumb of bread samples with different initial weights and baked at different temperatures: (a)~(c), 5 g, (d)~(f), 30 g, (g)~(i), 60 g; 175 °C (\square crust, \blacksquare crumb); 200 °C (\diamond crust, \blacklozenge crumb); 235 °C (\triangle crust, \blacktriangle crumb). The asterisk (*) means the residual viability of *L. plantarum* in crust was significantly different ($p < 0.05$) from that in the crumb for the sample baking time. The grey line in each figure indicates the calculated minimum baking time for different baking conditions, and the dashed lines are drawn to guide the eye. Error bars indicate the standard deviation.

Thermal inactivation of probiotics is affected by both temperature and the moisture content in the environment (Lievens et al., 1992; Perdana et al., 2013). As mentioned before, the temperature and moisture content profiles of bread crust and crumb are not similar, therefore different survival behaviour of *L. plantarum* in the crust and crumb during baking may be expected. Interestingly, after 4-min baking, the residual viability of the bacteria in the crust was 1~2 log higher than that in the crumb of 5 g and 30 g bread baked at 175 °C ($p < 0.05$, Figures 4-

3a & d). However, this difference was not statistically significant for 60 g bread baked at 175 °C (Figure 4-3g). In addition, no significant differences ($p>0.05$) were observed in the survival curves of probiotics in crust and crumb of bread baked at 205 °C or 235 °C. These results indicate that the heat-tolerance of the bacteria might be higher in the crust due to its lower moisture content, although the temperature of the crust was much higher than that of the crumb during baking (Perdana et al., 2013). Two environmental factors, i.e. moisture content and temperature, had the opposite effects on the thermal inactivation kinetics of probiotic bacteria during bread baking. As a result, similar survival curves of *L. plantarum* in the crust and crumb were obtained (Figures 4-3b, 4-3e, 4-3f, 4-3h and 4-3i). Moreover, for 5 g bread baked at 235 °C, residual viability of *L. plantarum* in the crumb became higher than that in the crust after 4-min baking (Figure 4-3c). This may be explained by the detrimental effect of the higher temperature in the crust exceeding the positive effect of the lower moisture content on the retention of bacterial viability (Chen and Patel, 2008).

To further evaluate the effect of temperature and moisture content on the inactivation of bacteria, the residual viability of *L. plantarum* was plotted against the corresponding temperature and moisture content of the crust or crumb, respectively (Figure 4-4). Results indicated a near linear correlation between the survival rate of bacteria and the temperature reached in crust and crumb (Figure 4-4a), while a similar trend was found for the residual viability and moisture content of the crust (Figure 4-4b). The bacterial inactivation data in the crust “shifted” towards the right side of the chart from those data of the crumb (Figure 4-4a), which indicated that a higher temperature was needed to inactivate the same amount of bacteria in the crust than in the crumb during baking. This might be explained by the positive effect of the decreasing moisture content in the crust on the retention of bacteria viability, as the moisture content in the crumb remained the same (Figure 4-2) and the inactivation of bacteria was mainly induced by heat stress.

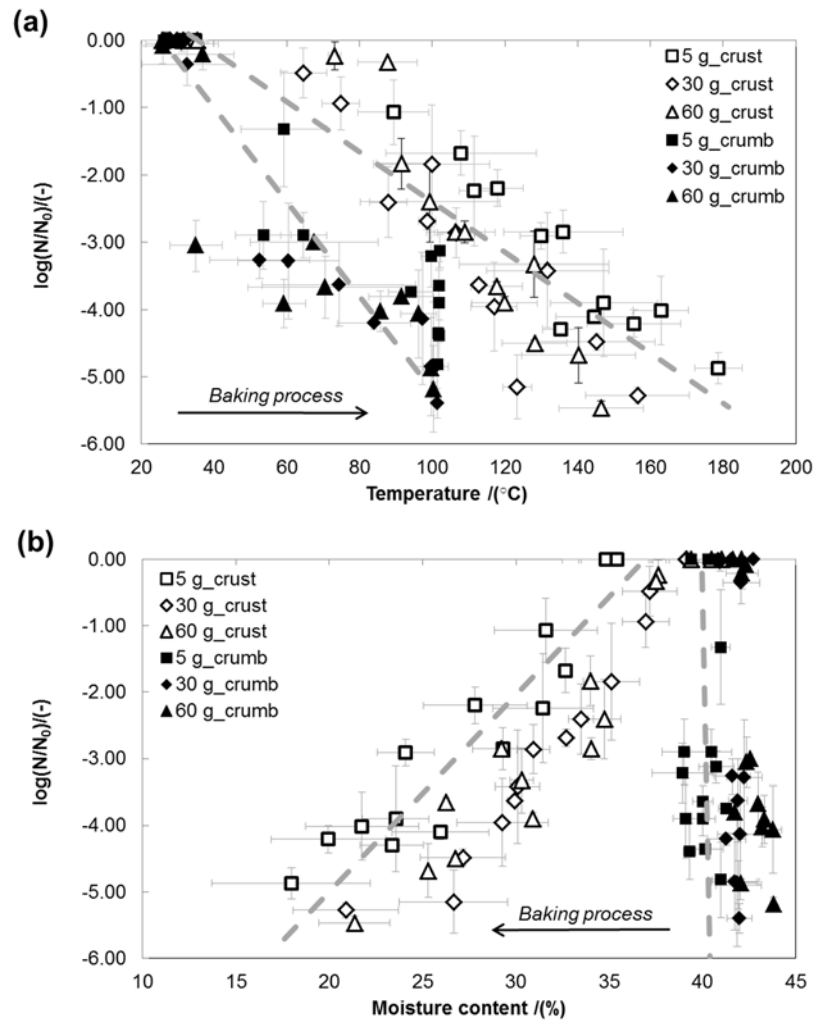


Figure 4-4. Residual viability of *L. plantarum* as a function of local moisture contents (a) or temperatures (b) in bread with different initial weights during baking: 5 g (\square crust, \blacksquare crumb), 30 g (\diamond crust, \blacklozenge crumb), and 60 g (\triangle crust, \blacktriangle crumb). Dashed lines are drawn to guide the eye. The arrow in each figure indicates the temperature increased in the crust and crumb during baking, while the moisture content of the crust gradually decreased. Error bars indicate the standard deviation.

4.3.4 Microstructure of bread crust and crumb

Figure 4-5 shows the microstructure of bread samples (30 g, 175 $^{\circ}\text{C}$, 8 min) with and without addition of *L. plantarum*. The microstructure of the crust was smoother and denser (Figures 4-5a & b), while the crumb showed a more porous microstructure (Figures 4-5c & d). Bacteria cells of *L. plantarum* were embedded in the glassy crust matrix (Figure 4-5b) while the cells were relatively freely distributed in the crumb (Figure 4-5d).

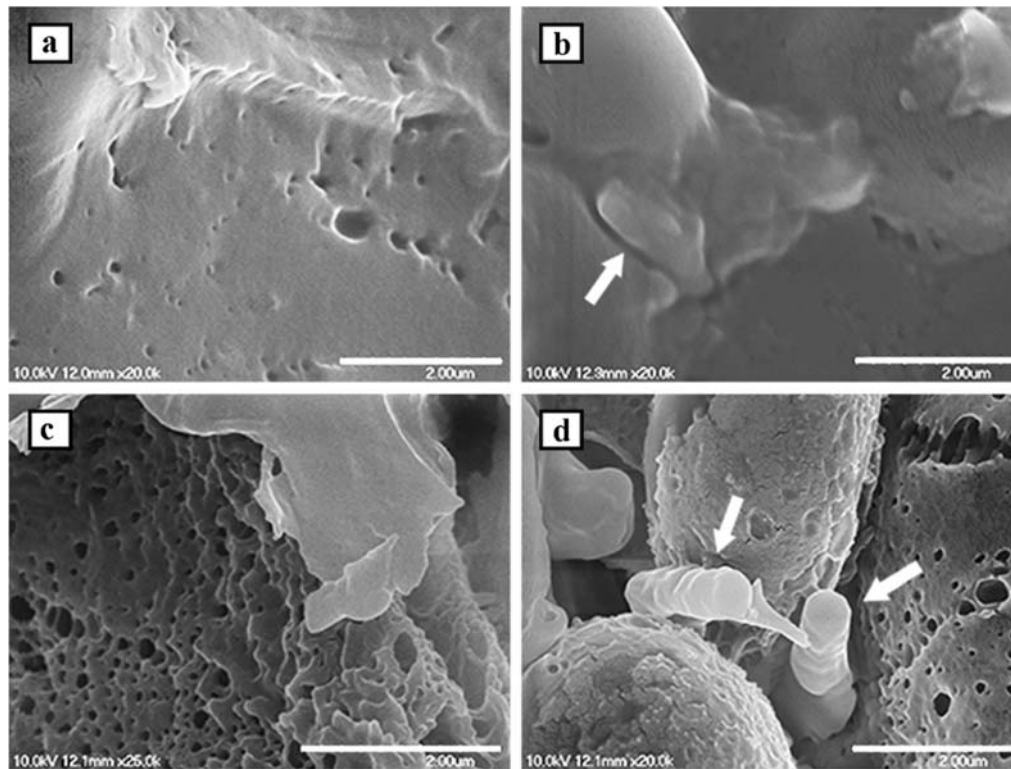


Figure 4-5. Microstructure of the control bread (a: crust; c: crumb) and bread supplemented with *L. plantarum* (b: crust; d: crumb) monitored by SEM, and bacteria cells in the bread matrix are pointed out with white arrows: scale bar represents 2.00 µm.

The entrapment of bacteria in the dense crust microstructure may provide a protective effect under heat treatment for *L. plantarum* by providing a drier extracellular environment and by reducing the molecular mobility (Hansen and Riemann, 1963; Morgan et al., 2006). This might also explain the higher survival of probiotics in the crust at a baking temperature of 175 °C. However, future research should further elucidate underlying mechanisms related to inactivation of bacteria during baking. This inactivation mechanism is expected to be affected by the temperature, moisture content and microstructure of the bread matrix.

4.3.5 Effect of storage on *L. plantarum* viability

In this study, the effect of storage on viability of *L. plantarum* was investigated using 30 g bread baked at 175 °C for 8 min. Re-growth of probiotic bacteria in the bread was observed during 5-day storage under well-controlled condition (Table 4-1). The bread matrix appears to be a suitable environment for probiotic bacteria to grow because nutrients for bacteria are abundantly present (Katina et al., 2005). Though, it is noted that the increase in viable counts during the first 2 days was not significant ($p>0.05$). This lag phase suggests that surviving cells after baking require time to recover from cellular damage and need to adapt to the new

environment (Corcoran et al., 2004; Huang et al., 2014). After this initial period, the viable counts of *L. plantarum* increased from 10^5 CFU/g to 10^8 CFU/g in the crust, and from 10^4 CFU/g to 10^6 CFU/g in the crumb, and stayed at the same level till day 5. After 4-day storage, the viability of *L. plantarum* achieved the recommended level (10^6 CFU/g) for probiotic foods (Mitropoulou et al., 2013). Therefore, to re-grow the probiotic bacteria inside the bread during storage could be one appropriate strategy to increase the viable counts of probiotics in the product before consumption.

Moreover, after 5-day storage the viable counts of *L. plantarum* in the crumb were about 2-log lower than that in the crust ($p < 0.05$, Table 4-1). This may be because the residual viability of bacteria in the crumb of the fresh baked bread was already 1-log lower than in the crust, indicating a smaller cell population of *L. plantarum* in the crumb at the beginning of the storage period. A lower population level of bacteria led to a longer recovery period (lag phase), which can result in lower viable counts in the end (Pérez-Rodríguez and Valero, 2013a). In addition, the moisture content of the crust increased while that of the crumb decreased during storage (Table 4-1). Water migrates from the core of the bread towards the surface during storage, until an equilibrium between crust, crumb and the environment is reached (Primo-Martín et al., 2006). This water migration can be expected favourable for the bacteria to re-grow in the dry crust (Soukoulis et al., 2014). Furthermore, *L. plantarum* is a facultative anaerobic organism, therefore the availability of oxygen in the crust may lead to a more efficient metabolism, and hence better re-growth.

As shown in Table 4-1, the pH of the bread crumb with addition of *L. plantarum* decreased while the total titrable acid (TTA) increased during storage due to acid formation by the heterofermentative *L. plantarum* (Vernocchi et al., 2004). Although these variations were not statistically significant ($p > 0.05$) during storage, the pH and TTA for bread samples with *L. plantarum* supplementation were significantly different from those of the control group with a pH remained at around 6.00, TTA around 2.33 mL. The decreased pH and increased TTA indicate the bread became “sour” during storage. Although sourdough bread is common in many regions, organoleptic properties of the probiotic-fortified bread should be evaluated in future research.

Table 4-1. Viable cell counts of *L. plantarum* and moisture content in the crust and crumb of dough, freshly baked bread and bread during storage (initial weight 30 g, baked at 175 °C for 8 min), and variation of pH and total titratable acidity (TTA) of dough and bread crumb during storage *.

Samples	Viability of LP /(log CFU/g)		Moisture content (% kg/kg)				pH	TTA
	crust	crumb	p<0.05	crust	crumb	p<0.05		
dough	9.12±0.14 ^a	9.12±0.14 ^a	-	40.33±0.48 ^a	40.33±0.48 ^a	-	4.79±0.05 ^a	7.38±0.11 ^a
baked	5.07±0.39 ^b	3.82±0.20 ^b	+	29.64±2.98 ^b	41.69±1.01 ^a	+	5.19±0.25 ^a	4.88±0.11 ^b
1-day	5.34±0.76 ^b	2.97±0.97 ^b	-	32.10±0.61 ^b	40.25±0.55 ^a	+	5.03±0.11 ^a	5.28±0.39 ^b
2-day	5.85±0.76 ^{bc}	4.06±0.58 ^b	-	32.73±1.25 ^b	39.31±0.63 ^{ab}	+	5.22±0.28 ^a	4.55±0.49 ^b
3-day	7.33±0.29 ^c	4.51±0.59 ^{bc}	+	33.73±1.23 ^b	39.23±0.64 ^{ab}	+	5.13±0.29 ^a	4.50±0.71 ^b
4-day	8.04±0.21 ^c	5.64±0.31 ^c	+	33.88±1.74 ^c	37.56±1.97 ^b	-	5.04±0.22 ^a	4.95±0.78 ^b
5-day	8.03±0.22 ^c	5.94±0.42 ^c	+	34.62±0.72 ^c	38.36±0.76 ^b	-	4.88±0.13 ^a	5.85±0.92 ^b

* values (mean ± SD) in the same column marked with different superscripts (a, b or c) are significantly different from each other ($p<0.05$), and the positive sign (+) indicates the difference in bacterial viability or moisture content between crust and crumb are significant ($p<0.05$), while the negative sign (-) indicates no significant difference.

4.4 Conclusions

The baking process significantly decreased the viability of *L. plantarum* to 10^{4-5} CFU/g in bread. Different bread sizes had little influence on the semi-logarithmic survival curves of probiotics during 8-min baking, however, higher residual viability can be obtained if the baking time is shortened. The bacteria in the bread crust were found more thermo-stable than those in the crumb in spite of the higher temperature in the crust during baking under certain conditions. The lower moisture content and the dense and glassy microstructure of the crust may have a positive effect on the thermo-stability of bacteria in the crust during baking. After 4-day storage, the population of probiotic bacteria recovered to an amount higher than 10^6 CFU/g in the crumb and 10^8 CFU/g in the crust, which was corresponding to the changing pH and TTA of bread during storage.

This study provided valuable experimental data of the inactivation of probiotic bacteria during bread baking. In future work, mathematical models could be established based on these experimental results, to describe the effect of physicochemical properties of the bread matrix on the inactivation kinetics of bacteria during baking. Future research should also focus on strategies to retain high viability of probiotics after baking which could involve encapsulation or optimization of processing parameters, etc.

Chapter 5

Kinetic study of the thermal inactivation of *Lactobacillus plantarum* during bread baking



This chapter has been published as:

Zhang, L., Schutyser, M.A.I., Boom, R.M., Chen, X.D. (2018). Kinetic study of the thermal inactivation of *Lactobacillus plantarum* during bread baking. *Drying Technology* (in press).

Link: <https://doi.org/10.1080/07373937.2018.1495647>

Abstract

Live probiotics can be supplemented to bread as functional ingredients. The viability of probiotics in bread needs to be sufficient to exert a beneficial effect on human health. To maximize the viability, a kinetic study on the inactivation of probiotics during baking was carried out. The thermal inactivation of *Lactobacillus plantarum* P8 during bread baking was evaluated with rate-dependent kinetic models. The influences of temperature, moisture content, drying rate and temperature variation rate on the inactivation kinetics were studied explicitly. A kinetic model $k_d = k_o \left(1 + a \left|\frac{dT}{dt}\right|\right) \exp\left(bX - \frac{E_d}{RT}\right)$, which included temperature (T), moisture content (X) and temperature variation rate (dT/dt) as variables, was found to best describe the concave and sigmoidal survival curves of probiotics in bread crust and in crumb during baking, respectively. The drying rate (dX/dt) was of little influence on the kinetics. The application of the proposed model is limited to baking processes, but could be used to maximize the survival of probiotics in bread products.

5.1 Introduction

Predictive microbiology describes the response of microorganisms to external conditions via mathematical modelling (McMeekin et al., 2008; Writing, 1995). In particular, predictive models are of interest to describe inactivation kinetics of microorganisms during thermal processing of foods. It is important to address sufficient inactivation of foodborne pathogens or maximum survival of living probiotics ingredients during thermal processing (Fu and Chen, 2011; Peleg and Cole, 1998).

Probiotics may be applied to produce functional bakery products (Majeed et al., 2016). However, inactivation of the probiotics during baking significantly affects the bacterial viability in the bakery products such as bread (Altamirano-Fortoul et al., 2012; Seyedain-Ardabili et al., 2016; Soukoulis et al., 2014; Zhang et al., 2014). Baking of bread is a dynamic process, during which the temperature and moisture content of the bread matrix change continuously (Zhang and Datta, 2006). In a previous experimental study, we found that the thermal inactivation of probiotic bacteria in the bread crust and crumb is affected by the distinct temperature-moisture content histories in these two domains within the bread during baking (Zhang et al., 2018). However, the underlying mechanism is not well-understood. We can deepen the understanding of the inactivation mechanisms of probiotics during baking via kinetic modelling.

Kinetic models can increase in complexity according to the following three different levels: i) a kinetic model that simply describes the inactivation percentage as function of time (e.g. by first-order kinetics); ii) a kinetic model that includes the effect of an environmental factor (e.g. temperature, pH or moisture content) towards stability of the microorganism (e.g., Arrhenius-type); and iii) a kinetic model that includes the two previous levels to predict the microbial responses to the changing conditions, e.g. the temperature or moisture gradient during processing (Isabelle and André, 2006; Pérez-Rodríguez and Valero, 2013b). Traditionally, kinetic models that have complexity up to level 2 are derived from isothermal experiments in model systems (Chen and Patel, 2007). Predictions of such kinetic models are often not in full agreement with inactivation data collected from dynamic processes. This is because rapid changing conditions during dynamic processes can dramatically alter the inactivation mechanism, and thus potentially lead to a disagreement between the experimental inactivation data and the predictions (Pérez-Rodríguez and Valero, 2013b).

Table 5-1 provides an overview of several studies that involved the kinetic modelling of inactivation of microorganisms during drying, a process that may be considered similar to

baking to certain extent. Main external factors considered in these studies are the temperature and the moisture content (or water activity) (Fu et al., 2013; Ghandi et al., 2012; Lievense et al., 1992; Valdramidis et al., 2006; Valero et al., 2014). Interestingly, only few studies incorporated the influence of the drying rate and/or the change in temperature to predict the inactivation kinetics of microorganisms (Bayrock and Ingledew, 1997; Foerst and Kulozik, 2012; Ghandi et al., 2012; Huang et al., 2009; Li et al., 2006; Marechal et al., 1999; Perdana et al., 2013). To the best of our knowledge, no previous work exists in the literature that deals with modelling of the influences of temperature, moisture content and their changes in time on inactivation kinetics of probiotics in the typical temperature range of baking processes. This is, however, of particular interest when the baking conditions need to be optimized to maximize viability of probiotics in final bread products.

Therefore, this study aims at providing a deeper understanding of the inactivation mechanism of probiotics during bread baking through kinetic modelling. We evaluated the feasibility of rate-dependent kinetic models to describe the inactivation of *Lactobacillus plantarum* P8 during bread baking as a function of several external factors (i.e., temperature, moisture content, drying rate and temperature variation rate). The model parameters are optimized using inactivation data of bacteria derived from real baking experiments of bread instead of from model systems, to increase the accuracy of model predictions. The obtained parameters are subsequently validated against inactivation data of bacteria in bread crust or crumb during baking generated from independent baking experiments.

Table 5-1. List of some studies on kinetic modelling of the inactivation of micro-organisms during dynamic drying processes.

Micro-organism strain	Medium	Drying condition	Kinetic model *	Variables	Reference
<i>Lactobacillus plantarum</i>	starch	fluidized-bed drying (T_{inlet} 30, 50, 60 °C)	$\ln(k_d) = \left[\left(a_1 - \frac{a_2}{RT} \right) X + \left(b_1 - \frac{b_2}{RT} \right) \right] + [1 - \exp(pX^q)] \left[\left(a'_1 - \frac{a'_2}{RT} \right) X + \left(b'_1 - \frac{b'_2}{RT} \right) \right]$	T, X	(Lieveuse et al., 1992)
<i>Escherichia coli</i> B200	n.a.	non-isothermic conditions (T 52.05~63.10 °C, pH 3~9, a_w 0.928~0.995)	$\ln(k) = C_0 + C_1/T + C_2pH + C_3pH^2 + C_4a_w^2$	T, pH, a_w	(Cerf et al., 1996)
<i>Bifidobacterium infantis</i> Bb1, <i>Streptococcus thermophilus</i> St10	milk droplet (10 wt % solids content)	flat-flow air drying (70, 90, 110 °C)	rate-dependent secondary model $k_d = k_o(1 + a \left \frac{dX}{dt} \right + b \left \frac{dX}{dt} \right ^2) \exp(-\frac{E_d}{RT})$	$T, dX/dt$	(Li et al., 2006)
<i>Listeria monocytogenes</i> Scott A	macerated potato	surface dry heating (90, 100 °C)	sigmoidal-like primary inactivation model Bigelow type secondary inactivation model	T, a_w	(Valdramidis et al., 2006)
<i>Saccharomyces cerevisiae</i> ATCC 2601	0.39 wt % yeast/water suspension	infrared drying (60, 70, 90 °C)	rate-dependent secondary model $k_d = k_o(1 + a \left \frac{dX}{dt} \right)(1 + b \left \frac{dT}{dt} \right) \exp(-\frac{E_d}{RT})$	$T, dT/dt, dX/dt$	(Huang et al., 2009)

<i>Lactobacillus paracasei</i> ssp. <i>paracasei</i> F19	water	vacuum drying	$k_d(a_w, T) = k_1 \exp(m \cdot T) + k_2 \cdot \exp\left(\frac{E_a}{RT} - 0.5 \left(\frac{a_w - a_{w0}}{b}\right)^2\right)$	T, a_w	(Foerst and Kulozik, 2012)
<i>Lactococcus lactis</i> ssp. <i>cremoris</i> ASCC930119	water droplet	convective air drying (45~95 °C)	$k_d = k_{d,ref} \left[1 - \frac{E_a}{R} \left(\frac{1}{T} - \frac{1}{T_{ref}} \right) \right]$	T	(Ghandi et al., 2012)
<i>Lactococcus lactis</i> ssp. <i>cremoris</i>	reconstituted skim milk (10 wt%, 20 wt% solids content)	convective air drying (70, 90, 110 °C)	$k_d = k_0 \exp\left(-\frac{E_d}{RT}\right)$	T	(Fu et al., 2013)
<i>Lactobacillus plantarum</i> WCFS1	20 % w/w maltodextrin DE 6	flat-flow air drying (50, 60, 70 °C)	A modified Weibull model $\ln\left(\frac{N(t)}{N_0}\right) = -\left(\frac{t}{\alpha}\right)^\beta, \alpha = f(T, X), \beta = 1$	T, X	(Perdana et al., 2013)
<i>Salmonella enterica</i> serovar Enteritidis	potato omelette	microwave (300, 450, 600, and 800 W)	Weibull model $\log\left(\frac{N(t)}{N_0}\right) = -b \cdot t^n, b = b(T), n = n(T)$	T	(Valero et al., 2014)

* primary level model was first-order reaction model except mentioned, and the meaning of each parameter is referred to the original publications.

5.2 Rate-dependent models

The inactivation of microbial cells by thermal processing is frequently described by first order kinetics (Eqns. 5-1 & 5-2):

$$\frac{d\left(\frac{N}{N_0}\right)}{dt} = -k_d \left(\frac{N}{N_0}\right) \quad (5-1)$$

or in an integrated form over a small discrete time interval Δt :

$$\log\left(\frac{N_{i+1}}{N_i}\right) = -\frac{1}{2.303} \cdot \bar{k}_d \cdot \Delta t \quad (5-2)$$

where N is the viable cell counts (CFU/mL, CFU: colony forming unit) at time t (s), N_0 is the initial viable cell counts (CFU/mL), and k_d is the inactivation rate constant (s^{-1}).

Generally, the rate of the thermal inactivation of bacteria increases with increasing temperature and decreases with reduced moisture content of the material (Chen and Patel, 2008; Lievense et al., 1992). However, the effect of the drying rate on the survival of microorganisms during drying processes remains unclear. Different studies report that a high drying rate has a positive, negative or no influence on the survival of microorganisms during drying (Foerst and Kulozik, 2012; Kuts and Tutova, 1983; Lievense et al., 1992; Perdana et al., 2013).

In previous studies, drying and temperature-rate dependent models were successfully applied to describe the survival data of different microorganisms (*Bifidobacterium infantis* Bb1, *Streptococcus thermophilus* St10, and *Saccharomyces cerevisiae* ATCC 2601) during drying (Huang et al., 2009; Li et al., 2006). An extensive theoretical appraisal of rate-dependent models can be found in the paper by Chen and Patel (2007).

In previously described rate-dependent models, the inactivation rate constant k_d is made dependent on the temperature (T), moisture content (X), drying rate (dX/dt), and the change of temperature in time (dT/dt). The latter two variables may be considered as “dehydration stress” and “thermal stress” experienced by the microorganisms during the process, respectively. The effect of these variables is described by the modification of the classical Arrhenius equation. However, different variations may be proposed for the rate-dependent correlations (Table 5-2

& Table 5-A1). In these models, k_o is a pre-exponential factor (s^{-1}), E_d is the activation energy ($J \cdot mol^{-1}$), and R is the ideal gas constant ($8.314 J \cdot mol^{-1} \cdot K^{-1}$).

The performance of different kinetic models in describing survival can be evaluated in different ways, for example with the parameters mean square error (MSE, Eqn. 5-3) and the corrected Akaike information criterion (AIC_c , Eqn. 5-4) (van Boekel and Zwietering, 2007). The advantage of the AIC_c is that both the number of parameters of the model and the goodness of fit are included in this parameter (Pérez-Rodríguez and Valero, 2013a).

$$MSE = \frac{\sum \left[\log \left(\frac{N}{N_0} \right)_{exp} - \log \left(\frac{N}{N_0} \right)_{model} \right]^2}{n - p} \quad (5-3)$$

and

$$AIC_c = n \ln \left(\frac{RSS}{n} \right) + 2(p + 1) + \frac{2(p + 1)(p + 2)}{n - p - 2} \quad (5-4)$$

where n is the number of observations, p is the number of optimized parameters, and RSS is the residual sum of squares. To compare multiple models, the models with smaller MSE and AIC_c values are preferred.

5.3 Materials and methods

5.3.1 Experimental inactivation data

Experimental inactivation data used in this study were derived from our previous study on the thermal inactivation of *Lactobacillus plantarum* P8 (ATCC 14917, Inner Mongolia Agricultural University) in bread during baking at different conditions. Detailed description of the experimental procedures can be found in Zhang et al. (2018). In brief, *Lactobacillus plantarum* P8 was cultured and supplemented to bread. Bread samples with varying dough weight (5, 30, and 60 g) were baked at different temperatures (175, 205, and 235 °C) for 8 min, and the residual viability of bacteria was determined every 2 min. The temperature and moisture content profiles of the bread crust and crumb were recorded. The corresponding diameter of the maximum cross sectional area of the bread was 2 cm, 6 cm and 8 cm for 5 g, 30 g and 60 g dough, respectively.

5.3.2 Generation of a new dataset for model validation

To validate the rate-dependent model, new experimental datasets were generated in this study. Bread samples with an initial weight of 0.1 g were prepared, for which the experimental procedures are described in the next sections.

5.3.3 Bacterial culture

A single colony of *L. plantarum* was inoculated in 10 mL sterile MRS broth (OXOID, United Kingdom) from a MRS agar plate stored at 4 °C. After 12-h incubation at 37 °C, 1 % v/v inoculum of *L. plantarum* was sub-cultured in 100 mL MRS broth for 24 h. Subsequently, the cell pellets were harvested by centrifugation (8000 g, 4 °C, 15 min) (Thermo Fisher Scientific, USA) and were re-suspended in UHT skim milk.

5.3.4 Bread baking experiment

Bread samples supplemented with *L. plantarum* were prepared according to Zhang et al. (2018). Miniature bread dough (0.1 g) with *L. plantarum* was baked at 145, 175 and 205 °C for 5 min in an electric oven (Changdi®, China). Type-K thermocouples (Omega®, USA) were used to monitor the temperature change inside the mini-bread with a sampling interval of 10 seconds. Only the average temperature and the average moisture content were measured because of the small dimensions (0.1 g) of the bread samples (the diameter of the dough ball was 0.5 cm). The moisture content of the mini-bread was determined every 1 min: the moisture content of the sample (kg/kg) was calculated by weighing the sample before and after drying at 105 °C in an oven for 24 h.

5.3.5 Microbiological analysis

The residual viabilities of *L. plantarum* in 0.1 g bread were determined every 1 min during baking. Briefly, the 0.1 g bread was crushed into pieces and transferred into a 2 mL centrifuge tube. Subsequently, 0.90 mL peptone water (0.1 % w/v, Solarbio®, China) was added and the suspension was vigorously homogenised using a vortex mixer (IKA®, Germany). Serial dilutions of the obtained suspension were made in peptone water and plated following the surface technique onto MRS agar (OXOID, United Kingdom) supplemented with natamycin (200 ppm, Antai®, China) (Zhang et al., 2014). The plates were incubated at 37 °C for 48 h. The residual bacterial viability was recorded as $\log(N/N_0)$, with N the viable count value after baking,

CFU/g, and N_0 the initial viable count, CFU/g. The initial viable count was $8.8 \pm 0.1 \log$ CFU/g for the 5 g, 30 g and 60 g dough, and $9.9 \pm 0.5 \log$ CFU/g for the 0.1 g dough.

5.3.6 Modeling procedures

The parameters of the models were estimated based on the data set for the 30 g bread, and the models with the best fit were subsequently validated against the data for 0.1 g, 5 g and 60 g bread. The survival data of the bacteria in the crust of 30 g breads during baking at each temperature were plotted against baking time (8 min) on semi-logarithmic coordinates. To improve the accuracy of the parameter estimation, the inactivation data $\log(N/N_0)$ in 30 g breads were first correlated with the baking time (Huang et al., 2009; Li et al., 2006) (Eqn. 5-5). This procedure enabled us to generate a more comprehensive set of experimental inactivation data (48 points in total) for each survival curve (Figure 5-1).

$$\log\left(\frac{N}{N_0}\right) = \frac{1}{2.303}(-Kt^m) \quad (5-5)$$

where K (s^{-m}) and m were two empirical parameters of this exponential equation. The values of K were 0.02, 0.07 and 0.15 for baking temperatures of 175, 205 and 235 °C, respectively, while the corresponding values of m were 1.00, 0.82 and 0.71, with a coefficient of determination (R^2) above 0.98.

More data were generated on the moisture content history during baking (Figure 5-A1), according to the Page's model (Eqn. 5-6) which is used to simulate the drying curves of food materials (Simal et al., 2005).

$$\frac{W - W_e}{W_0 - W_e} = \exp(-kt^n) \quad (5-6)$$

where W , W_e , W_0 are the average, equilibrium and initial moisture contents (kg/kg), respectively, and k and n empirical constants (s^{-n} and dimensionless). Therefore, absolute values of dX/dt were calculated using the data generated by the Page's model. Figure 5-A1 shows the variables (T , X , $\left|\frac{dT}{dt}\right|$ and $\left|\frac{dX}{dt}\right|$) of the rate-dependent kinetic models, which were plotted against the baking time for every interval of 10 seconds. The moisture removal rates were non-zero for 5 g, 30 g,

and 60 g bread at the end of baking, which indicates that the equilibrium moisture content was not achieved.

Subsequently, the unknown coefficients in the inactivation kinetic models were estimated using the non-linear least square minimization method solved using the add-in solver in Excel 2010 (Microsoft®, USA) based on the data set of 30 g bread. The coefficient of determination (R^2) was calculated using the RSQ function in Excel 2010 (Microsoft®, USA). The goodness of fitting was evaluated by comparing the MSE and AIC_c of each model (Eqns. 5-3 & 5-4) as mentioned before. The best-fit model was used to predict the survival data of *L. plantarum* in 0.1 g, 5 g and 60 g bread during baking, in combination with the drying kinetics for each baking condition.

5.3.7 Statistical analysis

All experiments were conducted at least in duplicate and results were presented as mean \pm standard deviations. The residual viability of bacteria during baking at different temperatures was analysed by two-factor analysis of variance (ANOVA) with replication with a significance level of $p < 0.05$. The ANOVA analysis was performed using Excel 2010 (Microsoft®, USA).

5.4 Results and discussion

5.4.1 Development of a rate-dependent model to describe survival in the crust

In this study, we investigate the influence of the drying rate and/or temperature variation rate on the inactivation of probiotic bacteria during baking, in addition to other factors (i.e., temperature and moisture content). However, the moisture content in the bread crumb stayed almost constant throughout baking (i.e., $dX/dt=0$) (Zhang et al., 2014), which makes it unrealistic to evaluate the influence of the drying rate in the crumb on the bacterial inactivation kinetics in the crumb. Therefore, it is more rational to evaluate first the rate-dependent models using the inactivation data of bacteria in the bread crust, where the temperature and moisture content changed dynamically during baking, as well as the drying rate and temperature variation rate. In section 5.4.4 the two most promising developed rate-dependent models on the basis of crust data were evaluated for prediction of inactivation in the crumb as well.

Figure 5-1 shows the residual viability of *L. plantarum* in the crust of 30 g bread against the baking time on semi-logarithmic coordinates. The dependency of the inactivation data of *L.*

plantarum on the baking temperature (175, 205 and 235 °C) was significant ($p < 0.01$). The survival curves were slightly concave especially for the baking temperature of 235 °C.

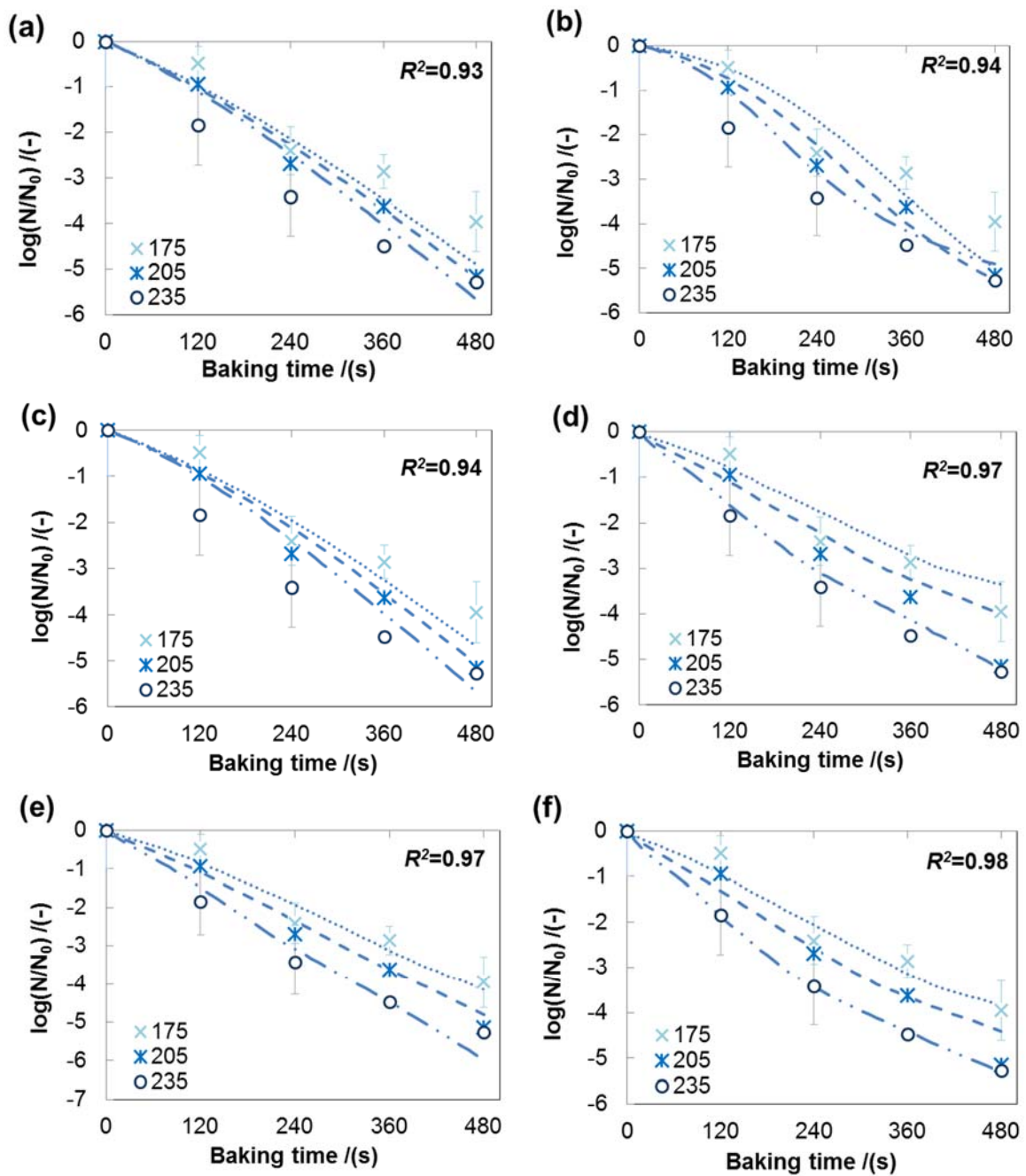


Figure 5-1. Experimental and simulated inactivation data of *L. plantarum* in the crust of 30 g bread during baking at different temperatures (experimental data: \times , 175 °C; $*$, 205 °C, \circ , 235 °C; simulated data:, 175 °C; - - -, 205 °C; - . . -, 235 °C), Simulated survival curves fitted with different rate-dependent models: (a)~(f) for model No. 1~6 in Table 5-2 (R^2 , square of correlation coefficient). Error bars indicate the standard deviation of the experimental data.

First, the classical Arrhenius model (model No.1, Table 5-2) was evaluated to describe the experimental inactivation data, which just considered the temperature-dependence of the inactivation rate. The fit is unsatisfactory: a large discrepancy remains between the measured residual viability and the predictions (Figure 5-1a). The estimated activation energy (E_d) for the Arrhenius model is low (Table 5-3), which implies that the influence of temperature on the inactivation process is relatively small (model No.1, Table 5-2), which explains the overlap of the different survival curves in Figure 5-1a.

Subsequently, the moisture content (X) was incorporated in the next kinetic model (model No.2, Table 5-2) (Meerdink and van't Riet, 1994): the moisture content of the food matrix has a profound effect on the thermal inactivation rate of bacteria when the moisture content changes strongly, e.g. during drying (Fu and Chen, 2011). Visually, the fitting results slightly improved (Figure 5-1b), even though the mean square error (MSE, Table 5-3) in fact increased somewhat.

Table 5-2. Rate-dependent models tested in this study to describe the inactivation rate constant k_d of *Lactobacillus plantarum* P8 inactivation during bread baking

Model No.	Expression	Variables
1	$k_d = k_o \exp(-\frac{E_d}{RT})$	T
2	$k_d = k_o \exp(aX - \frac{E_d + bX}{RT})$	T, X
3	$k_d = k_o(1 + a \left \frac{dX}{dt} \right + b \left \frac{dX}{dt} \right ^2) \exp(-\frac{E_d}{RT})$	$T, dX/dt$
4	$k_d = k_o(1 + a \left \frac{dX}{dt} \right)(1 + b \left \frac{dT}{dt} \right) \exp(-\frac{E_d}{RT})$	$T, dT/dt, dX/dt$
5	$k_d = k_o(1 + a \left \frac{dT}{dt} \right) \exp(-\frac{E_d}{RT})$	$T, dT/dt$
6	$k_d = k_o(1 + a \left \frac{dT}{dt} \right) \exp(bX - \frac{E_d}{RT})$	$T, X, dT/dt$

Then, two rate-dependent models (models No. 3 & 4, Table 5-2) were used to describe the inactivation kinetics, which include the effect of the dynamics of the process on the inactivation as shown in Table 5-1 (Huang et al., 2009; Li et al., 2006). Model No. 3 includes the drying rate or moisture removal rate (dX/dt) (Kuts and Tutova, 1983). The model No. 3 describes the inactivation of bacteria during drying of milk droplets reasonably well (Li et al., 2006), but it fails to describe the bacterial inactivation in our case (Figure 5-1c): its fit was even worse than the Arrhenius equation (larger values of MSE and AIC_c, Table 5-3).

The fit was dramatically improved by incorporating the changing rate of temperature (dT/dt) into the rate-dependent model No. 4 (Figure 5-1d & Table 5-3). A similar effect was observed in a study on infrared drying of yeast, where incorporation of both dX/dt and dT/dt also resulted in the best fit model (Huang et al., 2009). However, this was not seen in the study of single droplet drying (Li et al., 2006). This indicates that the temperature variation rate (dT/dt) may have different degrees of impact on the inactivation kinetics during different drying methods (i.e., convective drying, infrared drying, baking). There is no apparent delay in the temperature increase inside the matrix during bread baking (crust) and during infrared drying of yeast (Figure 5-A1), whereas the temperature inside the single droplet remains almost constant for some time in the beginning of the drying process (i.e., $dT/dt \approx 0$). This may influence the inactivation of the bacteria during different drying processes.

It is worth noting that the value of coefficient a in model No. 4 was small (Table 5-3), suggesting that the drying rate (dX/dt) may have little influence on the inactivation rate k_d . Therefore, we evaluated model No. 5 (see Table 5-2) in which the term dX/dt was eliminated from the pre-exponential factor. As shown in Figure 5-1e, this simplified model describes the inactivation kinetics of *L. plantarum* in the crust during baking reasonably well; the corresponding MSE and AIC_c values were even smaller than those of model No. 4. However, model No. 5 was not able to predict the noticeable convexity of the inactivation curve at a baking temperature of 235 °C.

Table 5-3. Optimal parameters of the rate-dependent models based on the inactivation data of *Lactobacillus plantarum* P8 in the crust of 30 g bread.

Model No.	k_0 (s ⁻¹)	E_d (J·mol ⁻¹)	a	b	MSE	AIC _c
1	0.186	6.085×10 ³	–	–	0.262	-188
2	27.731	5.271×10 ⁴	31.550	9.979	0.303	-165
3	0.345	8.048×10 ³	0	99.400	0.287	-171
4	0.175	1.087×10 ⁴	0.863	16.873	0.131	-286
5	0.469	1.087×10 ⁴	4.365	–	0.084	-351
6	0.110	1.392×10 ⁴	12.788	5.309	0.029	-504

Finally, a new variety of the rate-dependent model was developed by introducing the variable moisture content (X) into the exponential term (model No. 6, Table 5-2), similar as for model No. 2. This new expression requires the temperature (T), the moisture content (X) and the temperature change rate (dT/dt) as input variables. The calculated inactivation curves were in good agreement with the experimental data (Figure 5-1f), while the MSE and AIC_c were the

smallest among all evaluated models (Table 5-3). The estimated activation energy (E_d) was smaller ($13.92 \text{ kJ}\cdot\text{mol}^{-1}$) than that found in other studies (Foerst and Kulozik, 2012; Fu et al., 2013; Ghandi et al., 2012; Huang et al., 2009; Li et al., 2006), which is probably due to the different food matrices used during drying (Aryani et al., 2016).

In addition to the six models discussed, other expressions of the rate-dependent models were evaluated (see Table 5-A1), but no significant improvement was found in terms of the goodness of fit (results not shown). Therefore, we do not elaborate on those expressions.

5.4.2 Validation of the rate-dependent model

Models No. 4 & 6 in Table 5-2 provided the best fit to the experimental data, by comparing the values of MSE and AIC_c (Table 5-3) and by judging their visual fit (i.e., the convexity of the simulated survival curves, Figure 5-1). Therefore, these two rate-dependent kinetic models were validated against newly-generated experimental results. Specifically, the temperature and moisture content profiles as well as the viability of *L. plantarum* were determined during 5-min baking of 0.1 g bread at 145 °C and 175 °C, and during 8-min baking of 5 g or 60 g bread at 175 °C, 205 °C and 235 °C, respectively.

The temperature-moisture trajectories in the crust of the 5 g and 60 g breads showed a similar trend as for the 30 g samples (see Appendix 5-A, Figures 5-A1a, A1c, A1d), which we interpreted in detail in our previous paper (Zhang et al., 2018). In contrast, the core temperature of the 0.1 g sample increased rapidly to a plateau of 100 °C (i.e., $dT/dt \approx 0$) after baking for 120 s at 145 °C and after 60 s at 175 °C, respectively. This plateau is explained by the evaporation-condensation mechanism, which keeps the temperature at a constant value within the dough (Purlis and Salvadori, 2009a). The temperature increased again after baking for 180 s at 175 °C, indicating internal transfer limitation or even depletion of moisture (Zhang et al., 2016). The change of moisture content (X) in 0.1 g samples was precisely described by the Page's model (Eqn. 5-6), and the drying rate (dX/dt) clearly increased with increasing baking temperature during the first 180 seconds of baking (Figure 5-A1b).

The bacterial viability of *L. plantarum* in the crust decreased substantially from the initial viable counts of 9 to 10 log CFU/g down to 5 to 6 log CFU/g for all breads. The survival curves of *L. plantarum* in the crust of 5 g and 60 g breads exhibited a similar trend as for the 30 g bread (Figures 5-2b & c), whereas a noticeable 'tail' was observed for the 0.1 g samples (Figure 5-2a). The survival curves of *L. plantarum* in the 0.1 g, 5 g and 60 g samples during baking were

predicted using the rate-dependent models (models No. 4 & 6), by using the parameters derived from the 30 g dataset (Table 5-3) and the measured temperature (T), moisture content (X), drying rate (dX/dt) and temperature variation rate (dT/dt) as input variables (Figure 5-A1).

Generally, the rate-dependent models predicted the survival curves of bacteria in 0.1 g and 60 g bread samples reasonably well, especially the “long tail” for 0.1 g samples (Figures 5-2 & 5-3). However, the inactivation of *L. plantarum* in the crust of 5 g breads was overestimated by the kinetic models (Figures 5-2b & 5-3b), which could be caused by the high heating rate (dT/dt , Figure 5-A1c) in this group of breads. A smaller discrepancy between the predicted and observed data was found when model No. 6 was used (Figures 5-2d & 5-3d).

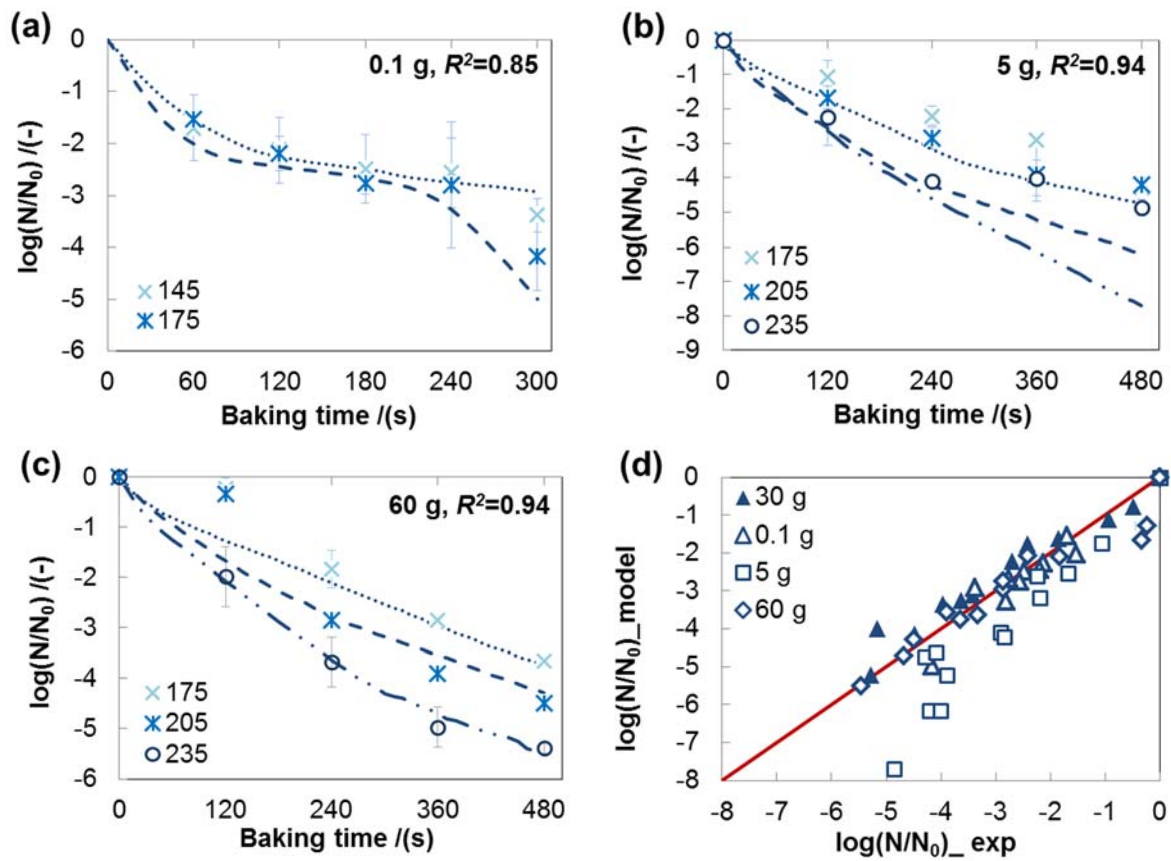


Figure 5-2. Validation of the rate-dependent model No. 4 in Table 5-2 using different inactivation datasets (a: 0.1 g; b: 5 g; c: 60 g) and a parity plot of the experimental and the simulated values of the residual viability of *L. plantarum* in the crust during baking (d: \blacktriangle 30 g, \triangle 0.1 g, \square 5 g, \diamond 60 g). Lines represent predicted survival curves calculated using parameters derived from 30 g dataset; Error bars indicate the standard deviation of the experimental data, R^2 the square of correlation coefficient.

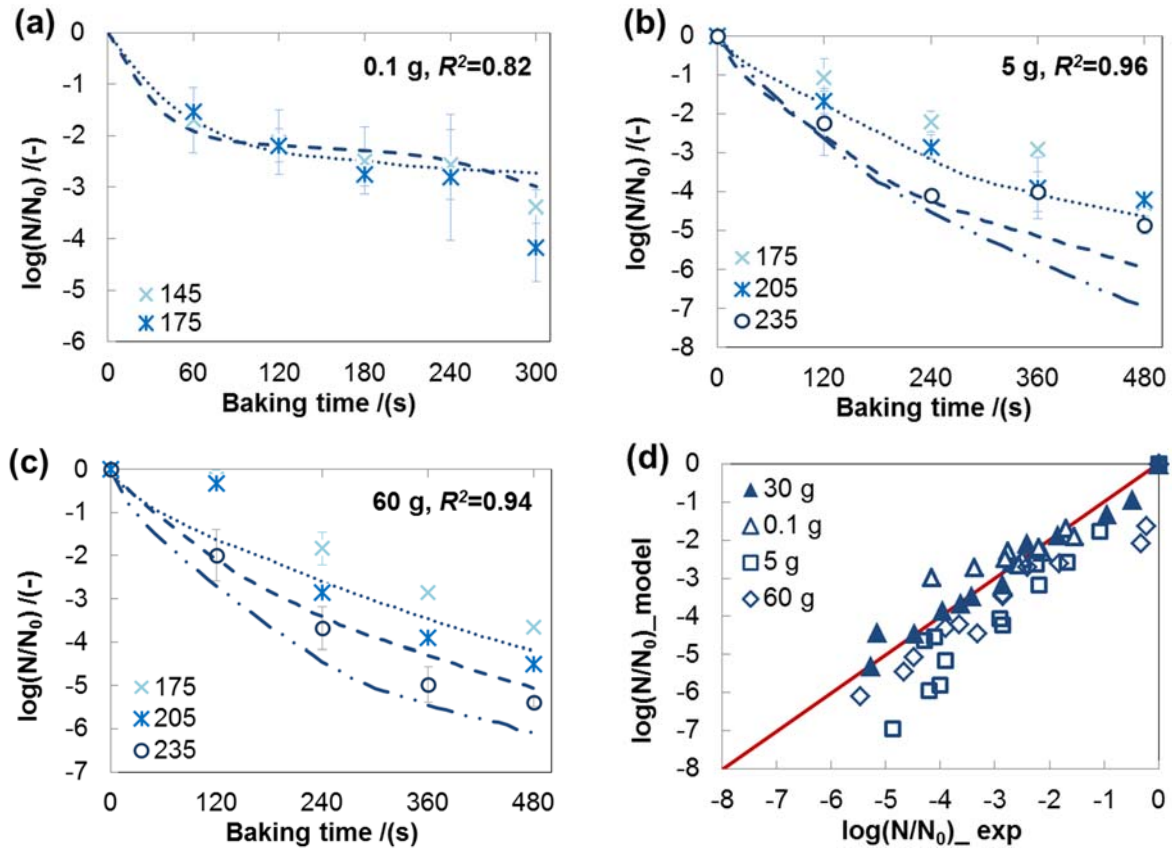


Figure 5-3. Validation of the rate-dependent model No. 6 in Table 5-2 using different inactivation datasets (a: 0.1 g; b: 5 g; c: 60 g) and a parity plot of the experimental and the simulated values of the residual viability of *L. plantarum* in the crust during baking (d: \blacktriangle 30 g, \triangle 0.1 g, \square 5 g, \diamond 60 g). Lines represent predicted survival curves calculated using parameters derived from 30 g dataset; Error bars indicate the standard deviation of the experimental data, R^2 the square of correlation coefficient.

5.4.3 Mechanistic interpretation of the rate-dependent model

The results discussed above suggest that the rate-dependent model No.6 best describes the inactivation kinetics of *L. plantarum* in bread crust during baking. In model No.6, the temperature variation rate (dT/dt), the reached moisture content (X) and the temperature (T) of the food matrix were identified as the main input variables to describe the bacterial inactivation during baking.

The exponential term of the rate-dependent model No. 6, i.e., $\exp\left(bX - \frac{E_d}{RT}\right)$ or $\exp(bX) \cdot \exp\left(-\frac{E_d}{RT}\right)$, may describe the opposite influence of increasing temperature (T) and decreasing moisture content (X) on the inactivation rate (Chen and Patel, 2008). Specifically, during baking,

the increasing temperature has a negative influence on the survival of bacteria (if $T \uparrow$, then $k_d \uparrow$), while the concurrently decreasing moisture content has a positive influence (if $X \downarrow$, then $k_d \downarrow$). The thermo-tolerance of bacteria is thus higher at low moisture contents than it is at high moisture contents (Ansari and Datta, 2003). In other words, the bacteria will be more heat-resistant once a lower moisture content is reached during drying (Perdana et al., 2013; Xing et al., 2014). This explains the slowing decrease in the residual viability of *L. plantarum* in 0.1 g bread (the ‘tailing effect’) in the later stages of baking when the moisture content becomes very low (Figures 5-2a & 5-A1b). The molecular mobility of the components in the matrix are expected to be lower at lower moisture content, and thus bacteria cells embedded in the glassy crust were better protected against thermal damage (Broeckx et al., 2016; Schutyser et al., 2012).

The pre-exponential term of the rate-dependent model $(1 + a \left| \frac{dT}{dt} \right|)$ describes the negative effect of the higher temperature variation rate on the heat resistance of bacteria (if $dT/dt \uparrow$, then $k_d \uparrow$). However, the term drying rate (dX/dt) is not present in model No. 6, which indicates that the inactivation induced by heat stress (dT/dt) is dominant over that of the stress due to dehydration. The latter may be significant during mild drying processes (Li et al., 2006; Perdana et al., 2013), but may be neglected when the dehydration takes place at much higher temperatures (i.e., the case of bread baking). This may be related to different inactivation mechanisms at different temperatures: dehydration inactivation is dominant at lower temperature ($< 45\text{ }^{\circ}\text{C}$), while thermal inactivation becomes more prominent at higher temperature (Fu and Chen, 2011). We conclude that the temperature variation rate must be considered as one of the prime extrinsic factors that influence the bacterial inactivation kinetics during severe thermal drying processes such as baking.

5.4.4 Prediction of the inactivation in bread crumb

During bread baking, the moisture content of the crumb was not affected ($X \approx 0.41$, $dX/dt \approx 0$) and the temperature in the crumb follows a sigmoidal pattern (Figure 5-A2) (Purlis and Salvadori, 2009a), which is distinct from the temperature profile and the moisture content history in the crust (Figure 5-A1). The inactivation data of *L. plantarum* in bread crumb were predicted using the rate-dependent models (models No. 4 & 6) with the same parameters in Table 5-3 found for the crust of 30 g bread (X was set to 0.41, dX/dt was set to 0).

As shown in Figure 5-4, the two rate-dependent models can predict the sigmoidal trend of the inactivation curves (with a ‘shoulder’ and a ‘tail’) of *L. plantarum* in the crumb during baking. The ‘shoulder’ is explained by the limited thermal inactivation in the initial stage of baking

because both the temperature and the changing-rate of temperature remained relatively low (Figure 5-A2). We attribute the ‘tail’ to the reasons mentioned before in section 5.4.3. Visual inspection shows the predicted trend of model No. 6 to be more realistic (Figures 5-4 d-f).

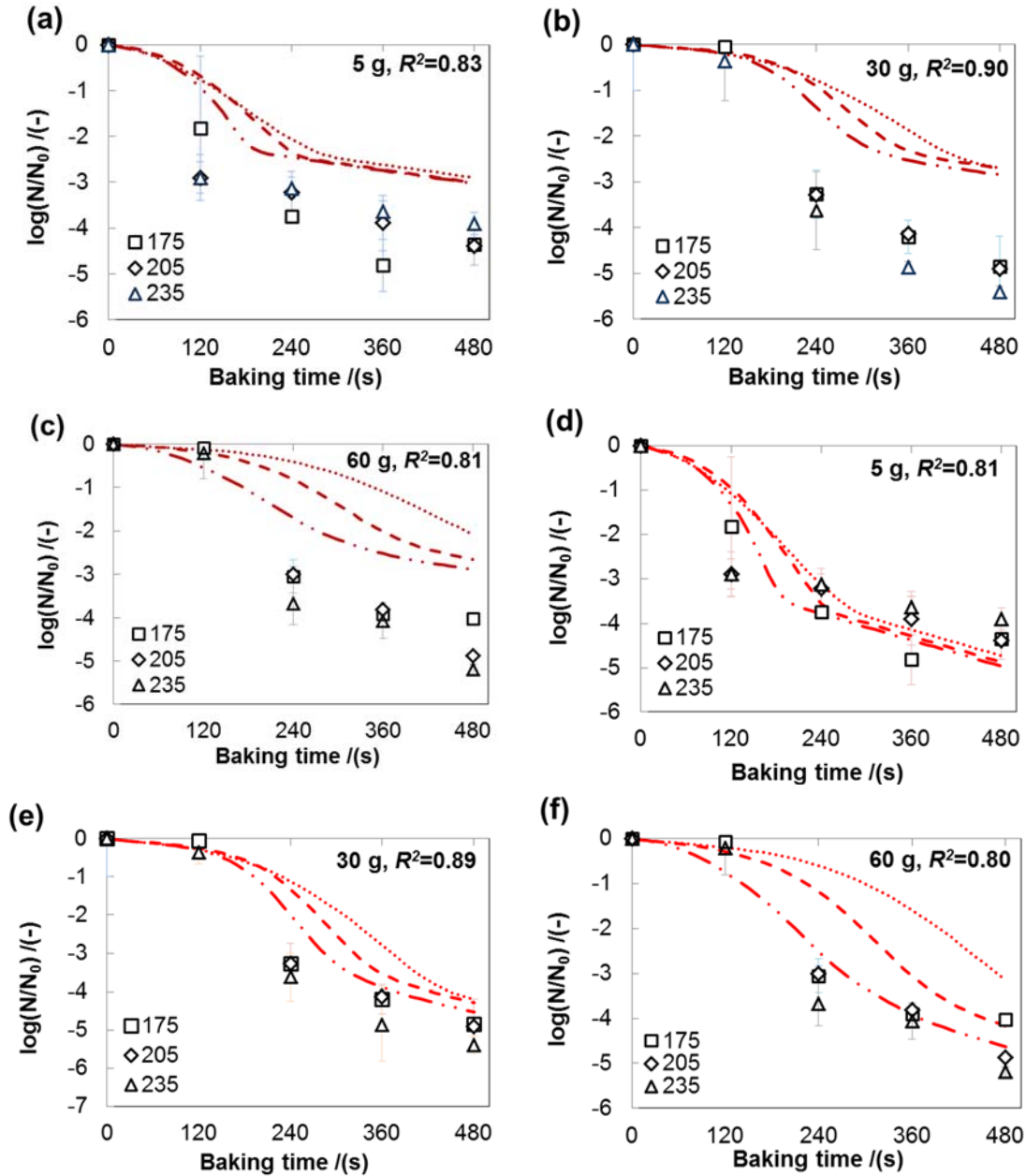


Figure 5-4. Experimental and simulated inactivation data of *L. plantarum* in the crumb of bread during baking at different temperatures (experimental data: \square , 175 °C; \diamond , 205 °C, Δ , 235 °C; simulated data:, 175 °C; - - -, 205 °C; - . . -, 235 °C), Simulated survival curves fitted with different rate-dependent models: (a)~(c) for model No. 4 and (d)~(f) for model No. 6 in Table 5-2 (R^2 , square of correlation coefficient). Error bars indicate the standard deviation of the experimental data.

The inactivation of *L. plantarum* in the crumb of 30 g and 60 g bread was systematically underestimated by the rate-dependent model (Figures 5-4e & f). This might have two reasons. First, the experimental inactivation curves of bacteria in crumb during baking at three temperatures were not significantly different (ANOVA, $p>0.05$) (Figure 5-4). Conversely, the temperature and its changing-rate in crumb of 30 g and 60 g bread were notably different at the three baking temperatures (Figures 5-A2b & A2c), which are two crucial variables (T and dT/dt) in the rate-dependent model (model No. 6) as the X was set to a constant. This may then in turn cause the inconsistency between the predicted and the observed inactivation data. We suggest that besides temperature and moisture content, also other environmental factors that are not included in this model (e.g., salt concentration, microstructure) and that are different in the crumb compared to the crust, may affect the inactivation of *L. plantarum* in the crumb (Peleg, 2006).

Second, the discrepancy could be caused by our assumption that the recorded temperature in the core zone of the bread is the average temperature of the crumb. In reality, the actual average temperature in the crumb (especially during the initial heating up phase) may well be higher than the value in the middle, due to a temperature gradient inside the bread matrix (Purlis and Salvadori, 2009a). Therefore, the accuracy of the prediction may be improved by considering the spatial temperature distribution inside the crumb.

5.4.5 Limitations to the application of the rate-dependent kinetic model

The parameters of the rate-dependent kinetic models were estimated from experimental baking data within a specific range of moisture contents (between 0.20~0.40) and temperatures (25~110°C). Therefore, application of the kinetic models to other processes than baking is not valid, especially if moisture contents or temperatures are outside the considered ranges. An alternative kinetic model development strategy could be to use experimental data from isothermal heating experiments with especially larger variations in moisture content. However, such a strategy may not provide a more accurate prediction of the inactivation during baking, because it is difficult to assess the influence of parameters other than temperature and moisture content (e.g. evolution of bread microstructure or certain stresses) on the inactivation kinetics in isothermal experiments.

5.5 Conclusions

The thermal inactivation of *L. plantarum* supplemented into bread before baking was investigated via kinetic modelling. The (semi-)empirical rate-dependent kinetic model proposed in this study describes the effects of the temperature (T), the temperature variation rate (dT/dt) and the moisture content (X) in the matrix on the survival rate of probiotics during baking. Reasonable agreement was found between the experimental and predicted inactivation data of *L. plantarum* in the crumb of 5 g bread and in the crust of other bread samples. A limitation of the presented rate-dependent kinetic model is that it is only applicable to describe survival during bread baking.

The predicted bacterial inactivation during thermal processing may be further improved by collecting more accurate data on the spatial distribution of temperature and water inside the food matrix and/or other factors that can affect the inactivation kinetics (e.g., salt concentration & microstructure). This will support development of more reliable kinetic models that describe inactivation of bacteria. In addition, optimization of the bread recipe and the baking conditions should contribute to further increase in the survival rate of probiotics after processing, without altering the organoleptic properties of the products. This leaves room for further study.

Nomenclatures

a	parameter of the rate-dependent model*	
a_w	water activity	(-)
b	parameter of the rate-dependent model or the Bigelow model	(K ⁻¹)
C	coefficient of surface response kinetic model	(-)
E_d	activation energy for deactivating cells	(J·mol ⁻¹)
k_0	a pre-exponential factor	(-)
k_d	rate constant of cell deactivation	(s ⁻¹)
K	empirical parameter of an exponential equation	(s ^{-m})
m	empirical parameter of an exponential equation	(-)
n	number of data points for non-linear regression	(-)
N	viable counts	(CFU/g)
p	moisture content dependency of parameter α for thermal	(-)
R	ideal gas constant	(8.314 J·mol ⁻¹ ·K ⁻¹)
R^2	square of the correlation coefficient	(-)
T	Temperature	(K)
t	Time	(s)
W	weight	(kg)
X	moisture content	(kg/kg)
dt	a short sampling time interval	(10 s)
dT/dt	changing rate of temperature	(K·s ⁻¹)
dX/dt	drying rate	(K·s ⁻¹)
α	scale parameter of Weibull distribution	(s)
β	shape parameter of Weibull distribution	(-)

Subscripts

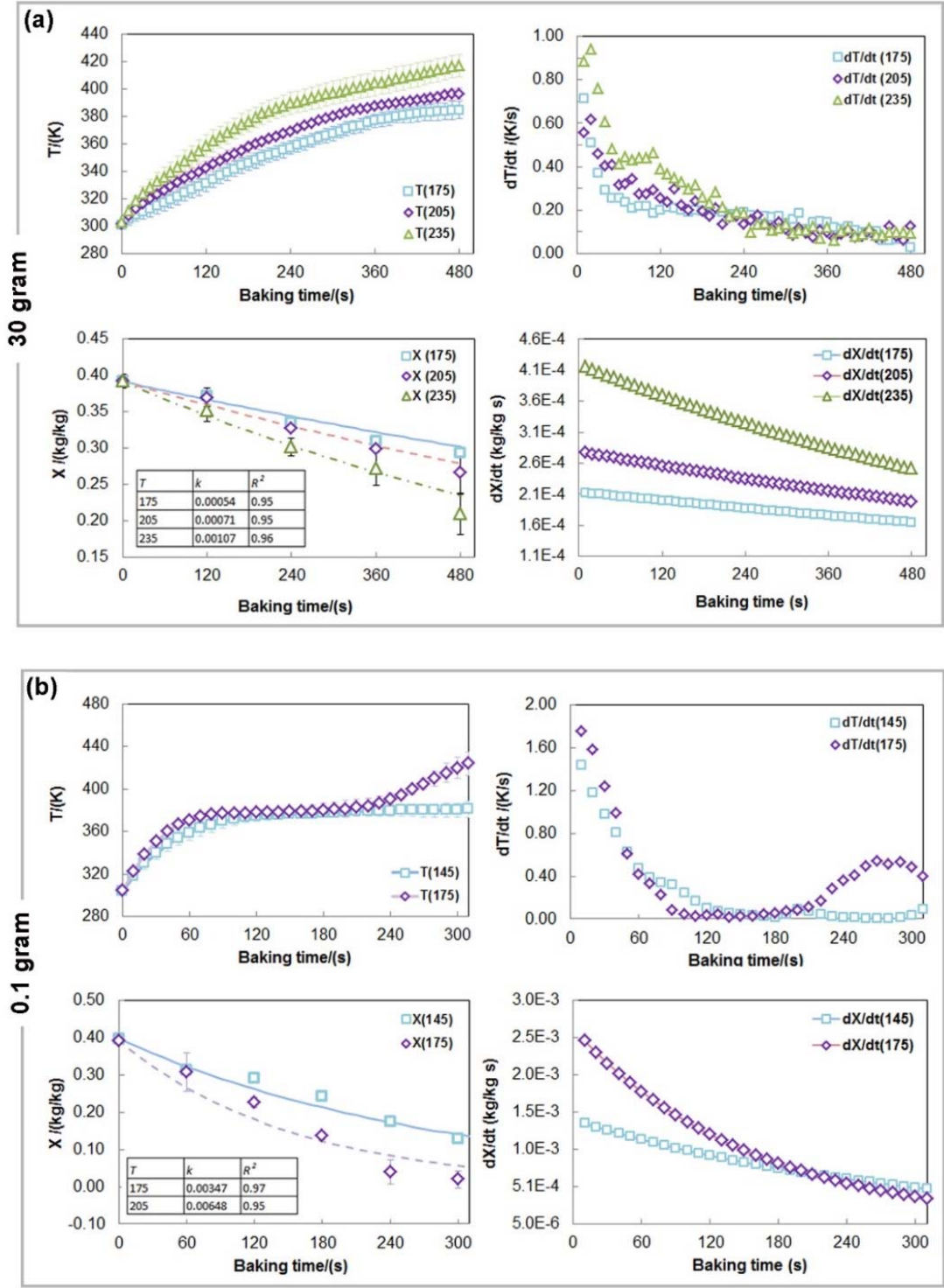
e	equilibrium
ref	reference
s	solid
w	water
0	initial
exp	experimental inactivation data
$model$	simulated inactivation data

Abbreviations

AIC_c	Akaike information criterion
MSE	mean square error
RSS	residual sum of squares

* The unit of a depends on the expression of the rate-dependent models (Table 5-2).

Appendix 5-A. Supplementary data



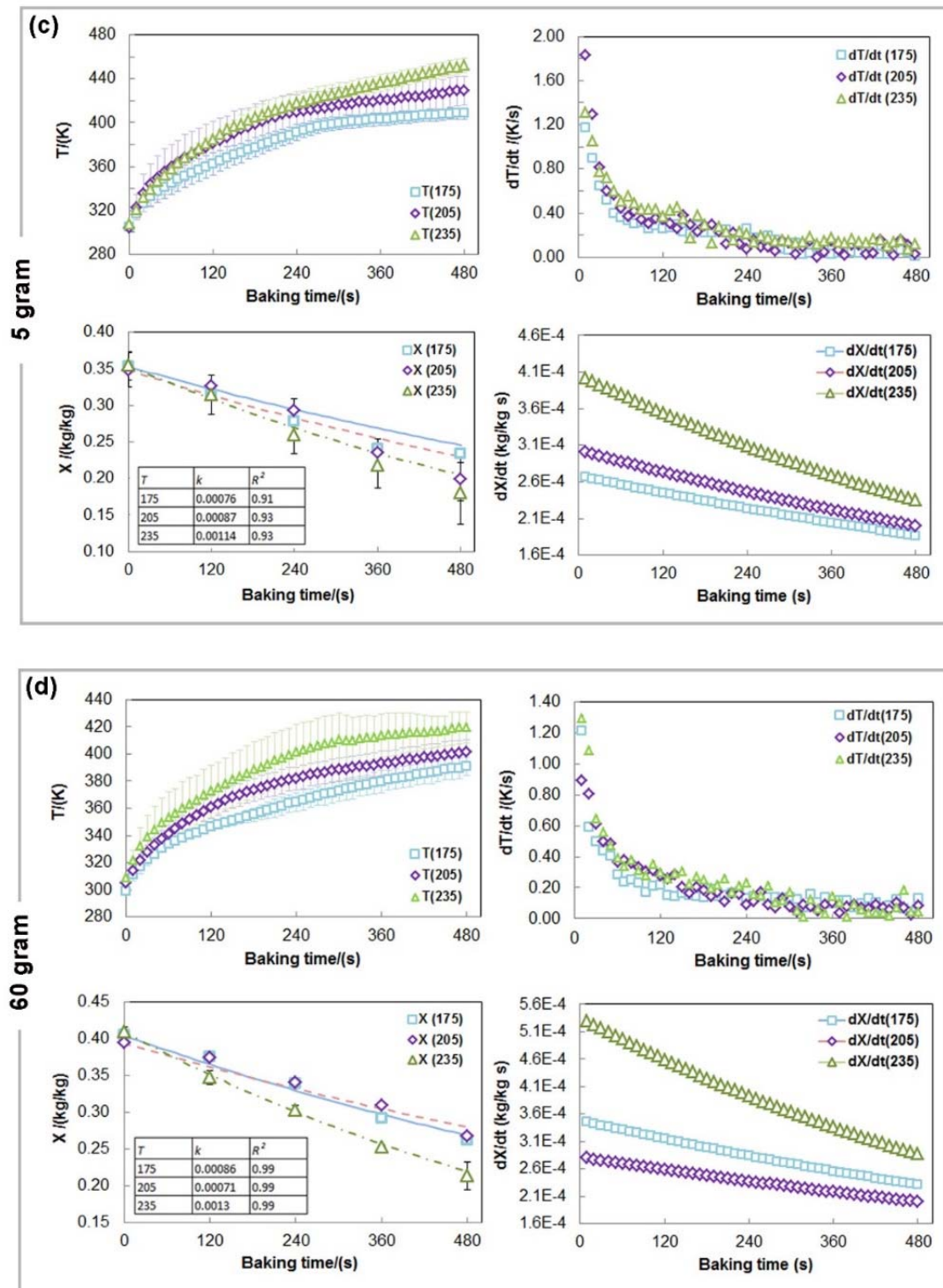


Figure 5-A1. Temperature (T) and moisture content (X) profiles, the changing rate of temperature (dT/dt) and drying rate (dX/dt) in the crust of bread samples with different initial weights during baking at different temperatures: (a) 30 g dough, \square 175 °C, \diamond 205 °C, Δ 235 °C; (b) 0.1 g dough, \square 145 °C, \diamond 175 °C; (c) 5 g dough, \square 175 °C, \diamond 205 °C, Δ 235 °C; (d) 60 g dough, \square 175 °C, \diamond 205 °C, Δ 235 °C. Straight and dotted lines represent the moisture content profiles fitted with the Page's model and parameters and the coefficient of determination (R^2) are listed in each corresponding subfigure; Error bars indicate the standard deviation.

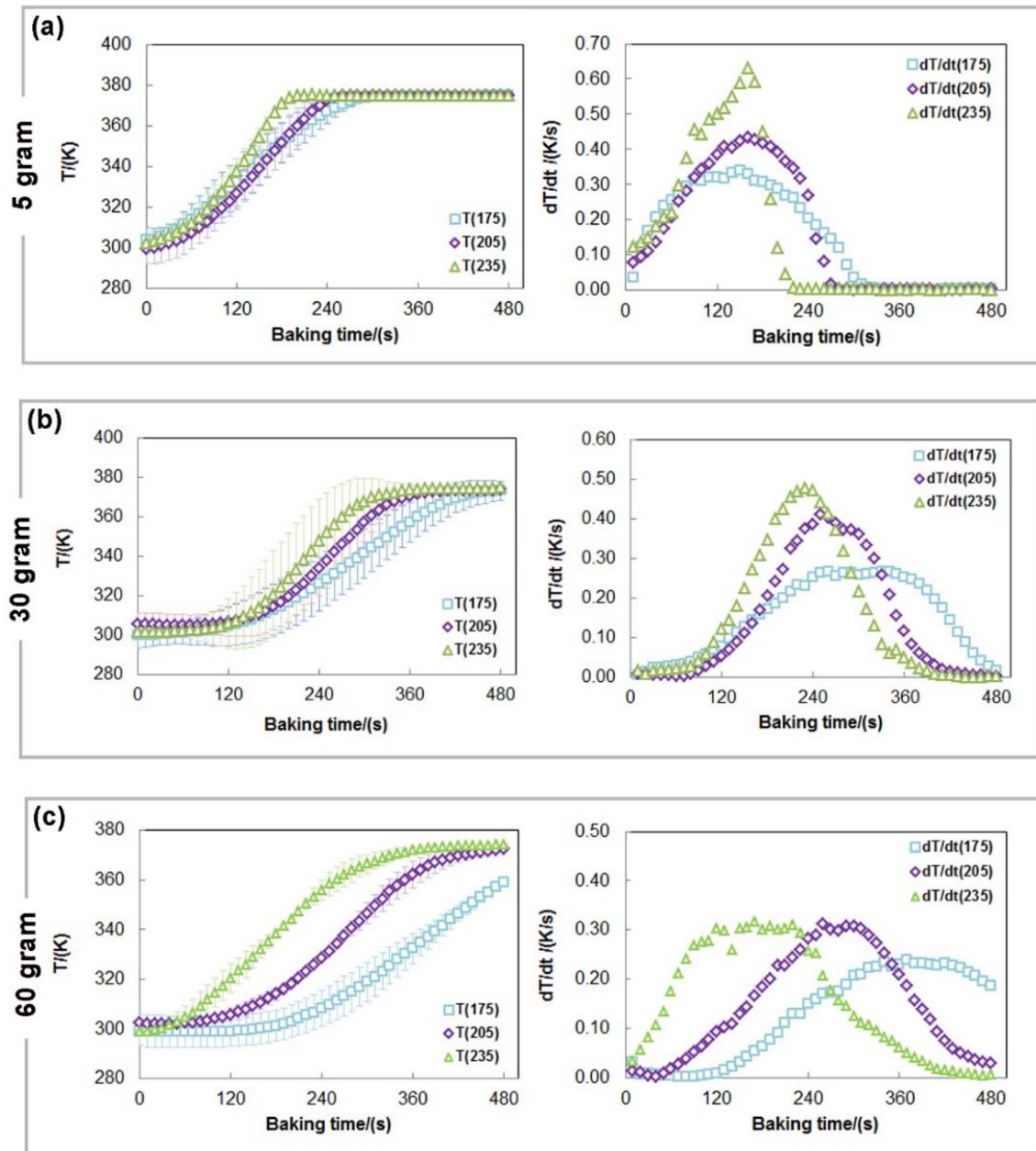


Figure 5-A2. Temperature (T) and the changing rate of temperature (dT/dt) in the crumb of bread samples with different initial weights (a: 5g, b: 30 g, c: 60 g) during baking at 175 °C (□), 205 °C (◇) and 235 °C (Δ); Error bars indicate the standard deviation.

Table 5-A1. Other possible expressions of the rate-dependent model to describe the inactivation rate constant k_d

Expression	Eqn. No.
$k_d = k_o \exp(aX - \frac{E_d + bT}{RT})$	(5-A1)
$k_d = k_o \exp(aT - \frac{E_d + bX}{RT})$	(5-A2)
$k_d = k_o(1 + a \left \frac{dX}{dt} \right) \exp(-\frac{E_d}{RT})$	(5-A3)
$k_d = k_o(1 + a \left \frac{dX}{dt} \right + b \left \frac{dX}{dt} \right ^2)(1 + c \left \frac{dT}{dt} \right + d \left \frac{dT}{dt} \right ^2) \exp(-\frac{E_d}{RT})$	(5-A4)
$k_d = k_o(1 + a \left \frac{dX}{dt} \right)(1 + b \left \frac{dT}{dt} \right) \exp(-\frac{E_d + cX}{RT})$	(5-A5)
$k_d = k_o(1 + a \left \frac{dX}{dt} \right)(1 + b \left \frac{dT}{dt} \right) \exp(cT - \frac{E_d + dX}{RT})$	(5-A6)
$k_d = k_o(1 + a \left \frac{dT}{dt} \right) \exp(bX - \frac{E_d + cT}{RT})$	(5-A7)
$k_d = k_o(1 + a \left \frac{dT}{dt} \right) \exp(bX - \frac{E_d + cX}{RT})$	(5-A8)
$k_d = k_o(1 + a \left \frac{dT}{dt} \right + b \left \frac{dT}{dt} \right ^2) \exp(cX - \frac{E_d}{RT})$	(5-A9)
$k_d = k_o(1 + a \left \frac{dT}{dt} \right) \exp(bX + cX^2 - \frac{E_d}{RT})$	(5-A10)
$k_d = k_o \exp(aX + bX^2 - \frac{E_d}{RT})$	(5-A11)
$k_d = k_o \exp(aX^2 + bT - \frac{E_d}{RT})$	(5-A12)

Chapter 6

Survival of encapsulated *Lactobacillus plantarum* during isothermal heating and bread baking



This chapter has been published as:

Zhang, L., Chen, X.D., Boom, R.M., Schutyser, M.A.I. (2018). Survival of encapsulated *Lactobacillus plantarum* during isothermal heating and bread baking. LWT - Food Science & Technology. 93, 396-404.

Link: <https://doi.org/10.1016/j.lwt.2018.03.067>

Abstract

The effect of encapsulation on the survival of *Lactobacillus plantarum* during isothermal heating and bread baking was investigated. Four encapsulating materials were evaluated, i.e., reconstituted skim milk (RSM), gum arabic (GA), maltodextrin (MD) and inulin. Freeze dried bacteria survived better in GA and RSM matrices during isothermal heating at 90 °C, which was explained by their high glass transition temperatures and physical entrapment of the bacterial cells in their dense microstructure. The survival of bacteria in bread during baking depended on the approach used to incorporate probiotics and physical properties of encapsulating materials, which was related to the exposure of the bacterial cells to moist-heat. Maximum survival of probiotic bacteria ($>10^8$ CFU/g bread) was achieved after 15 min baking at 100 °C when the RSM-probiotic powder was distributed on the dough surface. Furthermore, A Weibull model could describe the general trend of the inactivation kinetics of bacteria during isothermal heating (at 60, 75 and 90 °C) as influenced by the initial moisture content of the RSM-water mixtures (0.05, 0.60 and 0.90 kg/kg). Future development of bakery products with alive probiotic bacteria could benefit from this work.

6.1 Introduction

Foods fortified with probiotics are increasingly introduced into the market (De Prisco and Mauriello, 2016; Rivera-Espinoza and Gallardo-Navarro, 2010). Bakery products are an emerging category within the probiotic food segment and have attracted increasing research interest (Pinto et al., 2014; Reid et al., 2007; Soukoulis et al., 2014; Vitaglione et al., 2015; Zhang et al., 2014). To ensure that the addition of probiotic bacteria has the intended health benefit, a minimum number of living bacteria should be retained in the baked product at the time of consumption ($> 6\text{-}7 \log \text{CFU/g}$) (Tripathi and Giri, 2014). This is however a challenge for baked products due to the high temperatures employed during baking, which may lead to a significant loss of viable bacteria (Zhang et al., 2018). To facilitate the development of probiotic bakery products, it is important to study the survival of bacteria during the baking process.

A potential strategy to improve the survival of probiotic bacteria during baking is to encapsulate the bacterial cells in powder with protectants. Survival of probiotic bacteria in a solid matrix is influenced by the matrix composition when exposed to varying temperatures (Santivarangkna et al., 2011). Ideally, probiotic bacteria are embedded in a dry glassy matrix to secure maximum survival (Broeckx et al., 2016; Krasaekoopt, 2017). It is crucial that the moisture content of the system is kept low, because the glass transition temperature strongly decreases at increasing moisture content (Roos, 2010). Pitigraisorn, et al. (2017) encapsulated *Lactobacillus acidophilus* cells in alginate-based multi-layered microcapsules coated with an egg albumen-stearic acid composite. They found an increased survival of the encapsulated bacteria upon exposure to moist-heat (70°C , 100 %RH, 30 min), which was explained by the hydrophobic properties of the encapsulation matrix that limited moisture transfer into the capsules. However, the heating temperature used in that study was relatively low (70°C) compared to the actual temperature involved during baking. In another study, *Lactobacillus rhamnosus* R011 was entrapped in a whey protein gel, and the viability of the freeze dried cells were found higher during baking of biscuits (280°C , 5 min) due to the limited rehydration of the incorporated whey protein (Reid et al., 2007). Improved survival of living bacteria during thermal processing has thus been achieved by encapsulation (Corona-Hernandez et al., 2013). However, more quantitative insight is needed, especially to explore the possibilities of encapsulation in relation to improved survival of probiotics during bread baking.

Therefore, the aim of this study was to investigate the protective effect of encapsulating materials on the survival of dried probiotics subjected to isothermal heating and bread baking. A model probiotic strain (*Lactobacillus plantarum* P8) was freeze-dried in four different

matrices (reconstituted skim milk, gum arabic, maltodextrin and inulin) as protectants, respectively. The obtained powders were characterised on their physicochemical properties. Isothermal heating experiments with the dried powders were conducted to investigate the heat resistance of the bacteria as influenced by the encapsulation matrix and its initial moisture content. Subsequently, the probiotic powders were incorporated into bread using three different approaches and the survival of bacteria in bread after baking was evaluated.

6.2 Materials and methods

6.2.1 Bacterial culture

The probiotic strain of *Lactobacillus plantarum* P8 (ATCC-14917, hereafter termed LP) was provided by the Key Laboratory of the Education Ministry of China, Inner Mongolia Agricultural University. The bacteria were routinely cultured in MRS broth (OXOID®, United Kingdom). A single colony of LP was aseptically transferred from MRS agar plate to 10 mL sterile MRS broth, and pre-cultured at 37 °C for 12 h. Subsequently, 1 % v/v inoculum of LP was sub-cultured in 100 mL MRS broth at 37 °C for 24 h without agitation. The LP cell pellets were harvested by centrifugation (8000 g, 4 °C, 15 min), and were re-suspended in UHT skim milk or another solution as described in the next section.

6.2.2 Freeze drying of probiotic bacteria

The harvested LP cells were aseptically suspended in reconstituted skimmed milk (Devondale®, Australia), gum arabic from acacia tree (Sigma-Aldrich, Germany), maltodextrin (Dextrose Equivalent 13-17, Sigma-Aldrich, Germany), and inulin (Orafti GR®, Belgium) solutions with an initial solid content of 10 % w/w, respectively. Reconstituted skim milk (RSM) was sterilized in an autoclave at 105 °C for 15 min (Zealway GR60DR, USA), while gum arabic (GA), maltodextrin (MD) and inulin solutions were sterilized at 75 °C for 10 min (Yonekura et al., 2014). The LP cell suspensions in different solutions were transferred to sterile glass tubes and pre-frozen at - 20 °C for 12 h prior to the main vacuum-freeze-drying step in a freeze dryer (Sihuan Scientific Instruments Co., Ltd., China) for 50 h and the temperature was set at - 50 °C. Subsequently, the lyophilized matrices were fully grinded into fine powders in a mortar with a pestle. The powders were stored at 4 °C in sealed glass bottles in a desiccator.

6.2.3 Physicochemical analyses of the powders

Moisture content

To determine the moisture content of the freeze-dried powders (X_w , kg/kg), these were dried at 105 °C until a constant weight was reached. Subsequently, the moisture content was calculated as the weight of water removed during drying divided by the initial weight of the powder (AOAC, 2002).

Glass transition temperature

The glass transition temperature (T_g) of the freeze-dried powders was analysed by using differential scanning calorimetry (DSC, Mettler Toledo, USA) with a nitrogen-based cooling system (Behboudi-Jobbehdar et al., 2013). A portion of each powder (5-10 mg) was weighed in a stainless steel DSC pan and hermetically sealed. A sample was first scanned at the rate of 10 °C/min to 70 °C to erase the thermal history, and then cooled at 10 °C/min to 0 °C. A second scan was run up from 0 °C to 150 °C at a heating-rate of 10 °C/min. An empty pan was used as the reference. The onset and midpoint glass transition temperatures ($T_{g,onset}$ and $T_{g,mid}$) were analysed using Mettler Toledo Star (Columbus, OH, USA) software from the second heating scan thermographs.

Microstructure

Samples were fixed on an aluminium stub using a conducting carbon tape and coated with gold using a sputter to produce a conductive surface. Scanning electron microscopy (SEM) images were recorded using a Hitachi S4700 (Hitachi Ltd., Tokyo, Japan) to visualise the microstructure of the powders.

Hygroscopicity

The hygroscopicity of freeze-dried powders was determined according to a method modified from Fritzen-Freire et al. (2012). Samples of each powder were placed in aluminium weighing dishes, and stored at 75 % RH and 25 °C for 1 week. The hygroscopicity was expressed as grams of adsorbed water per 100 grams of dry solids (g/100 g).

6.2.4 Isothermal heat treatment

Isothermal heat treatment of powder (RSM, $X_w = 0.05$) or LP cell suspensions in RSM solutions ($X_w = 0.60$ & 0.90) was conducted using a Thermomixer (Eppendorf, Germany) at $60\text{ }^{\circ}\text{C}$, $75\text{ }^{\circ}\text{C}$ and $90\text{ }^{\circ}\text{C}$ for the designated time. For freeze-dried bacteria ($X_w = 0.05$), 0.100 ± 0.001 g sample was weighed and transferred into a 2 mL sterile centrifuge tube. To prepare cell suspension with a moisture content of 0.60, 150 μL sterile Milli-Q water was added to the centrifuge tube to dissolve 0.100 g powder by high-speed vortexing. To prepare suspension with a moisture content of 0.90, LP cells were harvested from 100 μL MRS broth by centrifugation (8000 g , $4\text{ }^{\circ}\text{C}$, 15 min) and then re-suspended into 100 μL 10 % w/w RSM. Samples in a 2 mL airtight centrifuge tubes were heated in the Thermomixer with a rotation speed of 300 rpm. The heating-up time was less than 60 s.

After heat treatment for the required time, the centrifuge tube was immediately transferred to an ice-water bath to avoid further inactivation of the bacteria. Subsequently, 900 μL cold peptone water (0.1 % w/w, $4\text{ }^{\circ}\text{C}$) was added to the sample (for $X_w = 0.60$, 1350 μL peptone water was added). All of the bacteria-suspended matrices were fully homogenized prior to making serial dilutions, and 100 μL diluted solution was spread onto MRS agar broth (OXOID, United Kingdom). The plates were statically incubated at $37\text{ }^{\circ}\text{C}$ for 48 h, and the survival curves of LP during heat treatment were obtained by plotting the $\log(N/N_0)$ versus the heating time, where N is the viable count (CFU/g) at time t and N_0 is the initial viable count (CFU/g). In addition, isothermal heat treatment of the other powders (i.e., GA, MD and inulin matrixes) at $90\text{ }^{\circ}\text{C}$ for 30 min were conducted using the same method described above.

6.2.5 Preparation of bread supplemented with *L. plantarum*

Bread dough was prepared in a mixer (Hauswirt[®] HM730, China), according to the following recipe: wheat flour (100 g), sugar (4 g), fine salt (1.5 g), instant yeast (1 g), non-salted butter (3 g), and UHT skimmed milk (65 g) (Zhang et al., 2018). Three approaches were applied to incorporate LP cells into bread: i) Cell suspension: LP cell suspension in UHT skimmed milk was directly utilized to prepare the dough (control group); ii) Dry powder: freeze-dried bacterial powder (1 g) was thoroughly mixed into the dough as the last item; iii) Powder distribution: 0.03 g powder was evenly distributed on the surface of a dough ball (5 g), which was done before proofing to ensure good adhesion of the powder to the dough. The dough was then divided into balls of 5 g for the first two approaches, and the dough balls were proofed at $40\text{ }^{\circ}\text{C}$, 85 % RH in a climate chamber (Yiheng, Shanghai, China) for 40 min. Subsequently, bread samples were

baked at 100 °C for 15 min and at 175 °C for 6 min in an electric oven (Changdi® CRTF30W, China), respectively. These temperature and baking time combinations were selected on the basis of 98 % estimated starch gelatinization as an indicator for proper baking (see Appendix 6-A, Figure 6-A1) (Zhang et al., 2018). Only the third approach was used to prepare bread with the GA, MD and inulin containing bacterial powders. Temperature profiles of the bread crust (surface) and crumb (core) during baking were recorded using K-type thermocouples (Omega®, USA). The moisture content of the bread after baking was determined according to the AOAC method 925.10 (AOAC, 2002).

6.2.6 Microbiological analysis

To determine the viable counts of LP in dough and baked bread, sample (5 g) was aseptically homogenized with 45 mL sterile peptone water (0.1 % w/w) in a stomacher (iMix®, Interlab, France). Serial dilutions of the suspensions (100 µL) were made in 900 µL sterile peptone water, and 100 µL solution was subsequently plated onto the MRS agar broth (OXOID®, United Kingdom) supplemented with 200 mg/L natamycin (Antai®, China). Natamycin was added to inhibit the growth of yeast on the MRS agar plate, which did not affect the growth of LP (Zhang et al., 2014). The plates were statically incubated at 37 °C for 48 h. After incubation, the viability of LP in bread was recorded as log CFU per gram of the sample (log CFU/g).

6.2.7 Weibull distribution model

The Weibull distribution function has been applied as a primary thermal inactivation model for vegetative bacteria (Pérez-Rodríguez & Valero, 2013; van Boekel, 2002). In this work, Weibull model is used to describe the survival of LP in RSM matrices with different initial moisture contents ($X_w = 0.05, 0.60$ and 0.90 , see section 6.2.4). Weibull model is a statistical model with an empirical nature, which describes the distribution of inactivation times. The cumulative function of Weibull model for a survival curve is:

$$\log S(t) = -\frac{1}{2.303} \left(\frac{t}{\alpha}\right)^\beta \quad (6-1)$$

$$S(t) = \frac{N(t)}{N_0} \quad (6-2)$$

where $S(t)$ is the survival rate of the bacteria after heat treatment for a certain time, α is the scale parameter that represents here the average death time of the microbial population, and β is the

dimensionless shape parameter (van Boekel, 2009). The scale parameter α can be described by the semi-empirical Bigelow model (Eqns. 6-3 to 6-5) (Perdana et al., 2013):

$$\alpha = \alpha_{w,T} \cdot \exp \left[\ln \left(\frac{\alpha_{s,T}}{\alpha_{w,T}} \right) \cdot \exp \left(-p \cdot \left(\frac{X_w}{1 - X_w} \right) \right) \right] \quad (6-3)$$

with

$$\log(\alpha_{w,T}) = \log(a_{w,T_{ref}}) - b_w(T - T_{ref}) \quad (6-4)$$

and

$$\log(\alpha_{s,T}) = \log(a_{s,T_{ref}}) - b_s(T - T_{ref}) \quad (6-5)$$

in which T is the temperature (K), X_w is the moisture content (kg/kg), p is a dimensionless parameter that describes the dependency of α on the moisture content. The $\alpha_{w,T}$ and $\alpha_{s,T}$ are Weibull parameters at $X_w = 1$ (infinite dilution) and $X_w = 0$ (pure solid form), respectively, which are described with the empirical equations (Eqns. 6-4 & 6-5) with parameters of $a_{T_{ref}}$ and b , where T_{ref} is set to 323.15 K (Mohács-Farkas, Farkas, Mészáros, Reichart, & Andrásy, 1999; van Boekel, 2009). The unknown parameters in the Weibull model, i.e., $a_{w,T_{ref}}$, $a_{s,T_{ref}}$, b_w , b_s , p , were estimated using the add-in Solver in Excel 2010 (Microsoft®, USA).

6.2.8 Statistical analysis

All the experiments were done independently in duplicate or more and all the data are presented as mean \pm standard deviation (SD). One-way ANOVA and Student's t-test were used to evaluate the difference between two means, and a p -value smaller than 0.05 meant that the difference between two means was significant ($p \leq 0.05$).

6.3 Results and discussion

6.3.1 Effect of moisture content on the survival of bacteria in RSM powder

Figure 6-1 shows the survival curves of *L. plantarum* in RSM matrices with different initial moisture contents (i.e., 0.05, 0.60 and 0.90) during isothermal heating at 60, 75 and 90 °C, respectively (see also section 6.2.4). At the same heating temperature, the survival of LP strongly increased as the moisture content of the matrix decreased (Figures 6-1a-c). For example, the viability of LP in solutions ($X_w = 0.60$ and 0.90) decreased by 5 log after 300-s heating at 90 °C

(Figure 6-1b & c), whereas the bacterial viability in dried RSM powder ($X_w = 0.05$) decreased only by 0.75 log after the same treatment (Figure 6-1a). This result is consistent with other studies, confirming that the heat resistance of bacteria increases at lower moisture content (Hansen and Riemann, 1963; Yesair et al., 1946). In a previous study, the heat resistance of *Lactobacillus plantarum* embedded in skim milk powder during heating at 150 and 200 °C was found highest when the initial water activity a_w of the powder was between 0.20 and 0.50 (Laroche et al., 2005). The water activity a_w of the dried RSM powder in our study ($X_w = 0.05$ kg/kg) was approximately 0.30 according to the sorption isotherm of skim milk powder (Murrieta-Pazos et al., 2011). However, the water activity in the RSM-water mixtures with an initial moisture content of 0.60 and 0.90 is very high ($a_w > 0.9$). This difference in water activity and moisture content and subsequent improved survival behaviour upon heat treatment observed in this study is thus in agreement with the previous study (Laroche et al., 2005).

The general trend of the pronounced influence of moisture content on survival of LP in the RSM/water system could be described by Weibull model (Eqns. 6-1 & 6-2, see lines in Figures 6-1a-c), although discrepancy was found between the prediction and the actual inactivation data. This discrepancy may be attributed to the isothermal heating method, where time required to heat and cool samples was neglected, which may influence the results especially at elevated temperatures (see Figure 6-B1 in Appendix 6-B). In this study, the shape parameter α of Weibull model was estimated for each survival curve by assuming that cells are equally susceptible to heat throughout the treatment at all conditions (i.e., $\beta=1$) (Pérez-Rodríguez and Valero, 2013b) (see Table 6-B1 in Appendix 6-B). A contour plot of different isothermal temperature conditions (45-135 °C) was made as a function of moisture content and α according to Eqns. 6-3 to 6-5 (lines in Figure 6-1d), and a high coefficient of determination was found ($R^2=0.99$). The parameters in the Bigelow model (Eqns. 6-3 to 6-5), $a_{w,T_{ref}}$, $a_{s,T_{ref}}$, b_w , b_s and p were estimated: 321 (s), 3810 (s), 0.031 (1/°C), 0.026 (1/°C) and 0.864 (-), respectively. An increase in the magnitude of α was observed at decreasing moisture contents and temperatures, indicating a higher survival of probiotics under these conditions (see Figure 6-1d). However, at higher moisture contents ($X_w > 0.90$), α was not sensitive to changes in moisture content anymore, and thus depended only on the heating temperature (Figure 6-1d). A similar observation was reported for *L. plantarum* WCFS1 incorporated in maltodextrin solutions (Perdana et al., 2013).

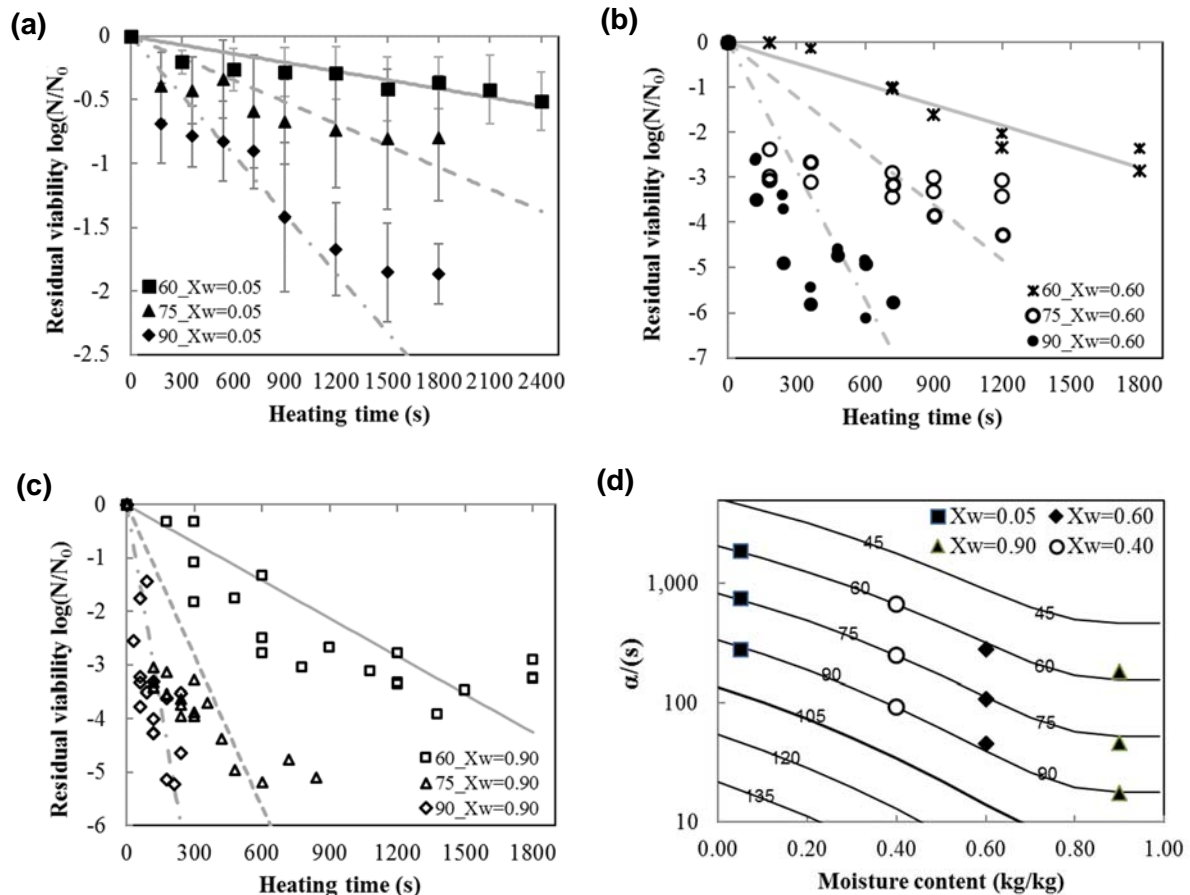


Figure 6-1. Survival curves of *L. plantarum* in RSM matrixes with different initial moisture contents (a: $X_w=0.05$; b: $X_w=0.60$; c: $X_w=0.90$) during isothermal heat treatment at 60 °C, 75 °C and 90 °C; solid lines and dashed lines represent fitted results of Weibull model, and error bars represent standard deviation ($n=4$). d: The scale parameter α estimated based on experimental data for each T - X_w combination (\blacksquare , $X_w=0.05$; \blacklozenge , $X_w=0.60$; \blacktriangle , $X_w=0.90$) and the predicted α (\circ , $X_w=0.40$); lines represent the contour plot of temperature as a function of α and moisture content based on Eqns. 6-3 to 6-5 ($R^2=0.99$).

6.3.2 Physicochemical properties of freeze-dried probiotic powder

Table 6-1 shows several physicochemical properties of the probiotic powders freeze-dried in different matrices (i.e. RSM, gum arabic, maltodextrin and inulin). The moisture content of the dried probiotic powder ranged from 0.028 kg/kg to 0.046 kg/kg and varied little when different carrier matrices were used (t-test, $p>0.05$). Moreover, the moisture content was similar to that of other freeze-dried probiotic powders (Chávez and Ledebor, 2007; Zayed and Roos, 2004). No significant difference in the final viability of LP was found among groups (all above 10.5 log CFU/g, t-test, $p>0.05$), while the bacterial viability before drying was about 11 log CFU/mL in

the cell suspensions, suggesting that the drying matrices used in this study had little influence on the viability variation of LP during freeze drying (Broeckx et al., 2016).

The glass transition temperature (both onset and midpoint T_g) of the powder containing 10 wt. % gum arabic was the highest in comparison to that of other powders (Table 6-1). It is assumed that the measured T_g values are not affected by the presence of the bacterial cells (Fonseca et al., 2001; Santivarangkna et al., 2011). Because powders have similar water content, it is the anhydrous T_g of the drying matrix that has the largest influence on the measured T_g of the probiotic powders. Therefore, the high T_g of the GA bacterial powder is probably due to the high anhydrous T_g of gum arabic. Unfortunately, only an approximated anhydrous T_g of gum arabic of 170 °C was reported (Collares and Kieckbusch, 2004; Fernandes et al., 2014). This anhydrous T_g of gum arabic was higher than that of RSM (92 °C), maltodextrin (DE13-17, 153-158 °C) and inulin (119 °C) reported in previous studies (Bhandari and Howes, 1999; Jouppila and Roos, 1994; Perdana et al., 2014). It is worthy to mention that the anhydrous T_g of maltodextrin (DE13-17) was also approximated based on a linear correlation between T_g and the ‘Dextrose Equivalent (DE)’ of maltodextrin (Bhandari and Howes, 1999).

Table 6-1. Physicochemical properties of bacterial powders freeze-dried in different matrices with the same 10 wt.% initial solid (RSM = reconstituted skim milk, GA = gum arabic, MD= maltodextrin DE13~17).

Property	RSM	GA	MD	Inulin
Moisture content (kg/kg)	0.046 ^a ±0.011	0.034 ^a ±0.019	0.028 ^a ±0.016	0.034 ^a ±0.016
Viable cell count (log CFU/g)	10.87 ^a ±0.22	10.76 ^a ±0.08	10.63 ^a ±0.21	10.54 ^a ±0.09
$T_{g,onset}$ (°C)	53.79 ^b ±2.51	60.64 ^a ±2.24	54.71 ^b ±2.49	48.80 ^b ±4.52
$T_{g,mid}$ (°C)	70.79 ^c ±1.00	80.28 ^a ±2.74	73.58 ^b ±0.18	68.80 ^d ±0.91
Hygroscopicity (g/100 g)	12.05 ^a ±5.28	20.05 ^a ±3.32	16.79 ^a ±2.49	13.35 ^a ±4.03

^{a-d} Parameters with different superscript letters within the same row have significant differences ($p \leq 0.05$).

All the four freeze-dried powders can be classified as hygroscopic because their hygroscopicity was higher than 10 g/100 g (Schuck et al., 2012). In particular, the powders dried in gum arabic and maltodextrin appeared to be more hygroscopic than the other two, although no significant differences in hygroscopicity among groups was observed due to the large standard deviation ($p > 0.05$) (see Table 6-1). Among the tested encapsulating materials, gum arabic and maltodextrin are hydrophilic compounds (Comunian and Favaro-Trindade, 2016). The

hygroscopicity of RSM-probiotic powder was relatively low and close to the reported value for skim milk powder (10.2 g/100 g) (Schuck et al., 2012). The poor solubility of inulin in water can explain in the lower hygroscopicity of the corresponding probiotic powder (Mensink et al., 2015).

Figure 6-2 shows the morphology of the freeze-dried bacterial powders at the micrometre scale. Abundant intact LP cells were found fixed in the compact microstructure of RSM or GA matrices (Figures 6-2a & b). Nevertheless, the bacteria cells seemed not so well embedded in the maltodextrin or inulin matrices (Figures 6-2c & d): cells seemed to be included in the cavities of the continuous maltodextrin matrix, while the cells were stacked on top of each other in inulin, resulting in a less obvious boundary between the cells and the matrix. The distinct microstructure of the different bacterial powders is difficult to explain, but is probably also related to the ice crystallization process during freezing (Harnkarnsujarit et al., 2012).

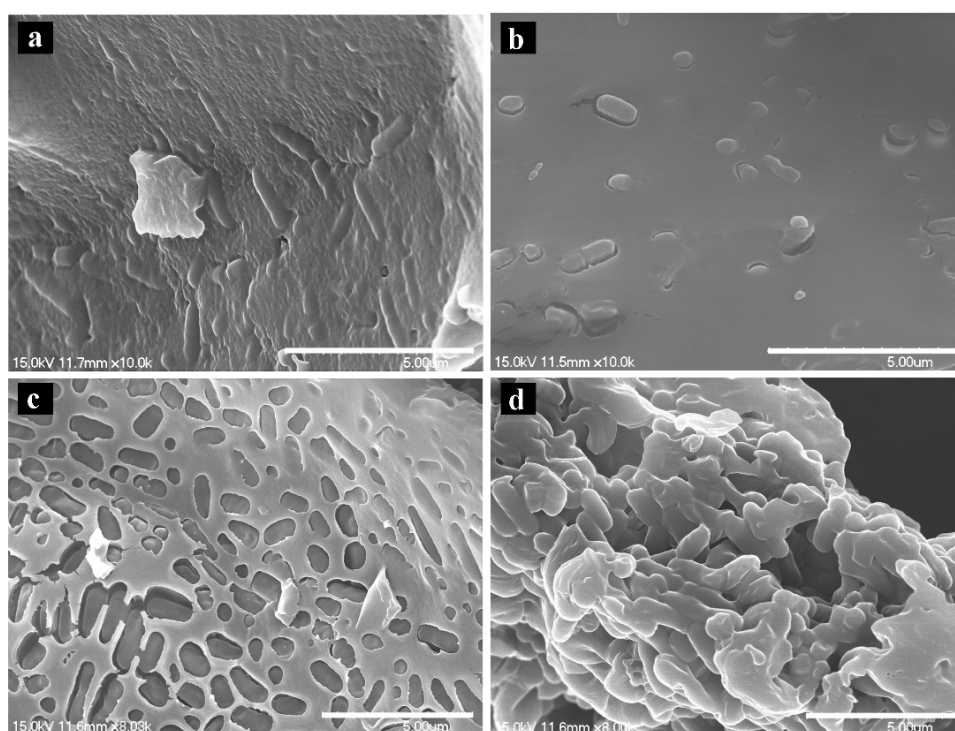


Figure 6-2. SEM images of *Lactobacillus plantarum* freeze dried in different matrices (a: RSM; b: gum arabic; c: maltodextrin DE13~17; d: Inulin), scale bars represent 5.00 µm.

6.3.3 Effect of matrices on survival of bacteria during isothermal heating

Figure 6-3 shows that survival of LP during isothermal heating at 90 °C is influenced by the drying matrices in which the cells are imbedded. The survival of LP cells was found the highest in the GA matrix, followed by the RSM matrix. The protective effects of maltodextrin and inulin

on the LP cells were limited: the log reductions of bacteria in GA, RSM, MD and inulin after 30-min heating at 90 °C were about 1.5, 2.75, 3.75 and 4.25, respectively (refer to Figure 6-3).

The higher LP survival observed in GA may be due to the high T_g of this formulation (Table 6-1), which is also suggested by Lodato, de Huergo, & Buera (1999) in a study on the thermal stability of a yeast strain freeze dried in difference matrices. Although none of the powders are in the glassy state at 90 °C, it may be expected that the mobility of the molecules in the GA matrix is lowest compared to the other formulations, which can explain the higher survival of the LP cells embedded in that matrix (Santivarangkna et al., 2011). Moreover, the physical embedding of LP cells in the RSM matrix or the compact GA matrix (Figures 6-2a & b) seems better compared to the embedding in the inulin and MD matrices (Figures 6-2c & d), which may assist in protection of the bacteria towards the harsh environmental conditions (Huang et al., 2014; Zheng et al., 2015). Specifically a large number of bacteria were observed on the surface of the MD and inulin powders, which suggests that bacteria in these matrices are less protected.

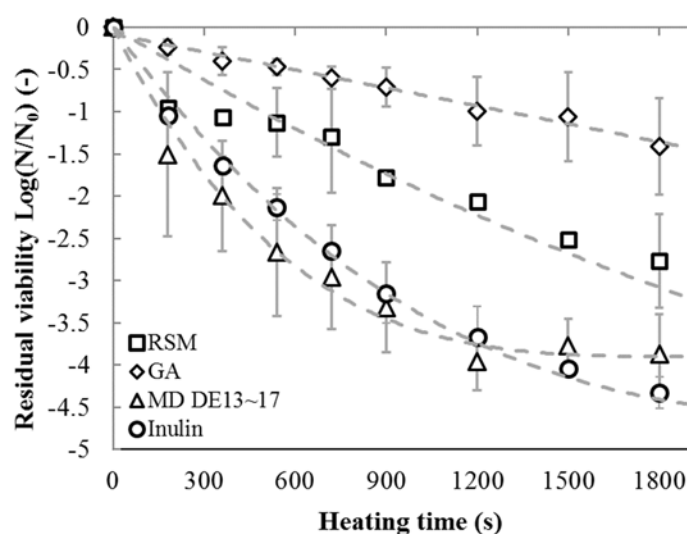


Figure 6-3. Semi-logarithmic survival curves of *L. plantarum* freeze-dried in different matrices during isothermal heat treatment at 90 °C for 1800 s (□, RSM; ◇, GA; △, MD DE13~17; ○, inulin). Dashed lines are drawn to guide the eye and the error bars indicate the standard deviation.

6.3.4 Different approaches to incorporate probiotics in bread

Different approaches may be applied to incorporate probiotic powders into bread, most probably resulting in different survival during baking. In this study, the following three approaches were used: i) addition of cell suspension in dough (control group); ii) addition of

dried probiotic powder to dough; and iii) application of dried probiotic powder onto the surface of dough (De Prisco and Mauriello, 2016), as described in detail in section 6.2.5. The final viability of bacteria in bread prepared with dried probiotic powders (using the second and third approaches) were compared to that of the control group. Only RSM powder was used for these experiments and compared to cells suspended in skim milk. As shown in Figure 6-4a, the application of powder onto the dough surface provided the highest viability of LP in baked bread, at the same baking conditions (i.e., 6-min at 175 °C or 15-min at 100 °C). This can be explained by the higher survival of LP at lower moisture content (see section 6.3.1), even though the temperature in the surface region of the bread is higher than in the core during baking at 175 °C (Figure 6-4b) (Zhang et al., 2018). The residual viabilities of the probiotics in breads prepared with free cell suspension and powder mixed in the dough (the second approach) were similar, i.e. 10^4 CFU/g after 6-min baking at 175 °C and 10^6 CFU/g after 15-min at 100 °C, respectively (Figure 6-4a). This suggests that the RSM matrix did not protect the LP cells during baking even when supplied as a dry powder. The reason is probably the fast hydration of the powder, which exposed the bacterial cells to a more moist environment, and thus the cells became more susceptible to thermal inactivation (van Boekel, 2008).

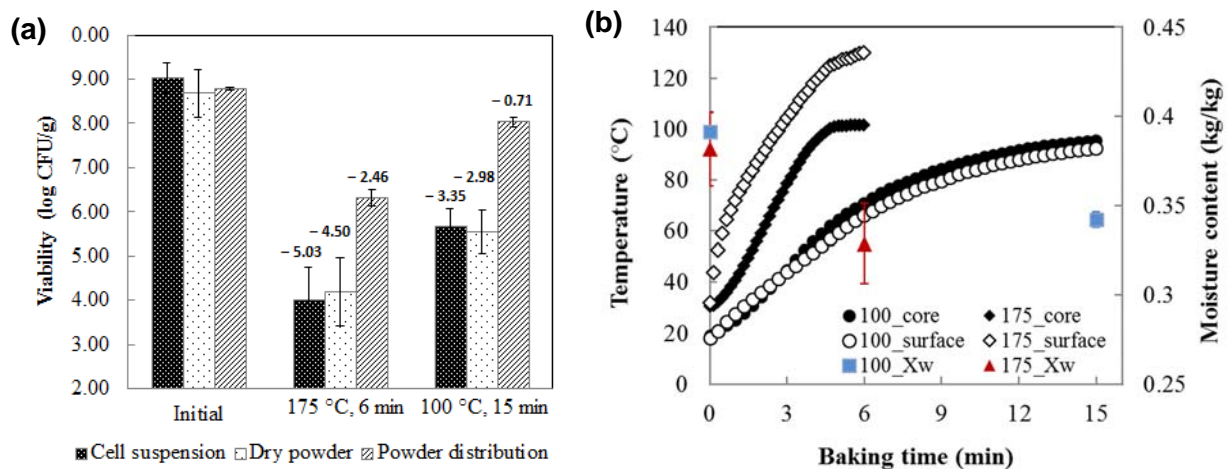


Figure 6-4. a: Viable counts of *L. plantarum* in bread before and after baking at 175 °C for 6 min or at 100 °C for 15 min with three different approaches to incorporate probiotics into bread (i.e., cell suspension, dry powder and powder distribution); the corresponding log reduction of the LP viability was marked on top of each bar; b: Temperature profiles of the core and the surface of bread during baking at 175 °C (6 min) and 100 °C (15 min), and the average moisture contents (kg/kg) of the dough and the baked bread (▲, 175 °C; ■, 100 °C).

Figure 6-4a shows that the viability of LP in all three kinds of bread baked at 100 °C was 2 log higher than that of breads baked at 175 °C. The higher survival rate of LP can be attributed to the relatively low temperature reached (< 100 °C) inside the bread (Figure 6-4b). The moisture contents of the bread crumb (0.34 kg/kg) was similar at the two baking temperatures (see Figure 6-4b), as well as the crumb structure (data not shown). Remarkably, a high bacterial viability of 10^8 CFU/g was observed after baking at 100 °C when the third approach was used. This bacterial viability was even higher than viabilities reported in other studies in which a probiotic-containing edible film was applied onto the surface of partially-baked bread (Altamirano-Fortoul et al., 2012; Soukoulis et al., 2014), or when a liquid sourdough was injected into baked bread (Lönner, 2008).

When the dried bacterial powder is applied onto the bread surface, the survival rate of LP after baking could be estimated with the earlier developed kinetic model in section 6.3.1 (Eqns. 6-5 & Figure 6-1d) and the measured temperature profiles of the bread surface during baking (Figure 6-4b). We considered two extreme conditions: i) the powder maintained its low moisture content after proofing ($X_w = 0.05$); ii) the powder absorbed water from the environment during proofing ($X_w = 0.40$, same as the dough). Based on these two more extreme situations, a linear semi-logarithmic survival curve is calculated ($\beta = 1$) using the temperature measurements retrieved each 10 s and using Eqns. 6-1 & 6-2, which are rewritten as:

$$\log\left(\frac{N_{i+1}}{N_i}\right) = -\frac{1}{2.303}\left(\frac{\Delta t}{\alpha}\right) \quad (i = 0, 1, 2, \dots, n) \quad (6-6)$$

where Δt is the discrete time interval ($\Delta t = 10$ s). The shape parameter α was changing along with the increasing temperature inside bread during baking (Figures 6-1d & 6-4b), and was calculated based on Eqns. 6-3 to 6-5 at each time interval. Finally, the accumulated reduction of LP viability during baking can be estimated, i.e. $\log(N/N_0)$. The log reduction of LP viability in bread was predicted between -2.23 and -8.16 after 6-min baking at 175 °C, and between -0.31 and -0.97 for baking at 100 °C for 15 min. The corresponding experimental results were -2.46 and -0.71 , respectively, which fell within the range of the predicted values (Figure 6-4a). Therefore, the kinetic model may be used to obtain a first approximation of the residual viability when the bacteria are applied as a powder on the dough surface.

6.3.5 Effect of matrices on survival of bacteria during bread baking

The influence of different drying matrices on the survival of LP during bread baking was investigated. The powder was added to bread by distributing it on the dough surface and a control group was made without adding probiotics (see Figure 6-5). The RSM matrix showed the highest protective effect on LP cells during baking at either 100 °C or 175 °C ($p \leq 0.05$), followed by the inulin matrix (Table 6-2). However, no protective effect was observed for gum arabic and maltodextrin during baking (Table 6-2), even though gum arabic performed the best during isothermal heating as discussed in section 6.3.3 (Figure 6-3).

Figure 6-5 shows that both GA and MD bacterial powders dissolved after proofing, while the RSM and inulin powders remained relatively dry, which is possibly due to the hydrophilic nature of GA and MD as compared to RSM and inulin (see section 6.3.2). The hydration of powder is expected to negatively affect the survival of embedded LP cells, as the initially glassy powder will enter the rubbery state due to the ‘plasticising effect’ of water (Crowley et al., 2016). Therefore, the dissolution of GA and MD powders after proofing is probably responsible for the low survival rate of LP during baking (Ansari and Datta, 2003). Furthermore, RSM led to higher viability compared to inulin, e.g. at 175 °C (log reduction was – 2.46 for RSM compared to – 4.01 for inulin), which may be related to the increased visual entrapment of bacteria into the matrix (Figure 6-2).

Table 6-2. Viability of *L. plantarum* in bread supplemented with different bacterial formulations before and after baking at 175 °C for 6 min or at 100 °C for 15 min.

Property	RSM	GA	MD	Inulin
Initial viable count (log CFU/g)	8.77 ^a ± 0.03	8.04 ^b ± 0.06	8.13 ^{ab} ± 0.18	8.17 ^{ab} ± 0.24
Viable count at 175 °C (log CFU/g)	6.31 ^a ± 0.19	2.99 ^c ± 0.12	2.95 ^c ± 0.24	4.16 ^b ± 0.16
Log reduction at 175 °C (-)	-2.46	-5.05	-5.18	-4.01
Viable count at 100 °C (log CFU/g)	8.03 ^a ± 0.10	4.95 ^c ± 1.23	6.57 ^b ± 0.43	7.42 ^b ± 0.11
Log reduction at 100 °C (-)	-0.74	-3.09	-1.56	-0.75

^{a-d} Parameters with different superscript letters within the same row have significant differences ($p \leq 0.05$).

It is important to note that in this study no browning of the surface of the breads occurred due to the relative low baking temperatures applied (Figure 6-5). Although the surface temperature of bread baked at 175 °C exceeded 120 °C (the minimum temperature required for initiating colour formation) in the late stage of baking (Figure 6-4b), the baking time was too short to

cause an obvious brown colour on the bread surface (Zanoni et al., 1995). In addition, although the extent of starch gelatinization was estimated to reach 100 % in the crumb after 15 min baking at 100 °C (see Appendix 6-A, Figure 6-A1), the core temperature of the bread just reached 98 °C after baking (Figure 6-4b). The short duration of the 98 °C baking plateau may have influence on the staling of the bread (Besbes et al., 2014; Le-bail et al., 2012).

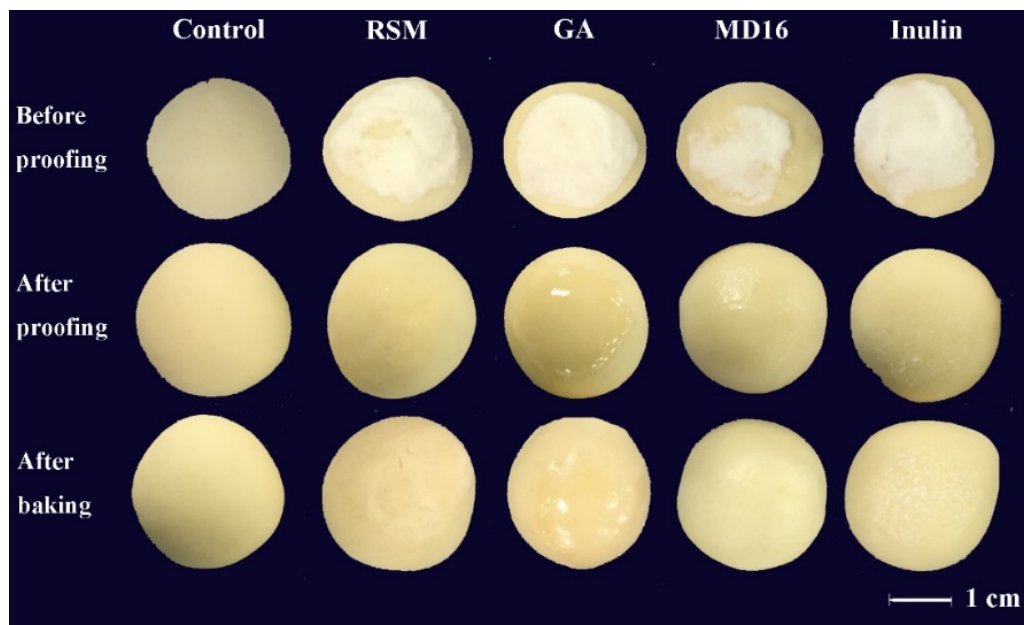


Figure 6-5. Digital images of the dough or the bread supplemented with different bacterial powders that were evenly distributed on the surface of the dough before proofing (bread was baked at 175 °C for 6 min or at 100 °C for 15 min, and the appearance of bread samples baked at these two conditions was similar, so only the images of one group were shown).

6.4 Conclusions

The survival of encapsulated *L. plantarum* (LP) during subsequent isothermal heating and baking is indeed strongly influenced by the matrix composition and processing conditions. In particular the moisture content appeared to have large influence on the survival of bacteria upon exposure to heat. The Weibull model could describe the general trend of the bacterial inactivation kinetics during isothermal heating as influenced by the initial moisture content of the RSM matrix, which could be used to predict the survival rate of bacteria in baked bread. Application of the RSM-probiotic powder onto the surface of the bread could best delay the water migration from the dough into the dry powder, which was critical to maximally preserve the bacterial viability during baking. Incorporation of the dry powder in the bread crumb

appeared not practical as the high moisture content in the crumb quickly rehydrates the powder and thus cancels out the protective effect of the encapsulation matrix. It is noted that application of powder on the dough surface slightly alters the appearance of the bread and baking time needs to be extended if browning of the crust is desired. Further evaluation of the organoleptic properties of the probiotic-fortified bread is therefore necessary.

Appendix 6-A. Starch gelatinization

The extent of starch gelatinization in dough was estimated using the method described in our previous study (Zhang et al., 2018). The starch gelatinization is described by a first-order kinetic model as a function of temperature (Figure 6-4b) and time, and the extent of starch gelatinization in the crumb of 5 g dough was estimated to reach 98 % after 10-min baking at 100 °C and after 4.5-min baking at 175 °C, respectively (see Figure 6-A1).

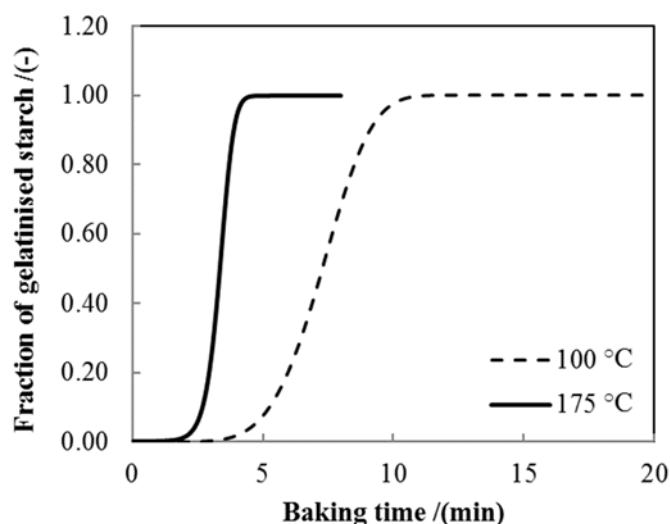


Figure 6-A1. Estimated extent of starch gelatinization in the crumb during baking of 5 g bread at 100 °C (dashed line) and 175 °C (black line).

Appendix 6-B. Supplementary results of Weibull model

Figure 6-B1 shows the parity plots of the logarithmic values of the residual viability of *Lactobacillus plantarum* obtained from experiments and calculated by Weibull model. The goodness-of-fit of Weibull model to the experimental inactivation data was acceptable in general, however some outliers were observed which was due to the large standard deviation of the original data. The estimated parameter of Weibull model α , the corresponding root mean square error (RMSE) and the coefficient of determination (R^2) were shown in Table 6-B1. A low RMSE value indicates a good fitting of the model to the data (Eqn. 6-B1).

$$RMSE = \sqrt{\frac{\sum_{i=1}^n (Y_i - \hat{Y}_i)^2}{n}} \quad (6-B1)$$

where Y_i is the experimental result, and \hat{Y}_i is the calculated value and n is the number of data points.

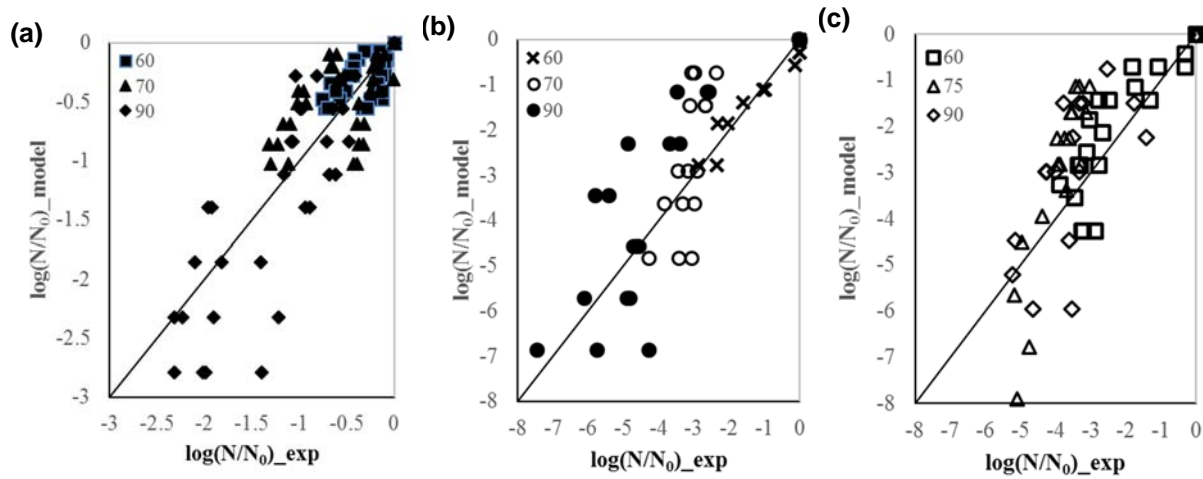


Figure 6-B1. Parity plots of the residual viability of *Lactobacillus plantarum* in RSM matrices during isothermal heating (at 60, 75 and 90 °C, respectively) obtained from experimental data and calculated by Weibull model. The symbols represent the results from all the replicates for each experimental condition, i.e., different initial moisture contents (kg/kg): (a) $X_w=0.05$; (b) $X_w=0.60$; (c) $X_w=0.90$.

Table 6-B1. Estimated Weibull parameter α , the corresponding root mean square error ($RMSE$) and the coefficient of determination (R^2) for each experimental condition as described in section 6.2.4 for isothermal heating of RSM-water mixtures with different initial moisture contents.

Moisture content X_w (kg/kg)	T (°C)	α (s)	R^2 values	$RMSE$ values
0.05	60	1900	0.84	0.19
	75	760	0.78	0.38
	90	280	0.76	0.61
0.60	60	282	0.94	0.26
	75	108	0.55	1.19
	90	46	0.69	1.40
0.90	65	184	0.72	0.75
	75	46	0.62	1.46
	90	17	0.63	1.27

Chapter 7

Fortification of bread with arabinoxylan-enriched fractions obtained by dry fractionation



Paper in preparation as:

Zhang, L., Grandia J., Chen, X.D., Boom, R.M.,
Schutyser, M.A.I. Fortification of bread with
arabinoxylan-enriched fractions obtained by dry
fractionation.

Abstract

An arabinoxylan-enriched fraction (AXF) was obtained from wheat bran by dry fractionation and evaluated as a food ingredient in bread baking. Dry fractionation consisted of milling, electrostatic separation and sieving, which is less intensive than the wet fractionation of arabinoxylans in terms of water and energy use. Bread was fortified with different amounts of the AXF and quality attributes of the fortified bread, such as colour, volume, textural properties and crumb structure were evaluated. The quality of bread fortified with 2 % AXF was not significantly different from the control bread, while breads with 5 % AXF were only slightly different. The addition of the AXF up to 10 % was however detrimental to the bread quality, giving decreased specific volume, harder crumb, darker appearance, and a coarser crumb structure. Enzymatic treatment of the AXF with feruloyl esterase improved the functional properties of the AXF and the quality characteristics of baked bread. Thus bread products with higher fibre content and improved nutritional value can be realized, without compromising the product quality.

7.1 Introduction

Daily consumption of more dietary fibre could lower the risk of cardiovascular disease and type 2 diabetes, may reduce the blood sugar level, and may inhibit the elevated cholesterol levels (Van Der Kamp et al., 2014). Given that bread constitutes a staple food worldwide, supplementation of dietary fibre to bread will participate to increase the consumption of dietary fibre. Arabinoxylan (AX) is a hemicellulose that has a xylose backbone with arabinose side chains, which is the major dietary fibre component in wheat grains particularly in the bran (Goesaert et al., 2005). Traditionally, wheat bran is an undervalued by-product during wheat flour production which is discarded or used as animal feed (Hemery et al., 2011, 2007). However, wheat bran contains also most of the micronutrients and phytonutrients of the wheat grain (Hemery et al., 2007). Therefore, AX-enriched fractions (AXF) obtained from wheat bran can be used to produce fortified bread.

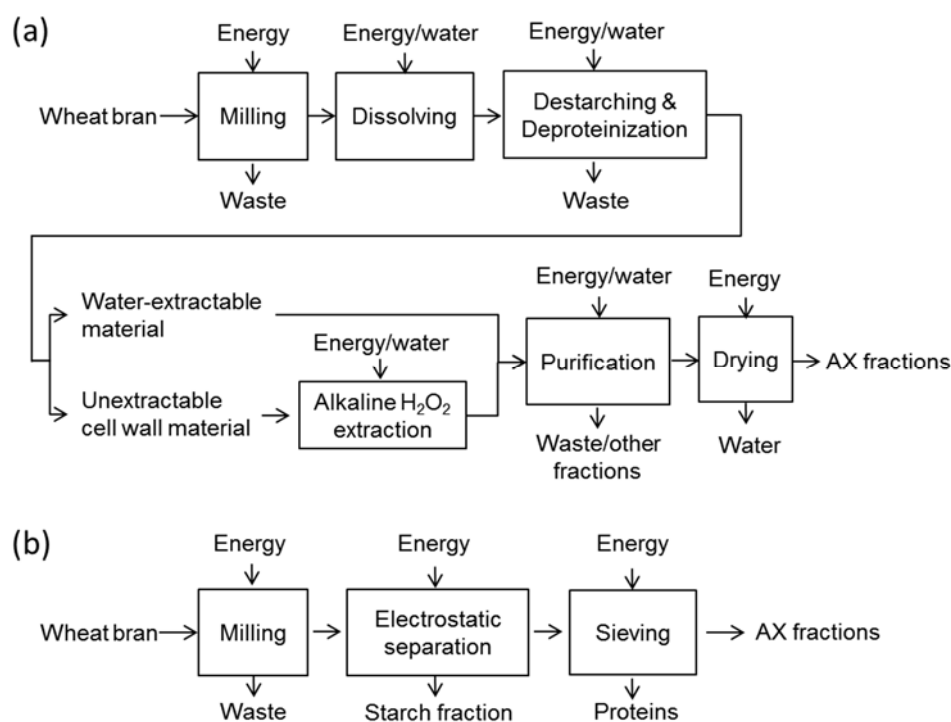


Figure 7-1. Scheme of the fractionation procedures of wheat bran to produce AX-enriched fractions: A, wet fractionation in Maes and Delcour (2002); B, dry fractionation in Wang et al., (2015).

Conventionally, a wet alkaline process is used to purify AX from wheat bran (Bataillon et al., 1998). The wet extraction process requires large amounts of water and consequently energy for dehydration, and results in the production of a lot of waste (Schutyser and van der Goot, 2011).

Besides, the harsh alkaline conditions may cause loss of functional groups of AX (e.g. phenolic acids esterified to the arabinose residues of AX) (Zhou et al., 2010). In this sense, a dry fractionation process that combines milling and electrostatic separation (ES) can be an alternative (see Figure 7-1), which consumes little energy and retains the native functionality of wheat bran components (van der Goot et al., 2016). Besides, dry fractionation allows efficient separation of the valuable components from the detrimental ones in wheat bran (i.e. contaminants, antinutrient compounds, and irritants) (Hemery et al., 2007). Electrostatic separation separates particles on their histological characteristics and charging behaviours rather than the size or density. AX-enriched fractions with an AX content of 43 % can be achieved by dry fractionation (Wang et al., 2015), which are mainly fragments of outer pericarp and intermediate layer of wheat bran. This dry-fractionated AXF contain starch and protein, which may show different effects on the quality of fortified breads compared to the purified AX obtained from the conventional wet fractionation process.

Fortification of bread with dietary fibres (i.e. wheat bran or AXF) has been intensively investigated in the past. The addition of AX or bran has been found to detrimentally influence the structural and organoleptic properties of bread (see Table 7-A1 in Appendix 7-A). This is because AX interferes with the development of the gluten network through two proposed mechanisms: i) the high water holding capacity of AX reduces the level of water available for the gluten, which disturbs the correct assembly of glutenin subunits; ii) the ferulic acid moieties of AX interact with gluten proteins via weak Van der Waals bonds. As a result, the dough becomes more viscous and less elastic, and ultimately the gas retention and the leavening potential are decreased (Gomes et al., 2018). To mitigate this, bioprocessing and/or enzymes may be used to improve the baking properties of AX-enriched flour (Messia et al., 2016). Feruloyl esterase may be added during dough preparation to release the ferulic acid from AX which decreases the water holding capacity and increases the elasticity of the dough and thus may also increase the quality of the final bread (Faulds et al., 2003).

This study aims at getting insight into the effect of added arabinoxylan-enriched fractions obtained by dry fractionation on bread quality, which has not been studied extensively before. First, the obtained AX-enriched fractions are characterized on their AX and moisture content and water holding capacity. Second, we investigate the effect of the AX-enriched fraction on the quality attributes of the fortified bread. Furthermore, we modify the AX-fraction using feruloyl esterase, to reduce the possibly negative influence of AX addition on quality of the fortified bread. We feel that the work reported here may facilitate the introduction of new functional

ingredient to bakery products and bring new insights into the manufacturing of a healthier AX-fortified bread employing fractionated wheat bran as a high-valued ingredient.

7.2 Materials and methods

7.2.1 Materials

Wheat bran was obtained from Koopmans Meel BV (Leeuwarden, the Netherlands), with the following specifications: moisture 15% (w/w), dietary fibre 44% (w/w), protein 15% (w/w), starch 13% (w/w), fat 6% (w/w) and ash 7% (w/w). Chemicals and reagents were of analytical grade and supplied by Sigma Aldrich (Germany). Wheat flour, UHT skim milk, instant yeast and other ingredients of bread were obtained from the local market. Milli-Q water (Merck Millipore, U.S.A.) was used during chemical analysis. Feruloyl esterase from rumen microorganisms (E-FAERU) was obtained from Megazyme (Megazyme International Ireland Ltd., Ireland).

7.2.2 Dry fractionation of arabinoxylans

The dry fractionation of an arabinoxylan-enriched fraction (hereinafter referred to as AXF) from wheat bran consists of three steps: milling, electrostatic separation and air jet sieving. The wheat bran was first milled using a pin mill (Type 100 UPZ, Hosokawa Alpine, Germany) at a speed of 20,500 rpm and an air flow of 75 m³/h. Four consecutive impact milling steps were carried out to obtain the starting material for the electrostatic separation (ES). During this milling the air flow was fixed at 80 m³/h, the milling speed at 8,000 rpm, the gas flow rate at 20 L/min and the classifier wheel speed at 2,500 rpm.

Subsequently, electrostatic separation was performed using a vertical bench-scale electrostatic separator as described in (Wang et al., 2015). The electrostatic separator consists of four parts: the feeding system, the charging slit, the separation chamber and the collection chamber. We used a dosing rate of 1.25 kg/h and an electric field strength of 200 kV/m, by applying a voltage of 20 kV to the positive electrode and 10 cm distance between the electrodes. The AX-enriched fraction was collected from the positive electrode as it was found in previous research that this fraction was enriched in AX (Wang et al., 2015), which was used as the starting material for the sieving step. Finally, the coarse AX-enriched fraction was separated from the fine fraction using a 50 µm air jet sieve (ALPINE Air Jet Sieve e200 LS, Hosowaka Alpine, Germany) for 2 minutes at 3000 Pa.

The separation efficiency of ES and sieving is defined as the percentage of AX recovered in the target fraction from the AX in the starting material, which is calculated by Eqn. 7-1.

$$\text{Separation efficiency} = \frac{Y_f \cdot C_{AX,f}}{C_{AX,i}} \quad (7-1)$$

where Y_f is the yield of the fraction, $C_{AX,f}$ is the AX content of the target fraction after ES or sieving, $C_{AX,i}$ is the AX content of the starting material for ES or sieving.

7.2.3 Characterization of the AX-enriched fraction

After dry fractionation, some properties of the obtained fractions were determined. Particle size distributions of the different powder fractions were measured using laser diffraction using a Mastersizer 2000 combined with a Scirocco 2000 dry dispersion unit (Malvern Instruments, UK). The AX content of different fractions was measured using a modified phloroglucinol method. The method is precisely described before (Wang et al., 2015), and yields the amount of pentosans, including both arabinoxylans and arabinogalactans. Arabinogalactans are present in low levels (0.27 to 0.38 % dm), and do not interfere with the determination of the AX content. The total dietary fibre (TDF) content of the AXF was determined with AOAC method 985.29, using the Megazyme TDF Test Kit (Megazyme International Ireland Ltd., Ireland).

The moisture content of the fractions was analysed according to AOAC method 925.10, by weighing 2 g of sample and dehydrating it at 105 °C in an oven for 24 h. The water holding capacity (WHC) of AXF was determined using AACC method 56-30: 5 gram of sample was weighed, after which incremental drops of water were added while stirring with a stirring rod until the sample was properly wetted. Samples were centrifuged at 2000 g for 10 min, excess water was poured off and samples were weighed again. The WHC (mL/g) was then calculated as:

$$\text{WHC} = \frac{(\text{wet weight sample}) - (\text{dry weight sample})}{(\text{dry weight sample})} \quad (7-2)$$

7.2.4 Bread baking

The fortification of bread with arabinoxylans was carried out by replacing a certain percentage of wheat flour with AXF, i.e., a 2 % AXF replacement means 2 g of wheat flour was replaced by 2 g of AXF in a total of 100 g of flour. The replacement was set to 0 % (control group), 2 %, 5 % and 10 %. A bread recipe modified from our previous study was used (Zhang et al., 2016): wheat

flour (100 g), UHT skimmed milk (66.67 g), sugar (10 g), salt (1.67 g), non-salt butter (3 g), instant yeast (1 g). The dough was made in a mixer (Bosch, Germany), and was divided into small pieces (5 g), which were then shaped into balls. Subsequently, the dough was proofed at 40 °C, 85 % RH for 45 minutes in a climate chamber (Memmert, Germany). The bread was baked at 205 °C in a preheated convection oven (Heraeus, Germany) for 8 minutes. After baking, the total moisture content of the bread was measured using the same method described before. The weight loss was determined by weighing the sample before and after baking:

$$\text{weight loss (\%)} = \frac{(\text{weight before baking}) - (\text{weight after baking})}{(\text{weight before baking})} \quad (7-3)$$

7.2.5 Texture profile analysis and colour measurement

Texture profile analyses (TPA) of the bread crumb were made using a texture analyser (Instron, Belgium) equipped with a 2.5 cm cylindrical probe. Crumb samples (2 cm × 2 cm) were 50 % compressed at a speed of 1 mm/s in a TPA double compression test, to imitate chewing actions. The delay time between the first and the second compression was 30 s. The parameters obtained were hardness, chewiness, cohesiveness and springiness. Surface browning of the bread crust after baking was monitored by a colorimeter (StellarNet Inc, USA). CIELab parameters (L^* , a^* , b^*) were measured at four different positions for each bread sample, and the mean values were calculated. The colour difference ΔE between the control breads and fortified bread with different levels of AXF replacement was calculated:

$$\Delta E = \sqrt{\Delta L^2 + \Delta a^2 + \Delta b^2} \quad (7-4)$$

where ΔL is the brightness difference, Δa is the redness difference and Δb is the yellowness difference.

7.2.6 Bread volume and cell structure

Bread samples were scanned using laser topography and the volume was analysed using VolCalc Software (Pertten instruments, Sweden). The specific volume (cm³/g) of the bread samples was expressed as the volume divided by the weight. The cellular structure of the bread was assessed by a C-Cell imaging system (Calibre Control International Ltd., UK). Briefly, images of the transection of bread sample were taken, and parameters such as cell volume, cell wall thickness and porosity were calculated by pixel analysis using the available image analysis software of the system.

7.2.7 Bioprocessing and biochemical analysis

The enzyme feruloyl esterase was added to release ferulic acid from AX, 10 g AXF was mixed with 66.67 g water and 0.7 mL feruloyl esterase (i.e. 42 U/g AXF). This mixture was stored overnight at 40 °C and 55 % RH in a climate chamber to produce enzyme-modified AXF (MAXF). Bread with 10 % MAXF replacement was subsequently made with this mixture directly using the method described above.

The amount of free ferulic acid (FFA) in the AXF and MAXF was quantified using HPLC (Thermo Scientific Ultimate 3000, USA). Specifically, to extract FFA from the AXF and the MAXF, 0.08 g sample was mixed with 2 mL water and 180 µL 4M HCl. Subsequently, 5 mL ethyl acetate was added and the suspension was mixed well in a tube. The ethyl acetate phase was collected in a round bottom flask using a separating funnel. This extraction was done twice; 10 mL ethyl acetate was collected in total. The ferulic acid was quantified using HPLC with a Gemini 3u C18 110A (the Netherlands) column, using a column temperature of 30 °C and diode array UV detection at 320 nm. The eluent used was 30 % acetonitrile in Milli-Q and 0.1 % trifluoroacetic acid. The flow rate was 0.75 mL/min and injection volume was 5 µL. The ferulic acid concentrations in the extracts were found by comparison to a pure ferulic acid standard curve (see Appendix 7-B, Figure 7-B1).

7.2.8 Statistical analysis

All data were presented as mean values of duplicates except where noted, and error bars represent standard error (\pm SE). The student t-test was used to compare means and the *P*-value was calculated using the T.TEST function in Excel (Microsoft®, USA).

7.3 Results and Discussion

7.3.1 Dry fractionation of AXF

During tribo-electrostatic charging, the aleurone layer and the endosperm of the wheat grain take positive charge while particles from the pericarp which are rich in AX take negative charge (Wang et al., 2015). Therefore, during electrostatic separation the enriched AX fraction was negatively charged and collected from the positive electrode, i.e., (-) charged fractions (Table 7-1). The separation efficiency (SE) of AX by ES using a vertical design electrostatic separator was 30.6 %, which was higher than the SE of 16 % that was obtained by using a horizontal system design (Wang et al., 2015). The yield of the negatively charged fractions was similar, which was

13.3 % in this study and 14 % in the previous one. The sieving step after ES enriched the AX from the negative-charged fraction (AX content, 44.2 % dm) to the final arabinoxylans-enriched fraction (AXF, AX content, 55.8 % dm) by removing starch and protein, with a high separation efficiency of 51.4 %. Overall, the dry fractionation process enriched the AX from 18.6 % dm in the wheat bran flour to 55.8 % in the AXF, with a total separation efficiency of 16 %.

Table 7-1. Properties of different fractions obtained by dry fractionation

Samples	Parameters		
	Weight (g)	Yield (% of WBF)	AX content (% dm)
WBF (start)	1534	-	18.6
AXF (final)	83	5.4	55.8
Fine fraction	110	7.2	40.1
(-) charged fraction	204	13.3	44.2
Right collector bag	426	27.7	14.8
(+) charged fraction	272	17.7	16.9
Left collector bag	538	35.1	18.7
Total*	1429	93.1	-
Lost	105	6.9	-

* Total is the sum of weights of arabinoxylan-enriched fraction (AXF), the fine fraction, fraction from right and left collectors, and fractions from the neutral electrode. The lost is the weight of wheat bran flour (WBF) minus total weight of those fractions. The negatively charged fraction was collected from the positive electrode. dm: dry matter.

A bottleneck of the employed AX enrichment procedure is the relatively low yield. The sieving step that was applied did increase the purity at the expense of the yield (from 13.3 % to 5.4 %). However, the AX content in the fine fraction after sieving was still as high as 40.1 % dm. In this study, we opted to incorporate the fractions with the highest purity in the breads, therefore the AXF was used for the baking experiments. It is possible to use the lower-purity fraction obtained with higher yield for other applications. In addition, the unused fractions after ES (i.e., the sum of the fractions in the collector bags and from the negative electrode) had an average AX content of 17.0 % which was close to that of the starting wheat bran flour (18.6 %). The yield of these unused fractions was high (80.6 %), therefore, recycling of the unused fractions may improve the yield of AXF (Wang, Zhao, Wit, Boom, & Schutyser, 2016).

7.3.2 Characterization of AXF

The AXF was characterized by several physiochemical properties, such as moisture content, particle size distribution and histological structure, etc. These properties may influence bread

baking performance of the AXF. The moisture content of the fractions was 8 % on a wet basis, which was lower than the wheat flour (14 %). The total dietary fibre (TDF) content in the AXF is 59.6 % dm, which indicates that most dietary fibres in the final fraction were arabinoxylans (Cui and Wang, 2009). The water holding capacity (WHC) of the AXF was found to be 3.20 mL/g, which was much higher than that of the wheat flour (0.76 mL/g). This high WHC of the AXF is expected to influence the quality of AX-fortified bread.

In addition, the particle size distribution analysis of the fractions yield the volume weighted means (D[4,3]) of the wheat bran flour, the arabinoxylans-enriched fraction and the fine fraction as 109 μm , 136 μm and 35 μm , respectively (Figure 7-2). The small particle size of the wheat bran flour may explain the low yield of negatively charged fractions via electrostatic separation in this study, as also reported by Wang et al. (2015) when the particle size was reduced to 110 μm by cryogenic milling. The coulombic interaction between the oppositely charged particles is more pronounced for smaller particles, resulting in an increase in the formation of agglomerates in the charging tube. The agglomerates are most likely to end up in the positive fraction, compromising the yield of the negative-charged fractions. Therefore, the particle size of the starting material may be optimized in the future to further increase the yield of the AXF.

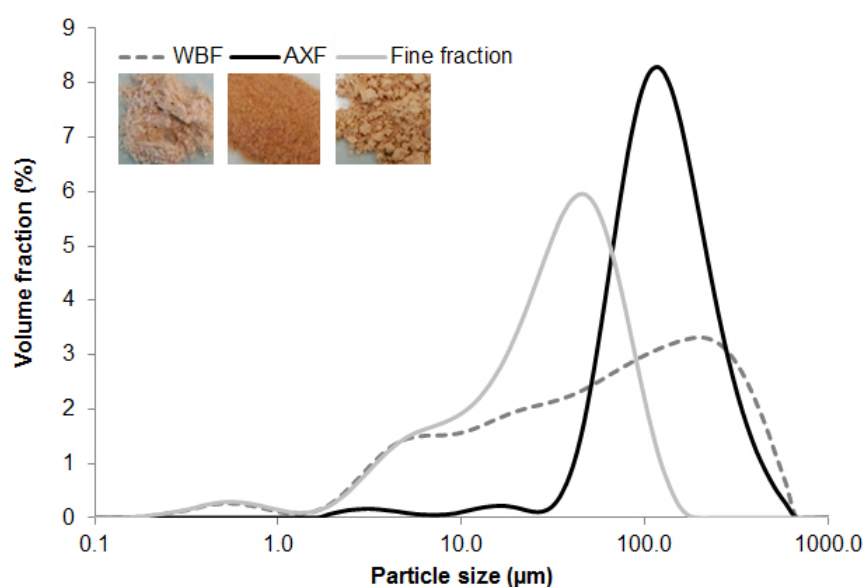


Figure 7-2. Particle size distribution and photos of wheat bran flour (WBF), arabinoxylans concentrates (AXF) and the fine fraction after sieving.

Moreover, as shown in Figure 7-2, the AXF had a brown colour due to the pigments naturally present in wheat bran (Žilić et al., 2012). The colour of the AXF was darker than the wheat bran

flour and the fine fraction obtained after air jet sieving. This is probably because the sieving step removed starch and protein which are lighter in colour. Finally, scanning electron microscope images showed the AXF contained mainly particles from the (outer) pericarp (Figure 7-3b), and the fine fraction obtained after sieving contained intact starch granules and small fragments of the pericarp (Figure 7-3c).

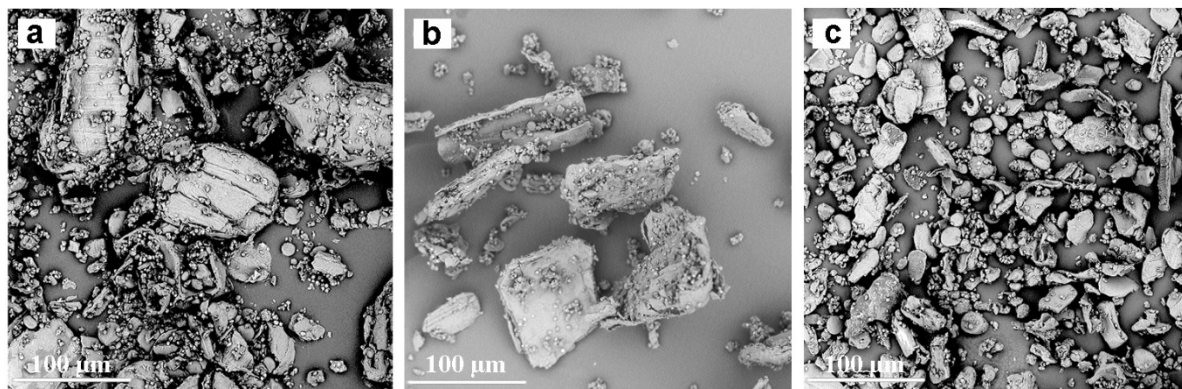


Figure 7-3. Scanning electron microscope (SEM) images of the wheat bran flour (a), the AX-rich fraction (b) and fine fraction after sieving (c). A Phenom Pure G2 SEM (Phenom-World B.V., the Netherlands) was used to record the image.

7.3.3 Quality attributes of bread fortified with AXF

According to our calculation, a loaf of 100 gram bread fortified with 2 %, 5 % or 10 % of AXF contains respectively 0.6 g, 1.6 g or 3.1 g more AX compared to the control bread. The physicochemical properties of these breads were evaluated in terms of moisture content, specific volume, colour, texture and crumb structure. In addition, the effect of enzymatic treatment on bread baking performance of the AXF was investigated.

Moisture content

Bread fortified with 10 % AXF retained significantly ($p < 0.05$) more water after baking than the control group (Figure 7-4), which is in agreement with the results of other studies (Biliaderis et al., 1995; Messina et al., 2016). This might be explained by the higher water holding capacity or water absorption of AXF, especially the water-unextractable form which has a much higher WHC (9.9 g water/g WUAX) than the water-extractable form (6.3 g water/g WEAX) (Courtin and Delcour, 2002; Goesart et al., 2008). The moisture content of the fortified bread with 10 % MAXF replacement was higher than the control mainly because the initial water content of the dough with MAXF was already higher because water was used to prepare the dough instead of

skim milk (water content $\approx 90\%$). The moisture content of the 10 % MAXF group was at the same level as the 10 % AXF group ($p>0.05$) although the initial moisture content in the dough was different, which could be attributed to the higher weight loss of the MAXF-fortified bread. In contrast, addition of 5 % AXF showed a slight decrease ($p<0.05$) in the moisture content of the baked bread, which is difficult to explain at this stage. Moisture content is an important property for bread because water acts as a plasticizer in bread and lowers the rigidity of the products. It can be expected that the textural properties of the bread can be affected by this significant change in moisture content (Besbes et al., 2014).

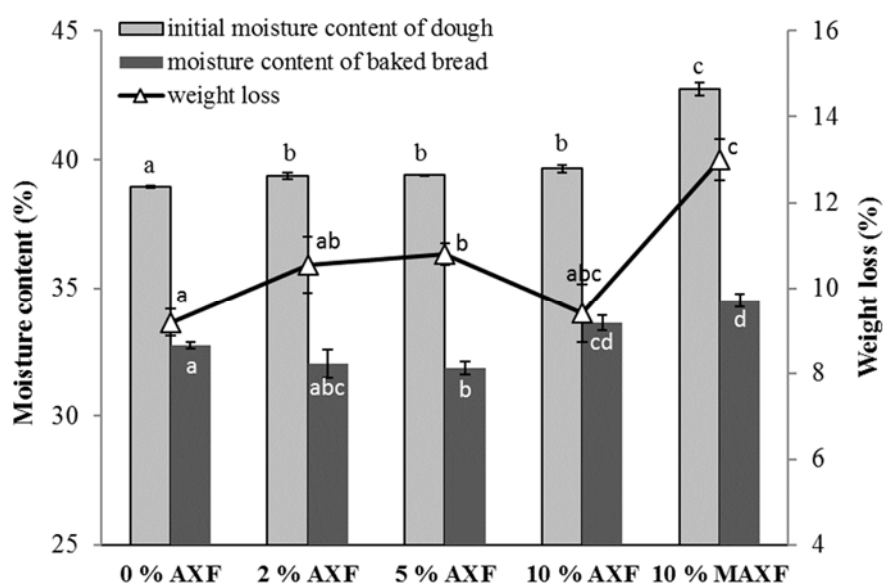


Figure 7-4. Total moisture content and weight loss of bread made with different recipes after baking (data with different superscript letters for each parameter have significant differences, $p<0.05$).

Colour analysis

As shown in Figure 7-5, the brightness (L^*) of the bread crust was negatively correlated to the level of AXF addition, while the other two parameters (a^* and b^*) increased with the increase of AXF replacement. The change in bread colour was only noticeable until an AXF replacement up to 5 %. As mentioned above, the AX-enriched fraction had a darker colour than wheat flour. Therefore, the addition of different levels of AXF results in fortified bread with different colours. Under the baking conditions in this study (205 °C, 8 min), the colour difference ΔE between the control group and the fortified bread was linearly correlated to the level of AXF supplement ($R^2=0.98$, Figure 7-5). However, the browning of the bread crust is also affected by the baking temperature and baking time, and the relatively pale colour of the control bread was due to the

short duration of baking. The colour difference between the fortified breads and the control bread is expected to be less significant when a higher baking temperature or a longer baking time is applied. Moreover, the difference in colour of the baked breads with addition of 10 % AXF and 10 % MAXF was not significant ($p>0.05$), indicating that the enzyme treatment did not alter the colour of the AXF.

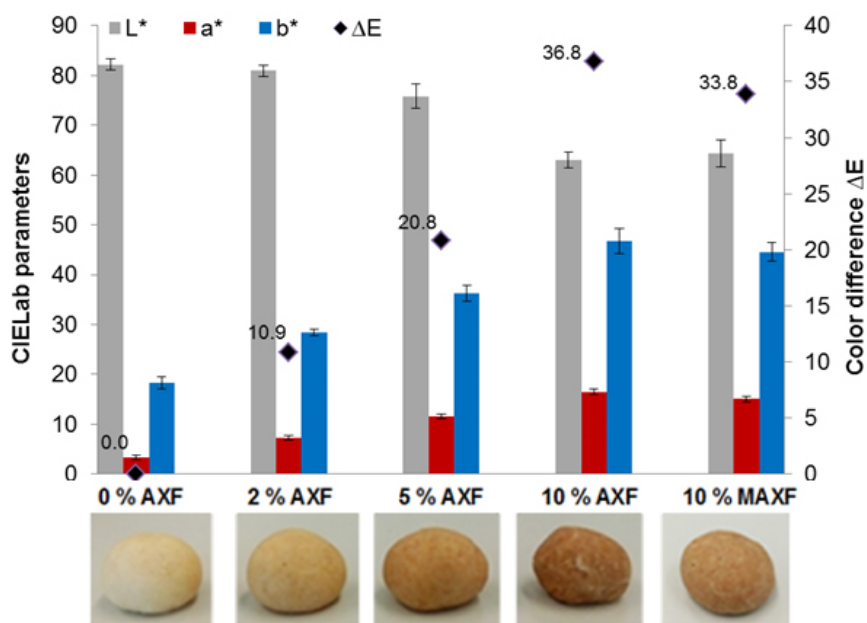


Figure 7-5. CIELab parameters and digital photos of the bread samples after baking, and the colour difference (ΔE) between the fortified breads and the control group.

Texture profile analysis

The texture of the crumb is one of the most important quality indicators of bread. Texture profile analysis (TPA) is used to imitate the chewing action of the teeth, and textural properties (hardness, chewiness, cohesiveness, elasticity) are determined (Bourne, 2002). Table 7-2 shows the impact of AXF addition on those textural properties. The change in crumb hardness (defined as the force required to compress the sample) was not significant ($p>0.05$) with replacement of AXF up to 5 %. However, the crumb hardness of bread with 10 % AXF replacement was found to be the highest ($p<0.05$), which is most likely explained by the interaction between AX and gluten forming a composite hydrated film network and the increased water absorption of AX in the dough, leaving less in the other components, which affects the texture of breadcrumb (Biliaderis et al., 1995). In addition, water-unextractable arabinoxylans (WUAX) molecules in the AXF have high water absorption, which can lower the stability of the dough foam and eventually reduce the loaf volume and increase the density of

the bread matrix. Consequently, the crumb hardness of the fortified bread (10 % AXF) increased because of its higher density (Curti et al., 2013).

Table 7-2. Textural profile analysis (TPA) of the fortified bread

Samples	Parameters			
	Hardness (N)	Chewiness (N)	Cohesiveness (-)	Elasticity (-)
0 % AXF	4.42 ^b ± 0.42	2.99 ^c ± 0.42	0.79 ^c ± 0.02	0.84 ^d ± 0.02
2 % AXF	3.90 ^{ab} ± 0.72	2.52 ^{abc} ± 0.42	0.77 ^c ± 0.01	0.85 ^{cd} ± 0.01
5 % AXF	3.55 ^{ab} ± 0.21	2.01 ^a ± 0.18	0.72 ^b ± 0.01	0.79 ^b ± 0.02
10 % AXF	7.13 ^c ± 0.69	3.05 ^c ± 0.20	0.63 ^a ± 0.02	0.69 ^a ± 0.01
10 % MAXF	2.94 ^a ± 0.55	1.37 ^b ± 0.16	0.68 ^{abc} ± 0.05	0.72 ^{abc} ± 0.04

^{a-d} Parameters (mean ± SE) with different superscript letters within the same column have significant differences ($p < 0.05$).


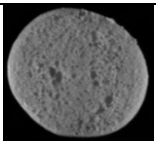
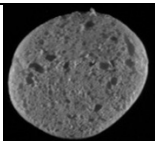
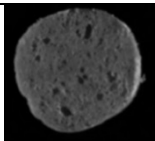
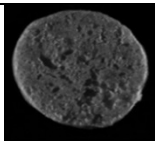
As for chewiness (defined as the energy required to masticate solid foods), a significant decrease was observed with 5 % AXF replacement. The crumb chewiness of 10 % AXF replacement was comparable to the control group, but significantly higher than the bread with 5 % AXF replacement, which is probably due to the change in the cellular structure of the crumb matrix with increasing of AXF concentration in bread. In addition, the cohesiveness and elasticity (or springiness) of bread crumb were negatively related to the level of AXF replacement. The cohesiveness is the ratio of the positive areas under the first and second compressions of the crumb, and the elasticity indicates how well the crumb physically springs back after a deformation caused by the first compression (Bourne, 2002). The decreased cohesiveness and elasticity of AXF fortified bread indicate the detrimental influence of added AXF on bread quality (Heiniö et al., 2016).

Our study shows that, in terms of textural properties, bread with 2 % AXF replacement was not significantly ($p > 0.05$) different from the control group, but a larger addition of AXF negatively affects the textural properties of the bread crumb. Moreover, the significantly decreased hardness (from 7.13 N to 2.94 N) and chewiness (from 3.05 N to 1.37 N) values for the 10 % AXF replacement and 10 % MAXF replacement, indicate a positive effect of the enzymatic treatment of the AXF on the textural properties of the final baked bread. However, as for the cohesiveness and elasticity, the influence of the enzymatic treatment was not statistically significant.

Specific volume and cellular structure analysis

Physical properties of bread that are related to crumb structure are cell wall thickness and porosity (Besbes et al., 2013). Table 7-3 shows that addition of the AXF up to 10 % leads to larger porosity ($p<0.05$) and a coarser, more irregular cellular structure of the fortified bread (see images of the cross section, Table 7-3). The coarseness of the crumb was probably caused by the high water retention of AX, which limits the amount of water available to participate in gluten formation in the bread dough, resulting in a poor gluten network (Li et al., 2012). In addition, WUAX in the AXF is reported for its negative effect on bread crumb structure, as it destabilizes gas cells by forming a physical barrier or inducing coalescence by disrupting the cell wall film (Courtin and Delcour, 2002; Kiszonas, 2013). In this study, a no-resting-time bread-making procedure was applied, which means the dough is divided into small pieces immediately after mixing and then moulded, proved and baked. In the industrial production process of bread, a bulk fermentation step can be added after dough mixing, which may result in better homogeneity and more regular cells in the end products of the fortified breads (Millar and Tucker, 2012). However, the difference in the average cell wall thickness among different groups was not statistically significant ($p>0.05$) in the present work, indicating a similar homogeneity of the crumb cellular structure among groups (Della Valle et al., 2014). This is inconsistent with our observation on the images of the cross-sections and the different porosity of the samples (Table 7-3), and therefore the mean cell wall thickness may not be used as the only parameter to quantify the bread crumb structure.

Table 7-3. Specific volume and structural properties of the bread crumb

Parameters	0 % AXF	2 % AXF	5 % AXF	10 % AXF	10 % MAXF
Cross-section (C-cell scan)					
Cell wall thickness (mm)	0.43 ^a ±0.06	0.37 ^a ±0.10	0.29 ^a ±0.03	0.44 ^a ±0.10	0.46 ^a ±0.03
Porosity (%)	39.95 ^a ±0.40	40.65 ^{ab} ±0.26	42.00 ^c ±0.27	42.63 ^{bc} ±0.71	46.58 ^d ±0.62
Specific volume (cm ³ /g)	7.09 ^b ±0.40	7.60 ^b ±0.17	7.60 ^b ±0.26	4.42 ^a ±0.62	6.50 ^{ab} ±0.72

^{a-d} Parameters (mean ± SE) with different superscript letters within the same row have significant differences ($p<0.05$).

Although a volume decrease was expected, a slight increase in the specific volume was observed when the wheat flour was replaced with AXF up to a level of 5 % (Table 7-3); however larger additions (10 %) gave a significant decrease in the specific volume. A similar observation was reported by Biliaderis et al. (1995): the initial increase in the volume is probably due to the increased strength and elasticity of the gluten-starch composite network, and the consequent decrease in volume is caused by the increased viscosity, imbalanced viscoelasticity and poor gas retention by the dough system with further addition of arabinoxylans. There is therefore an optimum concentration of AX with a maximum beneficial effect on the specific volume of bread. This optimum concentration will depend on the properties of the AX fractions such as the ratio of WUAX to WEAX (Goesaert et al., 2005).

The porosity of the fortified bread with 10 % MAXF (AXF that is enzymatically modified) replacement was larger obtained with 10 % AXF. The release of ferulic acid bound to arabinoxylans results in less cross-linking between AX and the gluten network, and subsequently more coalescence (Courtin and Delcour, 2002). This coalescence results in a more irregular and coarser crumb structure. The specific volume of the fortified bread with 10 % MAXF replacement was similar to the control group.

Free ferulic acid analysis

AX consists of β -(1,4)-linked D-xylopyranosyl residues, to which ferulic acid maybe linked as side group. D-xylopyranosyl residue can be substituted on C(O)-3 with a L -arabinofuranosyl residue, ferulic acid can be esterified to C(O)-5 of a L -arabinofuranosyl (Goesaert et al., 2005). The free ferulic acid (FFA) concentration increased by 226 % from 148.98 ± 3.91 $\mu\text{g/g}$ in the AXF to 338.61 ± 8.38 $\mu\text{g/g}$ in the MAXF upon the enzymatic treatment using feruloyl esterase. The main result of oxidative cross-linking caused by ferulic acid residues in AX molecules is a strong increase in the viscosity of AX (Courtin and Delcour, 2002). After enzymatic treatment, the bread fortified with 10 % of MAXF showed better textural properties and similar specific volume compared to the control bread. The reason for this might be the release of ferulic acid residues from AX, which reduces the water holding capacity. However, another explanation could be the increased moisture content of the dough which resulted in a relatively high moisture content of the baked bread (Figure 7-4). The moisture content may influence the expansion of the dough during proofing and thus the textural properties of the final baked bread. Therefore, Farinograph analysis is advised to adapt the amount of added water to the bread recipes to achieve optimal dough consistency (500 Farinograph Units) in future research (Shimizu et al., 2003).

In addition, the enzymatic treatment could improve the bioaccessibility of ferulic acid from the wheat bran matrix, and the increased levels of FFA are associated with anti-oxidative and anti-inflammatory effects (Anson et al., 2009). However, feruloyl esterase alone can release only a limited amount of ferulic acid from AX. The release of FFA is expected to be more efficient when xylanase (endo-1,4- β -d-xylanase, EC 3.2.1.8) is present due to the synergistic effect of xylanase on feruloyl esterase (Faulds et al., 2003). Xylanases can also solubilize WU-AX to decrease its water binding capacity and reduce WE-AX into small molecules (van Oort, 2010), which positively affect the quality of the fortified bread. To maximally mitigate the detrimental effect of AXF on quality attributes of bread, the enzymatic treatment procedure could be further optimized. Moreover, for future research, pre-treatment of the AXF without adding enzymes should be set as a blank group to eliminate the possible influence of endogenous xylanase present in the AXF on its bread baking performance (Gys et al., 2004).

7.4 Conclusions

Dry fractionation of wheat bran yielded an AX-enriched fraction (AXF) with an AX content of 55.6 % dm. The quality of bread with 2 % or 5 % of this AXF was not significantly different ($p>0.05$) or only slightly different from the control bread, respectively, while the addition of 10 % AXF strongly influenced the bread quality. After enzymatic treatment of the AXF, the fortified bread with 10 % modified AXF addition showed better textural properties and similar specific volume compared to the control bread. These results indicate that the palatability of the AX-fortified bread can be improved by optimizing the recipe or by enzymatic pre-treatment of the AXF. In conclusion, this work shows the potential of employing dry fractionated AX-enriched fractions as a supplement to bread, which may provide a new reference to prepare tasteful bread products with improved nutritional value.

Appendix 7-A. Literature review

Table 7-A1 listed some previous studies on the AX-fortified bread. The source of AX are mainly wheat bran or purified AX. It is difficult in establishing accurate comparisons among different studies due to the large variation in experimental conditions. Generally, the supplementation of wheat flour with bran and AX-rich fractions detrimentally affects the properties of dough and bread, e.g., (Farinograph) water absorption of dough was increased and specific volume of bread was decreased. Nevertheless, the baking properties of bread were improved by mixing enzyme solution into dough and by conducting (enzymatic) pretreatment on fiber-rich fractions.

Appendix 7-B. Calibration curve of ferulic acid

The calibration curve for HPLC analysis of ferulic acid was obtained by plotting the peak areas against the concentrations of pure ferulic acid (Figure 7-B1). The concentration of free ferulic acid in each fraction was calculated according to the calibration curve.

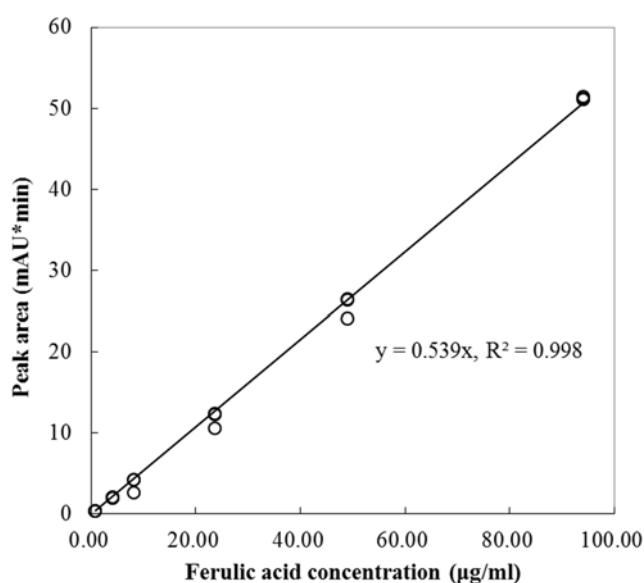


Figure 7-B1. Calibration curve of ferulic acid concentration.

Table 7-A1. List of some studies on the quality attributes of AX-fortified wheat bread.

Source of AX	AX content	Treatment	Effect	Reference
wheat bran	-	bran was ground into fractions with different particle size	fine bran had larger adverse effects than coarse or medium sized bran on loaf volume and crumb colour	(Zhang and Moore, 1999)
whole wheat flour	-	xylanase added to dough 12 U/g whole wheat flour	decreased water absorption; increased dough rising, final moisture content, specific volume; better sensory properties.	(Shah et al., 2006)
wheat bran	18 %	xylanase added to dough 5.1 U/g and 10.2 U/g bran-flour mix	increased AXOS content; increased bread loaf volume	(Damen et al., 2012)
wheat bran (toasted coarse wheat fibre)	-	0~20 g/100 g flour replacement level	reduced specific volume and crumb luminosity; increased high speed mixing time	(Almeida et al., 2012)
wheat bran	20.1 %, and 18.7 % before and after fermentation	pre-fermented bran using bacteria and enzyme mixture was added to dough	crumb chroma and crumb moisture content. AX solubility was affected, improving bread making quality, water balance and overall characteristics	(Messia et al., 2016)
wheat milling by-products	coarse bran 25.5 %; coarse weating 20.5 %; fine weating 16.1%; low grade flour 9.1 %	15 % replacement level	increased Farinograph water absorption and dough development time; fine weating and low grade flour decreased specific volume more than coarse bran and course weating	(Hemdane et al., 2015)

wheat bran	11.1~26.1 % in bran pearling fractions, 21.4 % in ground bran.	bran fractions was obtained from sequential pearling of wheat kernels; regular bran was ground to reduce particle size	the pericarp rich fraction (AX-rich) had the highest water binding/retention capacity, which negatively affected bread quality.	(Hemdane et al., 2016)
wholegrain concentrate	-	pre-fermentation of wholegrain concentrate using enzymes and yeast	optimised pre-fermentation of the wholegrain concentrate resulted in bread with higher volume and softer crumb	(Noort et al., 2017)
purified AX	-	AX with different molecular weight (MW) was evaluated: high MW(201600) and low MW (134600)	both increased water absorption and development time of dough, loaf volume; bread with HMW AX retained more water and bread was softer during storage	(Biliaderis et al., 1995)
purified AX	LMW-AX 87 % HMW-AX 88.6 %	AX with different molecular weight (MW) was evaluated: high MW(555300) and low MW (50300)	both increased loaf volume of small bread (10 g), addition level is correlated with loaf volume response	(Courtin and Delcour, 1998)
arabinoxylan	crude AX extract 44.3 %; partially purified AX extract 49.3 %	adjust the dosage of AX in the range of 2 to 3 % (w/w) flour replacement	increased water absorption; 2.5 % flour replacement level resulted in bread with similar quality as the control	(Koegelberg and Chimphango, 2016)

Chapter 8

General discussion



8.1 Introduction

Two major challenges in the development of functional bread are the retention of the functionality of bioactives during baking and the influence of the supplementation of the active ingredients on the product quality. Therefore, in this thesis, we aimed at understanding the impact of baking on the functionality of heat-sensitive bioactives (e.g. enzyme and probiotics), and the influence of fibre-fortification on the quality attributes of bread. This chapter discusses the main findings of this thesis and concludes with an outlook towards future research.

8.2 Main findings

An experimental miniature bread baking method was developed to study the bread baking process at lab scale (**chapter 2**). Mini-breads were observed to behave similar to regular-sized bread in terms of quality-related properties such as crumb formation, crust thickness and colour, and moisture content. Moreover, the spatial reaction engineering approach (S-REA) accurately described the browning kinetics during mini-bread baking. The results indicate that miniature bread baking approach is an efficient alternative to baking experiments with regular-sized breads, while being less time- and resource-consuming. This approach is especially practical when the active ingredients studied are expensive or not readily available in quantity. In this thesis the miniature bread baking approach was used to efficiently collect experimental data to better understand the impact of baking on active ingredients.

In **chapter 3**, the thermal inactivation of a model enzyme, β -galactosidase, was investigated during isothermal heating and bread baking experiments. The thermal inactivation of this enzyme in the wheat flour/water system during isothermal heating could be accurately described by a first order kinetic model which described the influence of both temperature and moisture content. During bread baking experiments, it was found that despite the higher temperature, the residual enzyme activity in the crust was higher than in the crumb, which suggests that the lower moisture content of the crust significantly enhances the thermostability of the enzyme. Another explanation of the improved thermostability is the dense and glassy microstructure of the crust, which may affect the kinetics of the inactivation as well.

Subsequently, the influence of baking on the retention of living probiotic bacteria was studied in **chapter 4**. The residual viability of *Lactobacillus plantarum* P8 was higher in the bread crust than in the crumb during baking at a relatively low temperature (175 °C) in spite of the higher temperature reached in the crust. Also here it is expected that the thermostability of bacteria is

better due to the lower moisture content and the dense glassy microstructure of the crust during baking. Moreover, re-growth of *L. plantarum* P8 in bread occurred during storage, leading to an increase in the bacterial viability by 2~3 log CFU/g. Overall, the results indicate that the inactivation mechanism of probiotic bacteria during baking is affected by the temperature, the moisture content and the microstructure of the bread matrix. The recovery of bacterial viability during storage is also relevant, and could constitute a strategy to increase the viable counts of probiotics in bread before consumption.

Chapter 5 investigates the inactivation mechanism of probiotics during baking via the development of rate-dependent kinetic models to describe the survival curves of bacteria during baking. Following several earlier studies, the changing rates of temperature and moisture content in the bread matrix were introduced as variables in these models, because they may induce thermal and dehydration stress to the cells and thus contribute to the inactivation of probiotics. Several models were evaluated using statistical criteria. Finally, a rate-dependent model that includes the temperature (T), the moisture content (X) and the rate of temperature change (dT/dt) was found to best describe the survival curves of bacteria during baking. The proposed rate-dependent model may be used to optimize baking processes to maximize the survival of probiotics. However, the applicability of the developed kinetic models is limited to baking applications given the small variation in moisture content and temperatures during the baking process.

Encapsulating probiotics with dry protectants may change the inactivation kinetics of bacteria during thermal treatment. In **chapter 6**, *L. plantarum* P8 was freeze-dried in reconstituted skim milk (RSM), gum arabic (GA), maltodextrin and inulin matrices. The dry bacterial powders were then exposed to heat, during which the survival of bacteria was assessed. The high glass transition temperature and the dense microstructure of RSM and GA favoured the survival of bacteria during isothermal heating. Subsequently, the dry powders were incorporated into bread using different approaches. Maximum survival of probiotics ($>10^8$ CFU/g bread) was obtained when the RSM-probiotic powder was applied on the dough surface and a lower baking temperature (100 °C) was used. The low hygroscopicity of RSM may delay the penetration of water into the powder, which maintained the relatively low moisture content of the environment where the bacteria cells were exposed to. Overall, the results indicate that the viability of probiotics in bread can be improved by rational design of the encapsulating materials and the processing conditions (e.g. low-temperature baking).

It is also of importance to understand how the addition of active ingredients affects the product quality. Arabinoxylans (AX) are the major dietary fibre in wheat bran, which can be enriched by dry fractionation. Fortification of bread with AX increases the daily consumption of dietary fibre which may provide health benefits to the consumers. However, as studied in **chapter 7**, the addition of large amounts of dry-fractionated arabinoxylans-enriched fraction (AXF) strongly influences the quality of the bread. Pre-treatment of AXF using enzyme (feruloyl esterase) mitigated the detrimental effect of AXF on the quality attributes of bread. In this way, bread with high fibre content and acceptable sensory properties can be obtained.

8.3 Outlook

The development of novel functional foods is accelerated by the increasing health awareness among consumers. Bakery products, as an emerging category within the functional food segment, have stimulated much research interest. The baking industry is seeking for technologies to introduce innovative ingredients (e.g. probiotics, prebiotics), to improve the product quality (e.g. longer shelf-life, better sensory properties), and to develop products for specific market segments (e.g. gluten-free, lactose-free products). Based on the findings of this thesis, it is clear that the interaction between the baking process and the fate of active ingredients is rather complex. To better retain the functionality of active ingredients and to produce products with good quality, there are still many questions to be resolved. This section discusses these research questions from the combined perspective of process engineering, microbiology and human nutrition.

8.3.1 Mild baking procedures

The active ingredients supplemented to bread partially or completely lose their bioactivity due to the high temperature encountered during baking. It is clear that lowering the baking temperature can increase the viable counts of probiotics in the baked bread. However, the physicochemical properties of bread are influenced by changing the processing conditions. For example, the sensory properties of bread are significantly altered when the mini-bread was baked at 100 °C; bread with a very thin crust and a light crust colour was obtained (see Figure 6-5 in **chapter 6**). Therefore, to maximally retain the functionality of active ingredient, the baking process should be optimized without influencing the quality of bread to any great extent.

Using microwave as a heating resource during baking may benefit the survival of the probiotics due to the shortened processing time. The microwave generates heat inside the product by

enhancing the movement of water molecules, thus accelerating the evaporation of water in the product. It is worth noting that using microwave alone may cause incomplete starch gelatinization, poor flavour development and less browning of the crust due to the short baking time. Nevertheless, a combined convective and microwave operation could be a viable solution, which can effectively shorten the baking time and at the same time better control the quality of bread (Hadiyanto, 2007).

8.3.2 Model development to optimise baking process

Kinetic models were used to describe the thermal inactivation of enzyme and probiotics in this thesis (**chapters 3, 5, and 6**). The kinetic analyses show that besides temperature the moisture content of the bread matrix has a major influence on the thermostability of heat-sensitive ingredients. It is therefore wise to maximize this positive effect of the low moisture content on the thermostability of active ingredients by optimizing the baking process, for example by incorporation of bioactives primarily in the crust region or in products which have low moisture content. Although the models describe the inactivation kinetics during isothermal heating of the model systems in an accurate manner, the ability of these models to accurately predict the residual enzyme activity or bacterial viability during actual baking process is still challenging.

For process optimisation, more reliable kinetic models could be developed by: i) collecting more accurate inactivation data during isothermal experiments for model development and/or validation; ii) considering the spatial distribution of temperature and moisture content inside the bread matrix during baking; and iii) including the influence of other factors (e.g. food microstructure, salt content, pH) on the inactivation kinetics, amongst other factors. Ideally, one would map the viability of active ingredients inside the bread matrix by combining kinetic models with physical models of baking, for example, heat and mass transfer models (Papasidero et al., 2015; Zhang and Datta, 2006) or the S-REA model (**chapter 2**) (Putranto et al., 2015). However, such an approach is challenging, not only due to the complexity of the physical phenomena, but also due to the difficulty in acquiring accurate experimental data for model validation.

8.3.3 Protecting probiotics during thermal processing

Encapsulation of probiotics

Encapsulation is employed in food systems to increase the chemical or physical stability of the active ingredients, to reduce the incompatibility between active ingredients and the food matrix, or to improve the bioavailability of nutrients (Ubbink and Kruger, 2006). In **chapter 6**, freeze-dried probiotic powders were incorporated into the bread matrix in two ways: i) mixing the powder with the other ingredients before preparing the dough; ii) distributing the powder onto the surface of the dough. Compared to the first approach, the second approach is more effective to delay the water absorption of the powder from the dough; indeed, the structure of the microcapsules was better maintained, and the viability of probiotics in bread produced by using the second approach was higher than the first one due to the positive effects of the lower moisture content and the presence of protectant on the survival of bacteria during baking. For application onto the surface of dough, encapsulating materials with a lower hygroscopicity (e.g. RSM) are superior because the penetration of water from the food matrix into the microcapsules was hindered to some extent. Hence, the direct environment of the bacteria cells stayed relatively dry.

A stronger protective matrix for probiotics is required when the microcapsules are intended to be supplemented into the whole bread matrix or when a higher baking temperature ($>175\text{ }^{\circ}\text{C}$ in chapter 6) is used. In this context, a multi-layered encapsulation structure as proposed by Pitigraisorn, et al. (2017) could be promising. *Lactobacillus acidophilus* cells were encapsulated in alginate-based microcapsules coated with egg albumin (EA) and stearic acid (SA) as the first layer, and with cassava starch granules as a second layer. The resistance of *L. acidophilus* upon exposure to a humid and hot environment ($70\text{ }^{\circ}\text{C}$ and 100 \% RH) was significantly improved, because the increased gel strength of the EA-starch composite matrix led to a higher level of heat resistance, while the SA inhibited the diffusion of water into the microcapsules. Therefore, based on the abovementioned results, it is envisaged that the heat resistance of probiotics can be further improved by protecting the cells in microcapsules (Figure 8-1) with the following properties: i) high glass transition temperature T_g ; ii) low thermal diffusivity and iii) high hydrophobicity. However, the considerable difference in moisture content between the dough matrix and the microcapsules is still of concern, which can provide a driving force for the fast moisture migration from the dough to the dry powder during processing.

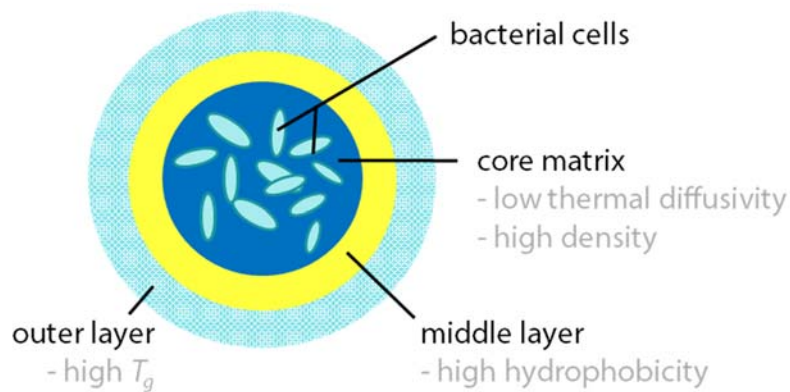


Figure 8-1. A conceptual design of multi-layered microcapsules: the core matrix provides mechanical support to the bacterial cells; the hydrophobic middle layer hinders the penetration of water towards the core; the outer layer maintains the whole structure in a glassy state upon heating.

Moreover, the influence of the food microstructure on the thermal inactivation and the functionality of active ingredients is considerable (Jin and Chen, 2018). The microstructure of a food matrix may yield a shielding effect against thermal degradation of active ingredients. For example, the degradation rates of anthocyanins (cyaniding-3-glucoside and cyaniding-3-rutinoside) were lower in a bread system than in aqueous solutions (Sui et al., 2015), which might be attributed to the high solid content or the low availability of oxygen in bread. In addition, the matrix of microcapsules (such as gum acacia and milk protein) may function as a buffering agent which protects probiotics during transit through the upper gastrointestinal tract (Huang et al., 2017), and the bread matrix may set up a physical barrier which hinders or delays the loss of functionality during digestion as well.

Enhancing the robustness of bacteria

From a microbiological perspective, enhancing the robustness of probiotics during thermal processing could be a feasible strategy to improve the retention of bacterial viability in bakery products. One approach to enhance the robustness of probiotics is through intracellular protection, which is less intensively studied compared to extracellular protection (i.e. encapsulation) (Termont et al., 2006). For example, increased intracellular trehalose content in *Lactobacillus plantarum* WCFS1 cells after pulsed electric field (PEF) treatment may enhance bacterial robustness during drying (Vaessen et al., 2018). Optimization of such treatment is required for real application, to improve the population of reversibly electroporated cells which contain trehalose. The protective effect of intracellular accumulation of trehalose on drying (thermal- and cryo-) damage should be investigated as well. Furthermore, there are other

strategies to increase the thermal tolerance of probiotics: i) inducing heat shock proteins expression in the cells after exposure to sub-lethal heat stress (De Angelis et al., 2004); ii) selecting robust probiotic strains with regard to their successful inclusion in bakery products (Sánchez et al., 2012).

8.3.4 Innovative food processing

3D food printing

The probiotics survived better in the crust of the mini-bread than in the crumb under certain baking conditions (**chapter 4**). Thus, creating more crust area by increasing the surface-to-volume ratio of food structures may improve the survival of probiotics. In this context, wheat-flour-based food structures with a high surface-to-volume ratio (Figure 8-2) were created by using extrusion-based three-dimensional (3D) printing which offers more flexibility in achieving complex structures compared to conventional methods. An optimal formulation formed by wheat flour (39 g), water (30 g), calcium caseinate (1.17 g) and *Lactobacillus plantarum* WCFS1 (initial viable count $\approx 10^9$ CFU/g) was used for 3D printing. The addition of calcium caseinate significantly improved the printability by shifting the viscoelastic properties of the dough towards a strong gel (Ahmed et al., 2017).

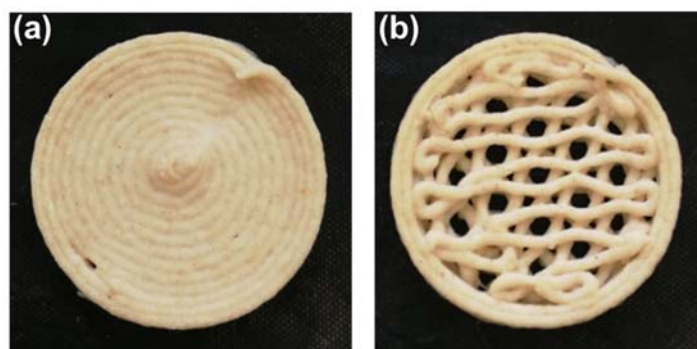


Figure 8-2. Digital photos of 3D-printed wheat-flour-based food structures with two different geometric designs (a: concentric; b: honeycomb); diameter: 4 cm, printed layer: 4, thickness: 0.32 cm; the estimated surface-to-volume ratio of the concentric design was $7.2 \text{ m}^2/\text{m}^3$ while the value of the honeycomb design was $9.2 \text{ m}^2/\text{m}^3$.

After printing, post-processing (i.e. baking) was carried out to solidify the structures. The survival of probiotics incorporated in the structure was determined after baking. When the residual viability of *L. plantarum* WCFS1 was plotted against the baking time, the difference in

the survival of probiotics in the two structures was not significant (Figure 8-3 a1~a3). However, the completion of the baking process may also be judged by the moisture content of the structure. In this case, the required baking time for the ‘honeycomb’ design was shorter than the ‘concentric’ one due to its higher surface-to-volume ratio (i.e. higher drying rate). Thus, at a baking temperature of 145 or 175 °C, the residual viability of the bacteria in the ‘honeycomb’ structure was about 1 log higher than in the ‘concentric’ one at the same moisture content (e.g. 40 %) (Figure 8-3 b1~b2). Nevertheless, further increase of the baking temperature to 205 °C resulted in an even faster drying process but a similar survival of bacteria in the two designs was observed (Figure 8-3 b3). These results indicate that it is possible to improve the survival of probiotics in food structures during baking by applying 3D printing technique, but optimization of the formulation of the printing materials, the geometric design and the post-processing conditions are necessary to obtain an even higher viability of probiotics in the final products.

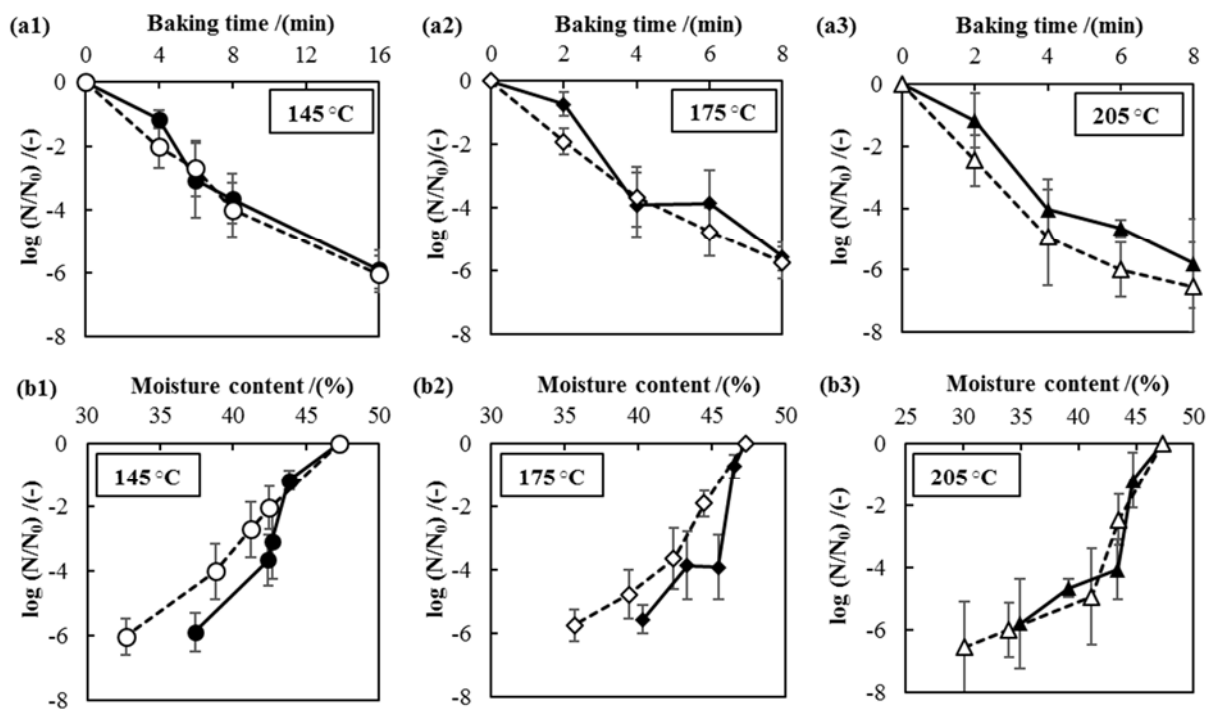


Figure 8-3. Residual viability of *L. plantarum* WCFS1 in two 3D-printed structures during baking at 145 °C (○ honeycomb, ● concentric); 175 °C (◇ honeycomb, ◆ concentric); 205 °C (Δ honeycomb, ▲ concentric), which was plotted against the baking time (a1~a3) and the residual moisture content of the object (b1~b3), respectively.

Synbiotic bread production

Briefly, synbiotics can be defined as synergistic combinations of probiotics and prebiotics. As mentioned above, survival of probiotics during thermal processing can be improved by physical protection by encapsulation. The incorporation of prebiotics in the protective agents can result in microcapsules with decreased moisture content and water activity after drying and a higher stability during storage (Fritzen-Freire et al., 2012). In this case, “synbiotic bread” may be produced by supplementation of such synbiotic microcapsules (Seyedain-Ardabili et al., 2012). In addition, Damen et al. (2012) reported the *in situ* production of arabinoxylan oligosaccharides (AXOS) during bread baking due to the degradation of arabinoxylans (AX) by xylanases. Therefore, enzymatic treatment of dry-fractionated AX-enriched fractions using xylanases is expected to increase the AXOS content in the final bread. Thus, synbiotic bread can be obtained by incorporating probiotics in bread with high content of AXOS which have prebiotic properties.

8.3.5 Impact of functional bread on health

The main reason for the development of functional foods is the potential effects of some active ingredients on human health. The interest in probiotic foods is growing because the understanding of the link between the human gut microbiome and certain disease is rapidly expanding (Gilbert et al., 2018). Long-term dietary interventions (e.g. daily consumption of probiotics) largely affect the gut microbiome composition, which may modulate an individual's enterotype (Wu et al., 2011). However, contradictory results are reported for the effects of probiotics on consumers. Thus, the demand of personalization of nutritional recommendation is of concern given the large intersubjective variation. Therefore, studies should be carried out to investigate the actual health-promoting benefits of functional bread or other functional bakery products, comprising all aspects of the digestion process, preferably with consumer or through clinical trials.

On the one hand, the bioactivity in functional foods should be well-preserved (e.g. by encapsulating using protectants) before consumption and/or during digestion to exert positive effects on human health. However, the protective effect of the encapsulating matrix may hinder the interaction between the probiotics and host mucosa, which may alleviate the beneficial effects of probiotic metabolite (Huang, 2017). Therefore, the protectants and the encapsulation strategy used to produce microcapsules of active ingredients should be well-chosen, to better control the targeted delivery of these ingredients without silencing their beneficial effects.

8.4 General conclusion

Bread is an interesting vehicle for the delivery of functional ingredients into the human diet due to its large daily consumption over the world. However, the harsh conditions encountered during baking significantly affect the activity of those ingredients. Therefore, feasible strategies need to be developed to better protect the active ingredients during baking. In this thesis experimental study on mini-breads was combined with kinetic modelling, to provide in-depth understanding of the interaction between the active ingredients and the baking process. The knowledge gained on the inactivation mechanisms of bioactives during baking and the influence of using microcapsules or fortification with fibre on the quality of the bread could accelerate the development of these functional bakery products.

References

References

- Adams, J.B., 1991. Review: Enzyme inactivation during heat processing of foodstuffs. *Int. J. Food Sci. Technol.* 26, 1–20.
- Ahmed, J., Ptaszek, P., Basu, S. (Eds.), 2017. *Advances in Food Rheology and Its Applications*. Elsevier Ltd.
- Al-Sheraji, S.H., Ismail, A., Manap, M.Y., Mustafa, S., Yusof, R.M., Hassan, F.A., 2013. Prebiotics as functional foods : A review. *J. Funct. Foods* 5, 1542–1553.
- Aleixandre, A., Miguel, M., 2016. Dietary fiber and blood pressure control. *Food Funct.* 7, 1864–1871.
- Almeida, E.L., Chang, Y.K., Steel, C.J., 2013. Dietary fibre sources in bread : Influence on technological quality. *LWT - Food Sci. Technol.* 50, 545–553.
- Altamirano-Fortoul, R., Moreno-Terrazas, R., Quezada-Gallo, A., Rosell, C.M., 2012. Viability of some probiotic coatings in bread and its effect on the crust mechanical properties. *Food Hydrocoll.* 29, 166–174.
- Ansari, M.I.A., Datta, A.K., 2003. An overview of sterilization methods for packaging materials used in aseptic packaging systems. *Trans IChemE.* 81, Part C, 57–65.
- Anson, N.M., Hemery, Y.M., Bast, A., Haenen, G.R.M.M., 2012. Optimizing the bioactive potential of wheat bran by processing. *Food Funct.* 3, 362–375.
- Anson, N.M., Selinheimo, E., Havenaar, R., Aura, A.M., Mattila, I., Lehtinen, P., Bast, A., Poutanen, K., Haenen, G.R.M.M., 2009. Bioprocessing of wheat bran improves in vitro bioaccessibility and colonic metabolism of phenolic compounds. *J. Agric. Food Chem.* 57, 6148–6155.
- AOAC, 2002. *Official Methods of Analysis*, third ed. Association of Official Agricultural Chemists, Inc., Washington DC.
- Arbolea, J.-C., Lasa, D., Olabarrieta, I., de Marañon, I.M., 2010. Chapter 11: New trends for food product design, in: Smith, J., Charter, E. (Eds.), *Functional Food Product Development*. Blackwell Publishing Ltd., pp. 229–243.
- Aryani, D.C., Zwietering, M.H., den Besten, H.M.W., 2016. The effect of different matrices on the growth kinetics and heat resistance of *Listeria monocytogenes* and *Lactobacillus plantarum*. *Int. J. Food Microbiol.* 238, 326–337.
- Bataillon, M., Mathaly, P., Cardinali, A.-P.N., Duchiron, F., 1998. Extraction and purification of arabinoxylan from destarched wheat bran in a pilot scale. *Ind. Crops Prod.* 8, 37–43.
- Bayrock, D., Ingledew, W.M., 1997. Fluidized bed drying of baker's yeast: moisture levels, drying rates, and viability changes during drying. *Food Res. Int.* 30, 407–415.

- Behboudi-Jobbehdar, S., Soukoulis, C., Yonekura, L., Fisk, I., 2013. Optimization of spray-drying process conditions for the production of maximally viable microencapsulated *L. acidophilus* NCIMB 701748. *Dry. Technol.* 31, 1274–1283.
- Besbes, E., Jury, V., Monteau, J.-Y., Le Bail, A., 2014. Effect of baking conditions and storage with crust on the moisture profile, local textural properties and staling kinetics of pan bread. *LWT - Food Sci. Technol.* 58, 658–666.
- Besbes, E., Jury, V., Monteau, J.-Y., Le Bail, A., 2013. Characterizing the cellular structure of bread crumb and crust as affected by heating rate using X-ray microtomography. *J. Food Eng.* 115, 415–423.
- Bhandari, B.R., Howes, T., 1999. Implication of glass transition for the drying and stability of dried foods. *J. Food Eng.* 40, 71–79.
- Bigliardi, B., Galati, F., 2013. Innovation trends in the food industry: The case of functional foods. *Trends Food Sci. Technol.* 31, 118–129.
- Biliaderis, C.G., Izydorczyk, M.S., Rattan, O., 1995. Effect of arabinoxylans on bread-making quality of wheat flours. *Food Chem.* 53, 165–171.
- Black, B.A., Zannini, E., Curtis, J.M., Gänzle, M.G., 2013. Antifungal hydroxy fatty acids produced during sourdough fermentation: microbial and enzymatic pathways, and antifungal activity in bread. *Appl. Environ. Microbiol.* 79, 1866–1873.
- Borneo, R., Kocer, D., Ghai, G., Tepper, B.J., Karwe, M.V., 2007. Stability and consumer acceptance of long-chain omega-3 fatty acids (eicosapentaenoic acid, 20:5, n-3 and docosahexaenoic acid, 22:6, n-3) in cream-filled sandwich cookies. *J. Food Sci.* 72, S49–S54.
- Bourne, M.C., 2002. Sensory methods of texture and viscosity measurement, in: *Food Texture and Viscosity (Second Edition)*. Academic Press, New York, pp. 257–291.
- Broeckx, G., Vandenheuvel, D., Claes, I.J.J., Lebeer, S., Kiekens, F., 2016. Drying techniques of probiotic bacteria as an important step towards the development of novel pharmabiotics. *Int. J. Pharm.* 505, 303–318.
- Brownlee, I.A., Chater, P.I., Pearson, J.P., Wilcox, M.D., 2017. Dietary fibre and weight loss: Where are we now? *Food Hydrocoll.* 68, 186–191.
- Burin, L., Jouppila, K., Roos, Y.H., Kansikas, J., Buera, M.P., 2004. Retention of β -galactosidase activity as related to Maillard reaction, lactose crystallization, collapse and glass transition in low moisture whey systems. *Int. Dairy J.* 14, 517–525.
- Bustos, P., Bórquez, R., 2013. Influence of osmotic stress and encapsulating materials on the stability of autochthonous *Lactobacillus plantarum* after spray drying. *Dry. Technol.* 31, 57–66.
- Cerf, O., Davey, K.R., Sadoudi, A. K., 1996. Thermal inactivation of bacteria - a new predictive

- model for the combined effect of three environmental factors: temperature, pH and water activity. *Food Res. Int.* 29, 219–226.
- Champagne, C.P., Gardner, N.J., Roy, D., 2005. Challenges in the addition of probiotic cultures to foods. *Crit. Rev. Food Sci. Nutr.* 45, 61–84.
- Charalampopoulos, D., Wang, R., Pandiella, S.S., Webb, C., 2002. Application of cereals and cereal components in functional foods: a review. *Int. J. Food Microbiol.* 79, 131–141.
- Chávez, B.E., Ledebøer, A.M., 2007. Drying of probiotics : optimization of formulation and process to enhance storage survival. *Dry. Technol.* 25, 1193–1201.
- Chen, X.D., Patel, K.C., 2008. Biological changes during food drying processes, in: Mujumdar, A.S., Chen, X.D. (Eds.), *Drying Technologies in Food Processing*. Blackwell Publishing, UK, pp. 90–112.
- Chen, X.D., Patel, K.C., 2007. Micro-organism inactivation during drying of small droplets or thin-layer slabs - A critical review of existing kinetics models and an appraisal of the drying rate dependent model. *J. Food Eng.* 82, 1–10.
- Chen, X.D., Putranto, A., 2013. *Modelling drying processes: a reaction engineering approach*. Cambridge University Press.
- Cizeikiene, D., Juodeikiene, G., Paskevicius, A., Bartkiene, E., 2013. Antimicrobial activity of lactic acid bacteria against pathogenic and spoilage microorganism isolated from food and their control in wheat bread. *Food Control* 31, 539–545.
- Clark, J.P., 2009. *Case Studies in Food Engineering Learning from Experience*. Springer Science+Business Media.
- Collares, F.P., Finzer, J.R.D., Kieckbusch, T.G., 2004. Glass transition control of the detachment of food pastes dried over glass plates. *J. Food Eng.* 61, 261–267.
- Comunian, T.A., Favaro-Trindade, C.S., 2016. Microencapsulation using biopolymers as an alternative to produce food enhanced with phytosterols and omega-3 fatty acids: A review. *Food Hydrocoll.* 61, 442–457.
- Corcoran, B.M., Ross, R.P., Fitzgerald, G.F., Stanton, C., 2004. Comparative survival of probiotic lactobacilli spray-dried in the presence of prebiotic substances. *J. Appl. Microbiol.* 96, 1024–1039.
- Corona-Hernandez, R.I., Álvarez-Parrilla, E., Lizardi-Mendoza, J., Islas-Rubio, A.R., de la Rosa, L.A., Wall-Medrano, A., 2013. Structural stability and viability of microencapsulated probiotic bacteria: A review. *Compr. Rev. Food Sci. Food Saf.* 12, 614–628.
- Corral, M.L., Cerrutti, P., Vázquez, A., Califano, A., 2017. Bacterial nanocellulose as a potential additive for wheat bread. *Food Hydrocoll.* 67, 189–196.
- Corsetti, A., Gobbetti, M., Balestrieri, F., Paoletti, F., Russi, L., Rossi, J., 1998. Sourdough lactic acid bacteria effects on bread firmness and staling. *J. Food Sci.* 63, 347–351.

- Courtin, C.M., Delcour, J.A., 2002. Arabinoxylans and endoxylanases in wheat flour bread-making. *J. Cereal Sci.* 35, 225–243.
- Courtin, C.M., Delcour, J.A., 1998. Physicochemical and bread-making properties of low molecular weight wheat-derived arabinoxylans. *J. Agric. Food Chem.* 46, 4066–4073.
- Crowley, S. V., Kelly, A.L., Schuck, P., Jeantet, R., O'Mahony, J.A., 2016. Rehydration and solubility characteristics of high-protein dairy powders, in: McSweeney, P.L.H, O'Mahony, J.A. (Eds.), *Advanced Dairy Chemistry: Volume 1B: Proteins: Applied Aspects: Fourth Edition*. Springer Science+Business Media, New York, pp. 99-132.
- Cruz, M., Ramírez-miranda, M., Díaz-ramírez, M., Alamilla-Beltran, L., Calderon-Domínguez, G., 2017. Microstructural characterisation and glycemic index evaluation of pita bread enriched with chia mucilage. *Food Hydrocoll.* 69, 141–149.
- Cui, S.W., Wang, Q., 2009. Cell wall polysaccharides in cereals: Chemical structures and functional properties. *Struct. Chem.* 20, 291–297.
- Curti, E., Carini, E., Bonacini, G., Tribuzio, G., Vittadini, E., 2013. Effect of the addition of bran fractions on bread properties. *J. Cereal Sci.* 57, 325–332.
- Damen, B., Pollet, A., Dornez, E., Broekaert, W.F., Haesendonck, I. Van, Trogh, I., Arnaut, F., Delcour, J.A., Courtin, C.M., 2012. Xylanase-mediated in situ production of arabinoxylan oligosaccharides with prebiotic potential in whole meal breads and breads enriched with arabinoxylan rich materials. *Food Chem.* 131, 111–118.
- De Angelis, M., Di Cagno, R., Huet, C., Crecchio, C., Fox, P.F., Gobbetti, M., 2004. Heat Shock Response in *Lactobacillus plantarum*. *Appl. Environ. Microbiol.* 70, 1336–1346.
- De Prisco, A., Mauriello, G., 2016. Probiotication of foods: A focus on microencapsulation tool. *Trends Food Sci. Technol.* 48, 27–39.
- De Vries, U., Sluimer, P., Bloksma, A.H., 1989. A quantitative model for heat transport in dough and crumb during baking. *Cereal Science and Technology in Sweden: Proceedings from an International Symposium*. 174–188.
- De Vos, P., Faas, M.M., Spasojevic, M., Sikkema, J., 2010. Encapsulation for preservation of functionality and targeted delivery of bioactive food components. *Int. Dairy J.* 20, 292–302.
- Della Valle, G., Chiron, H., Cicerelli, L., Kansou, K., Katina, K., Ndiaye, A., Whitworth, M., Poutanen, K., 2014. Basic knowledge models for the design of bread texture. *Trends Food Sci. Technol.* 36, 5–14.
- Della Valle, G., Chiron, H., Jury, V., Raitière, M., Réguerre, A.-L., 2012. Kinetics of crust formation during conventional French bread baking. *J. Cereal Sci.* 56, 440–444.
- Dewettinck, K., Van Bockstaele, F., Kühne, B., Van de Walle, D., Courtens, T.M., Gellynck, X., 2008. Nutritional value of bread: Influence of processing, food interaction and consumer perception. *J. Cereal Sci.* 48, 243–257.

- Doblado-Maldonado, A.F., Arndt, E.A., Rose, D.J., 2013. Effect of salt solutions applied during wheat conditioning on lipase activity and lipid stability of whole wheat flour. *Food Chem.* 140, 204–209.
- Dziki, D., Różyło, R., Gawlik-Dziki, U., Świeca, M., 2014. Current trends in the enhancement of antioxidant activity of wheat bread by the addition of plant materials rich in phenolic compounds. *Trends Food Sci. Technol.* 40, 48–61.
- Espitia, P.J.P., Batista, R.A., Azeredo, H.M.C., Otoni, C.G., 2016. Probiotics and their potential applications in active edible films and coatings. *Food Res. Int.* 90, 42–52.
- FAO/WHO, 2002. Guidelines for the evaluation of probiotics in food. Food and Agricultural Organization of the United Nations and World Health Organization Working Group Report. London Ontario, Canada.
- Faulds, C.B., Zanichelli, D., Crepin, V.F., Connerton, I.F., Juge, N., Bhat, M.K., Waldron, K.W., 2003. Specificity of feruloyl esterases for water-extractable and water-unextractable feruloylated polysaccharides: Influence of xylanase. *J. Cereal Sci.* 38, 281–288.
- Fernandes, R., Borges, S.V., Botrel, D.A., 2014. Gum arabic/starch/maltodextrin/inulin as wall materials on the microencapsulation of rosemary essential oil. *Carbohydr. Polym.* 101, 524–532.
- Foerst, P., Kulozik, U., 2012. Modelling the dynamic inactivation of the probiotic bacterium *L. paracasei* ssp. *paracasei* during a low-temperature drying process based on stationary data in concentrated systems. *Food Bioprocess Technol.* 5, 2419–2427.
- Fonseca, F., Obert, J.P., Béal, C., Marin, M., 2001. State diagrams and sorption isotherms of bacterial suspensions and fermented medium. *Thermochim. Acta* 366, 167–182.
- Fritzen-Freire, C.B., Prudêncio, E.S., Amboni, R.D.M.C., Pinto, S.S., Negrão-Murakami, A.N., Murakami, F.S., 2012. Microencapsulation of bifidobacteria by spray drying in the presence of prebiotics. *Food Res. Int.* 45, 306–312.
- Fu, N., Chen, X.D., 2011. Towards a maximal cell survival in convective thermal drying processes. *Food Res. Int.* 44, 1127–1149.
- Fu, N., Woo, M.W., Selomulya, C., Chen, X.D., 2013. Inactivation of *Lactococcus lactis* ssp. *cremoris* cells in a droplet during convective drying. *Biochem. Eng. J.* 79, 46–56.
- Garzón, R., Rosell, C.M., 2014. A sistematic study of breadmaking settings for obtaining small scale bread, in: Conference: AACC International Annual Meeting.
- Gawlik-Dziki, U., Dziki, D., Świeca, M., Sęczyk, Ł., Różyło, R., Szymanowska, U., 2015. Bread enriched with *Chenopodium quinoa* leaves powder - The procedures for assessing the fortification efficiency. *LWT - Food Sci. Technol.* 62, 1226–1234.
- Ghandi, A., Powell, I., Chen, X.D., Adhikari, B., 2012. Drying kinetics and survival studies of dairy fermentation bacteria in convective air drying environment using single droplet

- drying. *J. Food Eng.* 110, 405–417.
- Gilbert, J.A., Blaser, M.J., Caporaso, J.G., Jansson, J.K., Lynch, S. V, Knight, R., 2018. Current understanding of the human microbiome. *Nat. Med.* 24, 392–400.
- Goesaert, H., Brijs, K., Veraverbeke, W.S., Courtin, C.M., Gebruers, K., Delcour, J.A., 2005. Wheat flour constituents: How they impact bread quality, and how to impact their functionality. *Trends Food Sci. Technol.* 16, 12–30.
- Goesaert, H., Courtin, C.M., Delcour, J.A., 2008. Use of enzymes in the production of cereal-based functional foods and food ingredients, in: *Gluten-Free Cereal Products and Beverages*. Elsevier Inc., pp. 237–265.
- Gökmen, V., Mogol, B.A., Lumaga, R.B., Fogliano, V., Kaplun, Z., Shimoni, E., 2011. Development of functional bread containing nanoencapsulated omega-3 fatty acids. *J. Food Eng.* 105, 585–591.
- Gomes, H.A.R., Moreira, L.R.S., Filho, E.X.F., 2018. Chapter 3: Enzymes and food industry: A consolidated marriage, in: *Advances in Biotechnology for Food Industry*. Elsevier Inc., pp. 55–89.
- Guidini, C.Z., Fischer, J., de Resende, M.M., Cardoso, V.L., Ribeiro, E.J., 2011. β -Galactosidase of *Aspergillus oryzae* immobilized in an ion exchange resin combining the ionic-binding and crosslinking methods: Kinetics and stability during the hydrolysis of lactose. *J. Mol. Catal. B Enzym.* 71, 139–145.
- Gys, W., Gebruers, K., Sørensen, J.F., Courtin, C.M., Delcour, J.A., 2004. Debranning of wheat prior to milling reduces xylanase but not xylanase inhibitor activities in wholemeal and flour. *J. Cereal Sci.* 39, 363–369.
- Hadiyanto, 2007. Product quality driven food process design. PhD dissertation, Wageningen University, The Netherlands.
- Hansen, N.H., Riemann, H., 1963. Factors affecting the heat resistance of nonsporing organisms. *J. Appl. Microbiol.* 26, 314–333.
- Harnkarnsujarit, N., Charoenrein, S., Roos, Y.H., 2012. Microstructure formation of maltodextrin and sugar matrices in freeze-dried systems. *Carbohydr. Polym.* 88, 734–742.
- Hartemink, R., Domenech, V.R., Rombouts, F.M., 1997. LAMVAB—A new selective medium for the isolation of lactobacilli from faeces. *J. Microbiol. Methods* 29, 77–84.
- Hartmann, G., Piber, M., Koehler, P., 2005. Isolation and chemical characterisation of water-extractable arabinoxylans from wheat and rye during breadmaking. *Eur. Food Res. Technol.* 221, 487–492.
- Heiniö, R.L., Noort, M.W.J., Katina, K., Alam, S.A., Sozer, N., de Kock, H.L., Hersleth, M., Poutanen, K., 2016. Sensory characteristics of wholegrain and bran-rich cereal foods - A review. *Trends Food Sci. Technol.* 47, 25–38.

- Hemdane, S., Langenaeken, N.A., Jacobs, P.J., Verspreet, J., Delcour, J.A., Courtin, C.M., 2016. Study of the intrinsic properties of wheat bran and pearlings obtained by sequential debranning and their role in bran-enriched bread making. *J. Cereal Sci.* 71, 78–85.
- Hemdane, S., Leys, S., Jacobs, P.J., Dornez, E., Delcour, J.A., Courtin, C.M., 2015. Wheat milling by-products and their impact on bread making. *Food Chem.* 187, 280–289.
- Hemery, Y., Chaurand, M., Holopainen, U., Lampi, A.-M., Lehtinen, P., Piironen, V., Sadoudi, A., Rouau, X., 2011. Potential of dry fractionation of wheat bran for the development of food ingredients, part I: Influence of ultra-fine grinding. *J. Cereal Sci.* 53, 1–8.
- Hemery, Y., Rouau, X., Lullien-Pellerin, V., Barron, C., Abecassis, J., 2007. Dry processes to develop wheat fractions and products with enhanced nutritional quality. *J. Cereal Sci.* 46, 327–347.
- Hu, G., Huang, S., Cao, S., Ma, Z., 2009. Effect of enrichment with hemicellulose from rice bran on chemical and functional properties of bread. *Food Chem.* 115, 839–842.
- Huang, H., Brooks, M.S.-L., Huang, H.-J., Chen, X.D., 2009. Inactivation kinetics of yeast cells during infrared drying. *Dry. Technol.* 27, 1060–1068.
- Huang, S., 2017. Spray drying of probiotic bacteria : From molecular mechanism to pilot-scale production. PhD dissertation, INRA-Agrocampus Ouest, Rennes.
- Huang, S., Vignolles, M.-L., Chen, X.D., Loir, Y. Le, Jan, G., Schuck, P., Jeantet, R., 2017. Spray drying of probiotics and other food-grade bacteria : A review. *Trends Food Sci. Technol.* 63, 1–17.
- Huang, S., Yang, Y., Fu, N., Qin, Q., Zhang, L., Chen, X.D., 2014. Calcium-aggregated milk: a potential new option for improving the viability of lactic acid bacteria under heat stress. *Food Bioprocess Technol.* 7, 3147–3155.
- IGMB, 1959. 1959 IGMB in Wageningen bakt men speelgoedbroodjes [WWW Document]. TNO Inst. voor Graan Meel en Brood. URL <http://www.etnos-2.nl/videos/detail/id/10> (accessed 2.19.18).
- Illanes, A., Wilson, L., Tomasello, G., 2001. Effect of modulation of enzyme inactivation on temperature optimization for reactor operation with chitin-immobilized lactase. *J. Mol. Catal. - B Enzym.* 11, 531–540.
- Illanes, A., Wilson, L., Tomasello, G., 2000. Temperature optimization for reactor operation with chitin-immobilized lactase under modulated inactivation. *Enzyme Microb. Technol.* 27, 270–278.
- Isabelle, L., André, L., 2006. Quantitative prediction of microbial behaviour during food processing using an integrated modelling approach: a review. *Int. J. Refrig.* 29, 968–984.
- Izydorczyk, M.S., Chornick, T.L., Paulley, F.G., Edwards, N.M., Dexter, J.E., 2008. Physicochemical properties of hull-less barley fibre-rich fractions varying in particle size

- and their potential as functional ingredients in two-layer flat bread. *Food Chem.* 108, 561–570.
- Izydorczyk, M.S., Dexter, J.E., 2008. Barley β -glucans and arabinoxylans: Molecular structure, physicochemical properties, and uses in food products-a Review. *Food Res. Int.* 41, 850–868.
- Jakób, A., Bryjak, J., Wójtowicz, H., Illeová, V., Annus, J., Polakovič, M., 2010. Inactivation kinetics of food enzymes during ohmic heating. *Food Chem.* 123, 369–376.
- Jin, X., Chen, X.D., 2018. Microstructure and its relationship with release behavior of different vehicles, in: Devahastin, S. (Ed.), *Food Microstructure and Its Relationship with Quality and Stability*. Woodhead Publishing Limited, pp. 81–96.
- Jouppila, K., Roos, Y.H., 1994. Glass transitions and crystallization in milk powders. *J. Dairy Sci.* 77, 2907–2915.
- Kalita, D., Sarma, B., Srivastava, B., 2017. Influence of germination conditions on malting potential of low and normal amylose paddy and changes in enzymatic activity and physico chemical properties. *Food Chem.* 220, 67–75.
- Kar, S., Chen, X.D., 2011. Modeling of moisture transport across porcine skin using reaction engineering approach and examination of feasibility of the two phase approach. *Chem. Eng. Commun.* 198, 847–885.
- Kar, S., Chen, X.D., 2010. Moisture transport across porcine skin: experiments and implementation of diffusion-based models. *Int. J. Healthc. Technol. Manag.* 11, 474–524.
- Katina, K., Arendt, E., Liukkonen, K.-H., Autio, K., Flander, L., Poutanen, K., 2005. Potential of sourdough for healthier cereal products. *Trends Food Sci. Technol.* 16, 104–112.
- Kiszonas, A.M., 2013. Wheat grain arabinoxylan quantification, characterization, and fate during baking. PhD dissertation, Washington State University.
- Klibanov, A.M., 1989. Enzymatic catalysis in anhydrous organic solvents. *Trends Biochem. Sci.* 14, 141–144.
- Koegelenberg, D., Chimphango, A.F.A., 2017. Effects of wheat-bran arabinoxylan as partial flour replacer on bread properties. *Food Chem.* 221, 1606–1613.
- Korem, T., Zeevi, D., Zmora, N., Weissbrod, O., Bar, N., Lotan-Pompan, M., Avnit-Sagi, T., Kosower, N., Malka, G., Rein, M., Suez, J., Goldberg, B.Z., Weinberger, A., Levy, A.A., Elinav, E., Segal, E., 2017. Bread affects clinical parameters and induces gut microbiome-associated personal glycemic responses. *Cell Metab.* 25, 1243–1253.
- Krasaekoopt, W., 2017. Influence of non-equilibrium states and glass transition on the survival of bacteria, in: *Non-Equilibrium States and Glass Transitions in Foods*. Woodhead Publishing Limited, pp. 405–446.
- Kumar, B. V., Vijayendra, S.V.N., Reddy, O.V.S., 2015. Trends in dairy and non-dairy probiotic

- products - a review. *J. Food Sci. Technol.* 52, 6112–6124.
- Kuts, P.S., Tutova, E.G., 1983. Fundamentals of drying of microbiological materials. *Dry. Technol.* 2, 171–201.
- Ladero, M., Ferrero, R., Vian, A., Santos, A., Garcia-Ochoa, F., 2005. Kinetic modelling of the thermal and pH inactivation of a thermostable β -galactosidase from *Thermus* sp. strain T2. *Enzyme Microb. Technol.* 37, 505–513.
- Ladero, M., Santos, A., García-Ochoa, F., 2006. Kinetic modelling of the thermal inactivation of an industrial β -galactosidase from *Kluyveromyces fragilis*. *Enzyme Microb. Technol.* 38, 1–9.
- Lakkis, J.M., 2016. Chapter 8: Encapsulation and controlled release in bakery applications, in: Lakkis, J. (Ed.), *Encapsulation and Controlled Release Technologies in Food Systems*, Second Edition. John Wiley & Sons, Ltd., pp. 204–235.
- Lante, A., Tinello, F., Nicoletto, M., 2016. UV-A light treatment for controlling enzymatic browning of fresh-cut fruits. *Innov. Food Sci. Emerg. Technol.* 34, 141–147.
- Laroche, C., Fine, F., Gervais, P., 2005. Water activity affects heat resistance of microorganisms in food powders. *Int. J. Food Microbiol.* 97, 307–315.
- Laurikainen, T., Harkonen, H., Autio, K., Poutanen, K., 1998. Effects of enzymes in fibre-enriched baking. *J. Sci. Food Agric.* 76, 239–249.
- Le-bail, A., Agrane, S., Queveau, D., 2012. Impact of the baking duration on bread staling kinetics. *Food Bioprocess Technol.* 5, 2323–2330.
- Lencki, R.W., Arul, J., Neufeld, R.J., 1992. Effect of subunit dissociation, denaturation, aggregation, coagulation, and decomposition on enzyme inactivation kinetics: I. First-order behavior. *Biotechnol. Bioeng.* 40, 1421–1426.
- León, K., Mery, D., Pedreschi, F., León, J., 2006. Color measurement in $L^*a^*b^*$ units from RGB digital images. *Food Res. Int.* 39, 1084–1091.
- Li, J., Kang, J., Wang, L., Li, Z., Wang, R., Chen, Z.X., Hou, G.G., 2012. Effect of water migration between arabinoxylans and gluten on baking quality of whole wheat bread detected by magnetic resonance imaging (MRI). *J. Agric. Food Chem.* 60, 6507–6514.
- Li, X., Lin, S., Chen, X.D., Chen, L., Pearce, D., 2006. Inactivation kinetics of probiotic bacteria during the drying of single milk droplets. *Dry. Technol.* 24, 695–701.
- Lievense, L.C., Verbeek, M.A.M., Taakema, T., Meerdink, G., van 't Riet, K., 1992. Modelling the inactivation of *Lactobacillus plantarum* during a drying process. *Chem. Eng. Sci.* 47, 87–97.
- Liou, J.K., 1982. An approximate method for nonlinear diffusion applied to enzyme inactivation during drying. PhD dissertation. Wageningen University, The Netherlands.
- Liu, S.-Q., Tsao, M., 2009. Enhancement of survival of probiotic and non-probiotic lactic acid

- bacteria by yeasts in fermented milk under non-refrigerated conditions. *Int. J. Food Microbiol.* 135, 34–8.
- Lodato, P., Segovia de Huergo, M., Buera, M.P., 1999. Viability and thermal stability of a strain of *Saccharomyces cerevisiae* freeze-dried in different sugar and polymer matrices. *Appl. Microbiol. Biotechnol.* 52, 215–220.
- Lönnner, C., 2008. Probiotic bread and method of its production EP 1971231 A1, Google Patents.
- Lu, Z.X., Walker, K.Z., Muir, J.G., Mascara, T., O'Dea, K., 2000. Arabinoxylan fiber, a byproduct of wheat flour processing, reduces the postprandial glucose response in normoglycemic subjects. *Am. J. Clin. Nutr.* 71, 1123–1128.
- Lucas, T., 2014. Chapter 19: Baking, in: Zhou, W., Hui, Y.H., Leyn, I. De, M. A. Pagani, C. M. Rosell, J. D. Selman, N.T. (Eds.), *Bakery Products Science and Technology: Second Edition*. John Wiley & Sons, Ltd., pp. 335–354.
- Lumry, R., Eyring, H., 1954. Conformational changes of protein. *J. Phys. Chem.* 58, 110–20.
- Luyben, K.C., Liou, J.K., Bruin, S., 1982. Enzyme degradation during drying. *Biotechnol. Bioeng.* 24, 533–552.
- Maes, C., Delcour, J. A., 2002. Structural characterisation of water-extractable and water-unextractable arabinoxylans in wheat bran. *J. Cereal Sci.* 35, 315–326.
- Majeed, M., Majeed, S., Nagabhushanam, K., Natarajan, S., Sivakumar, A., Ali, F., 2016. Evaluation of the stability of *Bacillus coagulans* MTCC 5856 during processing and storage of functional foods. *Int. J. Food Sci. Technol.* 51, 894–901.
- Malmö, C., La Storia, A., Mauriello, G., 2013. Microencapsulation of *Lactobacillus reuteri* DSM 17938 cells coated in alginate beads with chitosan by spray drying to use as a probiotic cell in a chocolate soufflé. *Food Bioprocess Technol.* 6, 795–805.
- Marechal, P.A., de Marnañón, I.M., Poirier, I., Gervais, P., 1999. The importance of the kinetics of application of physical stresses on the viability of microorganisms: significance for minimal food processing 10, 15–20.
- Mazzobre, M.F., Buera, M.D.P., Chirife, J., 1997. Protective role of trehalose on thermal stability of lactase in relation to its glass and crystal forming properties and effect of delaying crystallization. *LWT - Food Sci. Technol.* 30, 324–329.
- McMeekin, T., Bowman, J., McQuestin, O., Mellefont, L., Ross, T., Tamplin, M., 2008. The future of predictive microbiology: Strategic research, innovative applications and great expectations. *Int. J. Food Microbiol.* 128, 2–9.
- Meerdink, G., van 't Riet, K., 1994. Prediction of product quality during spray drying., in: *Proc. 4th IChemE Food Process Engineering Conference*. University of Bath, pp. 235–242.
- Mensink, M.A., Frijlink, H.W., van de Voort Maarschalk, K., Hinrichs, W.L.J., 2015. Inulin, a flexible oligosaccharide I: Review of its physicochemical characteristics. *Carbohydr. Polym.*

- 130, 405–419.
- Messia, M.C., Reale, A., Maiuro, L., Candigliota, T., Sorrentino, E., Marconi, E., 2016. Effects of pre-fermented wheat bran on dough and bread characteristics. *J. Cereal Sci.* 69, 138–144.
- Millar, S., Tucker, G., 2012. Controlling bread dough development, in: *Bread Making: Improving Quality*. Woodhead Publishing Limited, pp. 401–423.
- Mitropoulou, G., Nedovic, V., Goyal, A., Kourkoutas, Y., 2013. Immobilization technologies in probiotic food production. *J. Nutr. Metab.* Article ID 716861, 1–15.
- Mohácsi-Farkas, C., Farkas, J., Mészáros, L., Reichart, O., Andrásy, É., 1999. Thermal denaturation of bacterial cells examined by differential scanning calorimetry. *J. Therm. Anal. Calorim.* 57, 409–414.
- Mohd Jusoh, Y.M., Chin, N.L., Yusof, Y. A., Abdul Rahman, R., 2009. Bread crust thickness measurement using digital imaging and L a b colour system. *J. Food Eng.* 94, 366–371.
- Mondal, A., Datta, A.K., 2008. Bread baking - A review. *J. Food Eng.* 86, 465–474.
- Moore, M.M., Bello, F.D., Arendt, E.K., 2007. Sourdough fermented by *Lactobacillus plantarum* FST 1.7 improves the quality and shelf life of gluten-free bread. *Eur. Food Res. Technol.* 226, 1309–1316.
- Morgan, C.A., Herman, N., White, P.A., Vesey, G., 2006. Preservation of micro-organisms by drying; A review. *J. Microbiol. Methods* 66, 183–193.
- Mundt, S., Wedzicha, B.L., 2007. A kinetic model for browning in the baking of biscuits: Effects of water activity and temperature. *LWT - Food Sci. Technol.* 40, 1078–1082.
- Murrieta-Pazos, I., Gaiani, C., Galet, L., Cuq, B., Desobry, S., Scher, J., 2011. Comparative study of particle structure evolution during water sorption: Skim and whole milk powders. *Colloids Surfaces B Biointerfaces* 87, 1–10.
- Noort, M.W.J., Outi, M., Katina, K., van der Kamp, J.W., 2017. HealthBread : Wholegrain and high fibre breads with optimised textural quality. *J. Cereal Sci.* 78, 57–65.
- Palacios, M.C., Sanz, Y., Haros, M., Rosell, C.M., 2006. Application of *Bifidobacterium* strains to the breadmaking process. *Process Biochem.* 41, 2434–2440.
- Papasidero, D., Manenti, F., Pierucci, S., 2015. Bread baking modeling: Coupling heat transfer and weight loss by the introduction of an explicit vaporization term. *J. Food Eng.* 147, 79–88.
- Patel, A.R., Velikov, K.P., 2011. Colloidal delivery systems in foods : A general comparison with oral drug delivery. *LWT - Food Sci. Technol.* 44, 1958–1964.
- Peleg, M., 2006. Advanced quantitative microbiology for foods and biosystems: Models for predicting growth and inactivation. CRC Press, Taylor & Francis Group, LLC, Boca Raton.
- Peleg, M., 2000. Microbial survival curves - The reality of flat “shoulders” and absolute thermal death times. *Food Res. Int.* 33, 531–538.

- Peleg, M., Cole, M.B., 1998. Reinterpretation of microbial survival curves. *Crit. Rev. Food Sci. Nutr.* 38, 353–380.
- Perdana, J., Bereschenko, L., Fox, M.B., Kuperus, J.H., Kleerebezem, M., Boom, R.M., Schutyser, M.A.I., 2013. Dehydration and thermal inactivation of *Lactobacillus plantarum* WCFS1: Comparing single droplet drying to spray and freeze drying. *Food Res. Int.* 54, 1351–1359.
- Perdana, J., den Besten, H.M.W., Aryani, D.C., Kutahya, O., Fox, M.B., Kleerebezem, M., Boom, R.M., Schutyser, M.A.I., 2014. Inactivation of *Lactobacillus plantarum* WCFS1 during spray drying and storage assessed with complementary viability determination methods. *Food Res. Int.* 64, 212–217.
- Perdana, J., Fox, M.B., Schutyser, M.A.I., Boom, R.M., 2012. Enzyme inactivation kinetics: Coupled effects of temperature and moisture content. *Food Chem.* 133, 116–123.
- Pérez-Rodríguez, F., Valero, A., 2013a. Chapter 2: Experimental design and data generation, in: Hartel R.W. (Ed.), *Predictive Microbiology in Foods*. Springer, New York, pp. 11–24.
- Pérez-Rodríguez, F., Valero, A., 2013b. Chapter 3: Predictive models: foundation, types, and development, in: Hartel R.W. (Ed.), *Predictive Microbiology in Foods*. Springer, New York, pp. 25–56.
- Pinto, D., Castro, I., Vicente, A., Bourbon, A.I., Cerqueira, M.A., 2014. Chapter 25: Functional bakery products: An overview and future perspectives, in: Zhou, W., Hui, Y.H., De Leyn, I., Pagani, M.A., Rosell, C.M., Selman, J.D., Therdthai, N. (Eds.), *Bakery Products Science and Technology: Second Edition*. pp. 431–452.
- Pitigraisorn, P., Srichaisupakit, K., Wongpadungkiat, N., Wongsasulak, S., 2017. Encapsulation of *Lactobacillus acidophilus* in moist-heat-resistant multilayered microcapsules. *J. Food Eng.* 192, 11–18.
- Primo-Martín, C., van de Pijpekamp, A., van Vliet, T., de Jongh, H.H.J., Plijter, J.J., Hamer, R.J., 2006. The role of the gluten network in the crispness of bread crust. *J. Cereal Sci.* 43, 342–352.
- Purlis, E., 2012. Baking process design based on modelling and simulation: Towards optimization of bread baking. *Food Control* 27, 45–52.
- Purlis, E., 2011. Bread baking: Technological considerations based on process modelling and simulation. *J. Food Eng.* 103, 92–102.
- Purlis, E., 2010. Browning development in bakery products – A review. *J. Food Eng.* 99, 239–249.
- Purlis, E., Salvadori, V.O., 2009a. Bread baking as a moving boundary problem. Part 1: Mathematical modelling. *J. Food Eng.* 91, 428–433.
- Purlis, E., Salvadori, V.O., 2009b. Bread baking as a moving boundary problem. Part 2: Model validation and numerical simulation. *J. Food Eng.* 91, 434–442.

- Purlis, E., Salvadori, V.O., 2009c. Modelling the browning of bread during baking. *Food Res. Int.* 42, 865–870.
- Purlis, E., Salvadori, V.O., 2007. Bread browning kinetics during baking. *J. Food Eng.* 80, 1107–1115.
- Putranto, A., Chen, X.D., 2013a. Multiphase modeling of intermittent drying using the spatial reaction engineering approach (S-REA). *Chem. Eng. Process. Process Intensif.* 70, 169–183.
- Putranto, A., Chen, X.D., 2013b. Spatial reaction engineering approach (S-REA) as a multiphase drying approach to model the heat treatment of wood under a constant heating rate. *Ind. Eng. Chem. Res.* 52, 6242–6252.
- Putranto, A., Chen, X.D., 2013c. Spatial reaction engineering approach as an alternative for nonequilibrium multiphase mass-transfer model for drying of food and biological materials. *AIChE J.* 59, 55–67.
- Putranto, A., Chen, X.D., Zhou, W., 2015. Bread baking and its color kinetics modeled by the spatial reaction engineering approach (S-REA). *Food Res. Int.* 71, 58–67.
- Quirós-Sauceda, A.E., Palafox-Carlos, H., Sáyago-Ayerdi, S.G., Ayala-Zavala, J.F., Bello-Perez, L.A., Álvarez-Parrilla, E., de la Rosa, L.A., González-Córdova, A.F., González-Aguilar, G.A., 2014. Dietary fiber and phenolic compounds as functional ingredients: interaction and possible effect after ingestion. *Food Funct.* 5, 1063–1072.
- Ramos, O.S., Malcata, F.X., 2011. Food-grade enzymes, in: Moo-Young, M. (Ed.) *Comprehensive Biotechnology*, Second edition. Elsevier Inc, pp. 555–269.
- Reid, A.A., Champagne, C.P., Gardner, N., Fustier, P., Vuilleumard, J.C., 2007. Survival in food systems of *Lactobacillus rhamnosus* R011 microentrapped in whey protein gel particles. *J. Food Sci.* 72, 31–37.
- Rivera-Espinoza, Y., Gallardo-Navarro, Y., 2010. Non-dairy probiotic products. *Food Microbiol.* 27, 1–11.
- Roos, Y.H., 2010. Glass transition temperature and its relevance in food processing. *Annu. Rev. Food Sci. Technol.* 1, 469–496.
- Ross, R.P., Desmond, C., Fitzgerald, G.F., Stanton, C., 2005. Overcoming the technological hurdles in the development of probiotic foods. *J. Appl. Microbiol.* 98, 1410–1417.
- Samborska, K., Guivarc'h, Y., Van Loey, A., Hendrickx, M., 2005. The influence of moisture content on the thermostability of *Aspergillus oryzae* α -amylase. *Enzyme Microb. Technol.* 37, 167–174.
- Sánchez, B., Ruiz, L., Gueimonde, M., Ruas-Madiedo, P., Margolles, A., 2012. Toward improving technological and functional properties of probiotics in foods. *Trends Food Sci. Technol.* 26, 56–63.

- Santivarangkna, C., Aschenbrenner, M., Kulozik, U., Foerst, P., 2011. Role of glassy state on stabilities of freeze-dried probiotics. *J. Food Sci.* 76, 152–156.
- Schuck, P., Anne, D., Jeantet, R., 2012. *Analytical Methods for Food and Dairy Powder*. John Wiley & Sons, Ltd. UK.
- Schutyser, M.A.I., Perdana, J., Boom, R.M., 2012. Single droplet drying for optimal spray drying of enzymes and probiotics. *Trends Food Sci. Technol.* 27, 73–82.
- Schutyser, M.A.I., van der Goot, A.J., 2011. The potential of dry fractionation processes for sustainable plant protein production. *Trends Food Sci. Technol.* 22, 154–164.
- Seyedain-Ardabili, M., Sharifan, A., Tarzi, B.G., 2016. The production of synbiotic bread by microencapsulation. *Food Technol. Biotechnol.* 54, 52–59.
- Shah, A.R., Shah, R.K., Madamwar, D., 2006. Improvement of the quality of whole wheat bread by supplementation of xylanase from *Aspergillus foetidus*. *Bioresour. Technol.* 97, 2047–2053.
- Shimizu, Y., Maeda, T., Hidaki, Y., Tani, H., Morita, N., 2003. Identification and effect of ethyl galactoside on the properties and baking quality of dough. *Food Res. Int.* 36, 373–379.
- Simal, S., Femenia, A., Garau, M.C., Rosselló, C., 2005. Use of exponential, Page's and diffusional models to simulate the drying kinetics of kiwi fruit. *J. Food Eng.* 66, 323–328.
- Sirbu, A., Arghire, C., 2017. Functional bread : Effect of inulin-type products addition on dough rheology and bread quality. *J. Cereal Sci.* 75, 220–227.
- Sivam, A.S., Sun-Waterhouse, D., Waterhouse, G.I.N., Quek, S. Y., Perera, C.O., 2011. Physicochemical properties of bread dough and finished bread with added pectin fiber and phenolic antioxidants. *J. Food Sci.* 76, 97–107.
- Soleimani Pour-Damanab, A., Jafary, A., Rafiee, S., 2014. Kinetics of the crust thickness development of bread during baking. *J. Food Sci. Technol.* 51, 3439–3445.
- Soukoulis, C., Yonekura, L., Gan, H.H., Behboudi-Jobbehdar, S., Parmenter, C., Fisk, I., 2014. Probiotic edible films as a new strategy for developing functional bakery products: The case of pan bread. *Food Hydrocoll.* 39, 231–242.
- Sui, X., Yap, P.Y., Zhou, W., 2015. Anthocyanins during baking: their degradation kinetics and impacts on color and antioxidant capacity of bread. *Food Bioprocess Technol.* 8, 983–994.
- Sui, X., Zhang, Y., Zhou, W., 2016. Bread fortified with anthocyanin-rich extract from black rice as nutraceutical sources: Its quality attributes and in vitro digestibility. *Food Chem.* 196, 910–916.
- Tan, A., Zhou, W., 2003. Colour development of bread during baking, in: *Proceedings of the 8th ASEAN Food Conference*. Hanoi, Vietnam, pp. 488–492.
- Tan, M.Y., Zhou, W., 2008. Modelling of bread crust colour development during baking. *Food Manuf. Effic.* 2, 9–15.

- Termont, S., Vandenbroucke, K., Iserentant, D., Neiryneck, S., Steidler, L., Remaut, E., Rottiers, P., 2006. Intracellular accumulation of trehalose protects *Lactococcus lactis* from freeze-drying damage and bile toxicity and increases gastric acid resistance. *Appl. Environ. Microbiol.* 72, 7694–7700.
- Therdthai, N., Zhou, W., 2003. Recent advances in the studies of bread baking process and their impacts on the bread baking technology. *J. food Sci. Technol. Res.* 9, 219–226.
- Therdthai, N., Zhou, W., Adamczak, T., 2002. Optimisation of the temperature profile in bread baking. *J. Food Eng.* 55, 41–48.
- Thorvaldsson, K., Janestad, H., 1999. A model for simultaneous heat, water and vapour diffusion. *J. Food Eng.* 40, 167–172.
- Tian, Y., Zhao, Y., Huang, J., Zeng, H., Zheng, B., 2016. Effects of different drying methods on the product quality and volatile compounds of whole shiitake mushrooms. *Food Chem.* 197, 714–722.
- Trinh, L., Campbell, G.M., Martin, P.J., 2016. Scaling down bread production for quality assessment using a breadmaker : Are results from a breadmaker representative of other breadmaking methods ? *Food Bioprod. Process.* 100, 54–60.
- Tripathi, M.K., Giri, S.K., 2014. Probiotic functional foods: Survival of probiotics during processing and storage. *J. Funct. Foods* 9, 225–241.
- Ubbink, J., Kruger, J., 2006. Physical approaches for the delivery of active ingredients in foods. *Trends Food Sci. Technol.* 17, 244–254.
- Vaessen, E.M.J., den Besten, H.M.W., Patra, T., van Mossevelde, N.T.M., Boom, R.M., Schutyser, M.A.I., 2018. Pulsed electric field for increasing intracellular trehalose content in *Lactobacillus plantarum* WCFS1. *Innov. Food Sci. Emerg. Technol.* 47, 256–261.
- Valdramidis, V.P., Geeraerd, A.H., Gaze, J.E., Kondjoyan, A., Boyd, A.R., Shaw, H.L., Van Impe, J.F., 2006. Quantitative description of *Listeria monocytogenes* inactivation kinetics with temperature and water activity as the influencing factors; Model prediction and methodological validation on dynamic data. *J. Food Eng.* 76, 79–88.
- Valero, A., Cejudo, M., García-Gimeno, R.M., 2014. Inactivation kinetics for *Salmonella Enteritidis* in potato omelet using microwave heating treatments. *Food Control* 43, 175–182.
- van Boekel, M.A.J.S., 2009. Kinetics of protein and enzyme denaturation, in: *Kinetic Modeling of Reactions in Foods*. CRC Press, Taylor & Francis Group, Boca Raton.
- van Boekel, M.A.J.S., 2009. Kinetics of inactivation of microorganisms, in: *Kinetic Modeling of Reactions in Foods*. CRC Press, Taylor & Francis Group, Boca Raton, pp. 13-1-13–44.
- van Boekel, M.A.J.S., 2008. Kinetic modeling of food quality: A critical review. *Compr. Rev. Food Sci. Food Saf.* 7, 144–158.

- van Boekel, M.A.J.S., 2002. On the use of the Weibull model to describe thermal inactivation of microbial vegetative cells. *Int. J. Food Microbiol.* 74, 139–159.
- van Boekel, M.A.J.S., Zwietering, M., 2007. Experimental design, data processing and model fitting in predictive modelling, in: Brul, S., van Gerwen, S., Zwietering, M. (Eds), *Modelling Microorganisms in Food*. Woodhead Publishing Limited, pp. 22–43.
- van der Goot, A.J., Pelgrom, P.J.M., Berghout, J.A.M., Geerts, M.E.J., Jankowiak, L., Hardt, N.A., Keijer, J., Schutyser, M.A.I., Nikiforidis, C. V., Boom, R.M., 2016. Concepts for further sustainable production of foods. *J. Food Eng.* 168, 42–51.
- van der Kamp, J.W., Poutanen, K., Seal, C.J., Richardson, D.P., 2014. The HEALTHGRAIN definition of 'whole grain'. *Food Nutr. Res.* 58, 1–8.
- van Nieuwenhuijzen, N.H., Tromp, R.H., Mitchell, J.R., Primo-Martín, C., Hamer, R.J., van Vliet, T., 2010. Relations between sensorial crispness and molecular mobility of model bread crust and its main components as measured by PTA, DSC and NMR. *Food Res. Int.* 43, 342–349.
- van Oort, M., 2010. Chapter 6: Enzymes in bread making, in: Whitehurst, R.J., van Oort, M. (Eds.), *Enzymes in Food Technology*, Second Edition. Blackwell Publishing Ltd., pp. 103–143.
- Vanin, F.M., Lucas, T., Trystram, G., 2009. Crust formation and its role during bread baking. *Trends Food Sci. Technol.* 20, 333–343.
- Vernocchi, P., Valmorri, S., Dalai, I., Torriani, S., Gianotti, A., Suzzi, G., Guerzoni, M.E., Mastrocola, D., Gardini, F., 2004. Characterization of the yeast population involved in the production of a typical Italian bread. *J. Food Sci.* 69, 182–186.
- Vitaglione, P., Troise, A.D., De Prisco, A.C., Mauriello, G.L., Gokmen, V., Fogliano, V., 2015. Chapter 15: Use of microencapsulated ingredients in bakery products: Technological and nutritional aspects, in: Sagis, L.M.C. (Eds.), *Microencapsulation and Microspheres for Food Applications*. Elsevier Inc., pp. 301–311.
- Wagner, M.J., Lucas, T., Le Ray, D., Trystram, G., 2007. Water transport in bread during baking. *J. Food Eng.* 78, 1167–1173.
- Wang, J., De Wit, M., Boom, R.M., Schutyser, M.A.I., 2015. Charging and separation behavior of gluten-starch mixtures assessed with a custom-built electrostatic separator. *Sep. Purif. Technol.* 152, 164–171.
- Wang, J., Rosell, C.M., Benedito de Barber, C., 2002. Effect of the addition of defatted date seeds on wheat dough performance and bread quality. *Food Chem.* 79, 221–226.
- Wang, J., Smits, E., Boom, R.M., Schutyser, M.A.I., 2015. Arabinoxylans concentrates from wheat bran by electrostatic separation. *J. Food Eng.* 155, 29–36.
- Wang, J., Zhao, J., Wit, M. De, Boom, R.M., Schutyser, M.A.I., 2016. Lupine protein enrichment

- by milling and electrostatic separation. *Innov. Food Sci. Emerg. Technol.* 33, 596–602.
- Wang, R., Zhou, W., 2004. Stability of tea catechins in the breadmaking process. *J. Agric. Food Chem.* 52, 8224–8229.
- Wong, S.Y., Zhou, W., Hua, J., 2007. CFD modeling of an industrial continuous bread-baking process involving U-movement. *J. Food Eng.* 78, 888–896.
- Writing, R.C., 1995. Microbial modeling in foods. *Crit. Rev. Food Sci. Nutr.* 35, 467–494.
- Wu, G.D., Chen, J., Hoffmann, C., Bittinger, K., Chen, Y., Keilbaugh, S.A., Bewtra, M., Knights, D., Walters, W.A., Knight, R., Sinha, R., Gilroy, E., Gupta, K., Baldassano, R., Nessel, L., Li, H., Bushman, F.D., Lewis, J.D., 2011. Linking long-term dietary patterns with gut microbial enterotypes. *Science*. 334, 105–109.
- Wu, Z., Dong, M., Lu, M., Li, Z., 2010. Encapsulation of β -galactosidase from *Aspergillus oryzae* based on “fish-in-net” approach with molecular imprinting technique. *J. Mol. Catal. B Enzym.* 63, 75–80.
- Xing, Y., Li, A., Felker, D.L., Burggraf, L.W., 2014. Nanoscale structural and mechanical analysis of *Bacillus anthracis* spores inactivated with rapid dry heating. *Appl. Environ. Microbiol.* 80, 1739–1749.
- Yam, K.L., Papadakis, S.E., 2004. A simple digital imaging method for measuring and analyzing color of food surfaces. *J. Food Eng.* 61, 137–142.
- Yesair, Y., Bohrer, C.W., Cameron, E.J., 1946. Effect of certain environmental conditions on heat resistance of micrococci. *J. Food Sci.* 11, 327–331.
- Yoshioka, S., Aso, Y., Izutsu, K., Kojima, S., 1994. Is stability prediction possible for protein drugs? Denaturation kinetics of β -galactosidase in solution. *Pharm. Res.* 11, 1721–1725.
- Yonekura, L., Sun, H., Soukoulis, C., Fisk, I., 2014. Microencapsulation of *Lactobacillus acidophilus* NCIMB 701748 in matrices containing soluble fibre by spray drying: Technological characterization, storage stability and survival after in vitro digestion. *J. Funct. Foods* 6, 205–214.
- Zanoni, B., Peri, C., Bruno, D., 1995. Modelling of browning kinetics of bread crust during baking. *LWT - Food Sci. Technol.* 28, 604–609.
- Zayed, G., Roos, Y.H., 2004. Influence of trehalose and moisture content on survival of *Lactobacillus salivarius* subjected to freeze-drying and storage. *Process Biochem.* 39, 1081–1086.
- Zhang, D., Moore, W., 1999. Wheat bran particle size effects on bread baking performance and quality. *J. Sci. Food Agric.* 79, 805–809.
- Zhang, J., Datta, A.K., 2006. Mathematical modeling of bread baking process. *J. Food Eng.* 75, 78–89.
- Zhang, J., Datta, A.K., Mukherjee, S., 2005. Transport processes and large deformation during

- baking of bread. *AIChE J.* 51, 2569–2580.
- Zhang, L., Huang, S., Ananingsih, V.K., Zhou, W., Chen, X.D., 2014. A study on *Bifidobacterium lactis* Bb12 viability in bread during baking. *J. Food Eng.* 122, 33–37.
- Zhang, L., Putranto, A., Zhou, W., Boom, R.M., Schutyser, M.A.I., Chen, X.D., 2016. Miniature bread baking as a timesaving research approach and mathematical modeling of browning kinetics. *Food Bioprod. Process.* 100, 401–411.
- Zhang, L., Taal, M.A., Boom, R.M., Chen, X.D., Schutyser, M.A.I., 2018. Effect of baking conditions and storage on the viability of *Lactobacillus plantarum* supplemented to bread. *LWT - Food Sci. Technol.* 87, 318–325.
- Zheng, X., Fu, N., Duan, M., Woo, M.W., Selomulya, C., Chen, X.D., 2015. The mechanisms of the protective effects of reconstituted skim milk during convective droplet drying of lactic acid bacteria. *Food Res. Int.* 76, 478–488.
- Zhou, S., Liu, X., Guo, Y., Wang, Q., Peng, D., Cao, L., 2010. Comparison of the immunological activities of arabinoxylans from wheat bran with alkali and xylanase-aided extraction. *Carbohydr. Polym.* 81, 784–789.
- Zhou, W., Therdthai, N., 2007. Three-dimensional CFD modeling of a continuous industrial baking process, in: Sun, D.-W. (Eds), *Computational Fluid Dynamics in Food Processing, Contemporary Food Engineering*. CRC Press, pp. 287–312.
- Žilić, S., Serpen, A., Akillioğlu, G., Janković, M., Gökmen, V., 2012. Distributions of phenolic compounds, yellow pigments and oxidative enzymes in wheat grains and their relation to antioxidant capacity of bran and debranned flour. *J. Cereal Sci.* 56, 652–658.
- Zubillaga, M., Weill, R., Postaire, E., Goldman, C., Caro, R., Boccio, J., 2001. Effect of probiotics and functional foods and their use in different diseases. *Nutr. Res.* 21, 569–579.

Summary

Summary of this thesis

Functional foods contain bioactive ingredients that may beneficially affect consumers' health. Bread is an interesting food 'vehicle' for the delivery of bioactive ingredients because bread is consumed by people around the world on a daily base. However, to exhibit the intended health benefits, the functionality of the supplemented bioactives should be maintained during bread baking. This is however challenging due to the sensitivity of most bioactive compounds towards high temperatures. Moreover, fortification of bread with bioactives may negatively influence the product quality as well. Therefore, it is essential to study the interactions between the baking process and the behaviour of bioactives and explore strategies to better retain the functionality of bioactives without compromising bread quality.

In **chapter 2**, a miniature bread baking approach was developed to study the bread baking process at lab scale. Results indicate that the mini-bread baking was essentially similar to the baking process of regular-sized bread in terms of the development of quality-related properties of bread (e.g. crust thickness and browning). In addition, the small-scale experimental approach required less time and resources which improved the efficiency of data collection. Moreover, the moisture content and temperature profiles in mini-bread were modelled by the spatial reaction engineering approach (S-REA), and these profiles were then used to describe the browning kinetics of mini-breads during baking.

Subsequently, the impact of baking on the bio-activity of β -galactosidase as a model enzyme (**chapter 3**) and *Lactobacillus plantarum* P8 as a model probiotics (**chapter 4**) were investigated through mini-bread baking experiments. Surprisingly, the residual enzyme activity and bacterial viability were found higher in the crust of mini-breads than in the crumb in spite of the higher temperatures reached in the crust during baking. This was attributed to the lower moisture content and the dense and glassy microstructure of the bread crust, which affected the thermal inactivation kinetics of enzyme and probiotic bacteria.

A kinetic modelling study was then conducted to further investigate the inactivation mechanisms of enzymes and probiotics as influenced by the temperature and moisture content of bread during baking. In **chapter 3**, a first order kinetic model accurately described the inactivation of β -galactosidase in the flour/water system during isothermal heating. The residual enzyme activity of β -galactosidase in the bread crumb was reasonably predicted by kinetic modelling using the same parameters derived from the isothermal experiments.

However, the model underestimated the residual enzyme activity in the crust, suggesting that food microstructure may affect the inactivation mechanism of bioactives during actual baking as well.

In **chapter 5**, a rate-dependent kinetic model was developed to describe the inactivation of *L. plantarum* P8 in bread during baking. The goodness of fit of different rate-dependent models were evaluated by comparing the values of the mean square error and the corrected Akaike information criterion, and by judging the visual fit. Thus, the rate-dependent model including the temperature (T), the moisture content (X), and the changing rate of temperature (dX/dt) of the bread matrix as variables was found to best describe the survival curves of bacteria in bread crust and crumb during baking.

The findings in chapters 4 & 5 indicate that besides the product temperature also the moisture content and microstructure of the bread matrix play an important role in the inactivation of probiotics. In **chapter 6**, *L. plantarum* P8 was freeze-dried in the presence of protectants (i.e. reconstituted skim milk, gum arabic, maltodextrin and inulin, respectively). The physicochemical properties of the protectants significantly influenced the heat resistance of the bacteria in the powders during processing. During isothermal heating, reconstituted skim milk (RSM) and gum arabic (GA) matrices protected the cells more effectively due to their high glass transition temperature and dense microstructure. Subsequently, the probiotic powders were incorporated into bread using different approaches. The RSM-probiotic powder was observed to be least hygroscopic, delaying moisture migration from the dough into the dry glassy powder, which is expected critical to the survival of probiotics. In addition, a lower baking temperature (100 °C) also favoured the survival of probiotics. These findings suggest that bread with sufficient viable probiotics ($>10^8$ CFU/g) can be obtained by carefully choosing the protectants for encapsulation and the processing conditions (e.g. incorporation approach, baking temperature and time).

Furthermore, it was investigated how the addition of bioactive ingredients (e.g. prebiotics) influences the quality of bread. In **chapter 7**, arabinoxylans-rich fractions (AXF) were separated from wheat bran by dry fractionation and was used to produce AX-fortified bread. Dry fractionation contained steps of milling, electrostatic separation and sieving, which is more sustainable than the conventional wet extraction in terms of water and energy consumption. The quality attributes of the fortified bread (e.g. colour, texture, volume) were negatively affected by a flour replacement level of AXF up to 10 %. Enzymatic pre-treatment of AXF

mitigated this detrimental effect. However, the process conditions for the pre-treatment need to be further optimized.

Mini-bread baking experiments and kinetic studies were combined in this thesis, which provided quantitative understanding of the interaction between the active ingredients and the bread baking process. Based on the findings, future research needs for the development of functional bakery products were discussed in **chapter 8**. To better retain the functionality of bioactives, the baking process may be optimized either with the aid of mathematical modelling or by changing the heating method. In addition, extracellular (i.e. encapsulation) and intracellular protection (i.e. pulsed electric field treatment) may be applied as strategies to enhance the robustness of probiotics during thermal processing. Moreover, 3D printing has been identified to manufacture innovative baked products containing bioactives. Finally, the actual health benefits of novel developed functional baked products are also of concern and should be assessed. All in all, the results reported in this thesis lay the foundation for further exploration.

Acknowledgements

Acknowledgements

Looking back on the last four years, I realize that doing a PhD abroad is truly the most life-changing decision I have ever made. I would like to take this opportunity to thank the people who went through this journey together with me.

To start with, I would like to thank my promoters and co-promotor for giving me the opportunity to do research and for cultivating me as a future professional. Dong, the word “thank you” itself is inadequate to describe my gratitude for your constant support and guidance in the past 8 years since my bachelor study. I am so lucky to be your student: “he who teaches me for one day is my teacher for life”. Hope I can have opportunities to work with you in the future. Remko, although we did not meet up that frequently, I got inspiration from you every time during our meetings. Thank you very much for all the constructive comments on my project. Maarten, I still remember four years ago you picked me up from Schiphol airport, and it seems like it was only yesterday. Thank you so much for being such a great supervisor and mentor. I look forward to continuing working together with you.

Many thanks to the staff members in FPE. Marjan and Ilona, thank you for your excellent administrative support. Jos, thank you for your instructions on pin mill, texture analyser, particle sizer, rotary evaporator, rheometer...and many others. Martin, thank you for your help with dry fractionation and 3D printing experiments, and for helping me reimburse my expenses during conferences which keeps me away from bankruptcy. Maurice, thank you for all your technical support in the lab, especially with HPLC, I hope I did not bother you too much with that... Jarno, thank you for your instruction in the lab and also in the FPE garden. I will make a nice signboard for the FPE garden as I promised.

My fellow PhD students, thank you for all the pleasant time we spend together. We will still see each other around in the coming two years, and I guarantee you there will be more “hotpot party”, “dumpling party”, and “karaoke party”! Special thanks to Jue who helped me so much in the beginning of my PhD, and thank you Fiona and Jun for being my paranymphs.

I would like to thank my thesis students, Sophie, Saskia, Kristina, Marieke, Jorinde, Lisanne, Yimin and Anneloes, for your contribution to this thesis. I learnt a lot from the supervision experience. The co-authors of my papers, Prof. Weibiao Zhou, Dr. Aditya Putranto and Jeroen Grandia, thank you for the nice collaboration we had. Remco from FBR, thank you for your

help with the X-ray tomography. Heidi and Ingrid from FHM, thank you for letting my student and I make use of the bacterial strain and the facilities in your lab.

Many thanks to the friends I met in Wageningen, Kun, Feifei, Yu, Zhili and my artist friends from Het Gelders Palet, for making my life here so colourful. Also, I want to thank my friends Xin, Song, Peggy, Nick, Ruosang, Liang, Juan & Chuang, for making my stay in Suzhou as delightful as it can be.

亲爱的爸爸妈妈，感谢你们一直以来对我的关心和支持，希望我今天的小小成就能让你们感到骄傲！女儿多年在外求学，没能好好对你们尽孝心，希望你们不要太责怪。我爱你们！家乡的亲人们，也感谢你们对我学业的支持！

Dearest Tom, I am so grateful to have you in my life! Thank you for being so supportive of my PhD study as well as my “artist dream”. Congratulations on completing your own PhD! I am looking forward to our future life together with a lot of fun adventures. I love you! >3<

About the author

Curriculum Vitae

Lu Zhang was born on July 27, 1989 in Anhui, China. After completing her secondary education in Anhui Bengbu No.2 Middle School in 2007, she started her higher education at Xiamen University, China, where she obtained her BSc degree in Chemical Engineering and a second BSc degree in Advertising. In 2011, Lu started her master programme of Chemical Engineering at Xiamen University, with a master thesis *Baking properties of probiotic bread*. In the second year of her MSc study, she was awarded a scholarship to visit the Food Science & Technology Programme at National University of Singapore, where she was supervised by Prof. Weibiao Zhou. During both her BSc (2009) and MSc (2013) studies, Lu was awarded the National Scholarship by the Ministry of Education of the People's Republic of China.



In September 2014, Lu started her PhD Program at the Laboratory of Food Process Engineering (FPE) at Wageningen University & Research, the Netherlands, in collaboration with the School of Chemical and Environmental Engineering (SCEE) at Soochow University, China, under the supervision of Dr. Maarten Schutyser, Prof. Remko Boom and Prof. Xiao Dong Chen. This thesis entitled *Bioactive ingredients during mini-bread baking* is the result of that PhD project. Currently, Lu works as a postdoctoral researcher at FPE.

Email: xmuzhanglu@gmail.com; lu1.zhang@wur.nl

List of publications

Journal articles

This thesis

Zhang, L., Putranto, A., Zhou, W., Boom, R.M., Schutyser, M.A.I., Chen, X.D. (2016). Miniature bread baking as a timesaving research approach and mathematical modelling of browning kinetics. *Food and Bioproducts Processing*. 100, 401–411.

Zhang, L., Chen, X.D., Boom, R.M., Schutyser, M.A.I. (2017). Thermal inactivation kinetics of β -galactosidase during bread baking. *Food Chemistry*. 225, 107–113.

Zhang, L., Taal, M.A., Boom, R.M., Chen, X.D., Schutyser, M.A.I. (2018). Effect of baking conditions and storage on the viability of *Lactobacillus plantarum* supplemented to bread. *LWT - Food Science & Technology*. 87, 318–325.

Zhang, L., Schutyser, M.A.I., Boom, R.M., Chen, X.D. (2018). Kinetic study of the thermal inactivation of *Lactobacillus plantarum* during bread baking. *Drying Technology* (in press).

Zhang, L., Chen, X.D., Boom, R.M., Schutyser, M.A.I. (2018). Survival of encapsulated *Lactobacillus plantarum* during isothermal heating and bread baking. *LWT - Food Science & Technology*. 93, 396-404.

Others

Schutyser, M.A.I., Both, E., Siemons, I., Vaessen, E., **Zhang, L.** (2018). Gaining insight on spray drying behaviour of foods via single droplet drying analyses. *Drying Technology* (in press).

Xu, F., Jin, X., **Zhang, L.**, Chen, X.D. (2017). Investigation on water status and distribution in broccoli and the effects of drying on water status using NMR and MRI methods. *Food Research International*. 96, 191–197.

Zhang, L., Huang, S., Ananingsih, V. K., Zhou, W., & Chen, X. D. (2014). A study on *Bifidobacterium lactis* Bb12 viability in bread during baking. *Journal of Food Engineering*, 122(1), 33–37

Huang, S., Yang, Y., Fu, N., Qin, Q., **Zhang, L.**, & Chen, X. D. (2014). Calcium-Aggregated Milk: a Potential New Option for Improving the Viability of Lactic Acid Bacteria Under Heat Stress. *Food and Bioprocess Technology*, 7(11), 3147–3155.

Zhang, L., Che, L., Zhou, W., & Chen, X. D. (2012). Rheological behaviour of agar solution in relation to the making of instant edible bird's nest products. *International Journal of Food Engineering*, 8(3).

Book chapter

Zhang, L., & Chen, X. D. (2014). Chapter 39: Bakery Products of China. in: Zhou, W., Hui, Y.H., Leyn, I. De, M. A. Pagani, C. M. Rosell, J. D. Selman, N.T. (Eds.), *Bakery Products Science and Technology: Second Edition*. John Wiley & Sons, Ltd., pp. 673–684.

Conference proceedings

Zhang, L., Taal, M.A., Boom, R.M., Chen, X.D., Schutyser, M.A.I. (2016). Viability of *Lactobacillus plantarum* P8 in Bread during Baking and Storage. In proceedings of the 19th *International Drying Symposium* (IDS2016) Gifu, Japan, 7-10 August, 2016.

Zhang, L., Boom, R.M., Chen, X.D., Schutyser, M.A.I. (2018). Recent developments in functional bakery products and the impact of baking on active ingredients. In proceedings of the 20th *International Drying Symposium* (IDS2018) Valencia, Spain, 11-14 September, 2018.

Overview of completed training activities

Discipline specific activities

Courses

Reaction Kinetics in Food Science (VLAG, NL)	2014
Advanced Food Analysis (VLAG, NL)	2015
Numerical Methods for Chemical Engineers (OPST, NL)	2015
Introduction of Numerical Analysis (SCEE, CHN)	2015
Food and Biorefinery Enzymology (VLAG, NL)	2017
Healthy Food Design (VLAG, NL)	2018

Conferences

* oral presentation

Symposium of the Dutch Working Party on Drying (NWGD, NL)	2014
Workshop on Multiscale Modeling in Food Engineering (KU LEUVEN, BE)	2015
2 nd PhD Symposium (WPC, NL)	2015
2 nd Frontiers in Chemical Engineering Suzhou International Symposium (SCEE, CHN)	2015
2 nd Food Structure and Functionality Forum (Elsevier, SG) *	2016
20 th International Drying Symposium IDS2016 (IDS, JP) *	2016
Soochow University Workshop on Modeling and Simulation in Multidisciplinary Engineering (SCEE, CHN) *	2016
5 th International Congress on Sustainability Science and Engineering (AIChE& SCEE, CHN)	2016
International Forum on Baking and Fermentation Biotechnology for Foods (Jiangnan Uni & KU LEUVEN, CHN)	2017
17 th Congress, Asian Pacific Confederation of Chemical Engineering (HK PolyU & HKUST, HK) *	2017
10 th World Congress of Chemical Engineering WCCE2017 (WCEE, ESP) *	2017
Symposium of the Dutch Working Party on Drying (NWGD, NL)	2017
3 rd Food Structure and Functionality Forum (Elsevier, CA) *	2018

General courses

VLAG PhD week in Baarlo (VLAG, NL)	2014
Data Management Planning (WGS, NL)	2014
Scientific Writing (WGS, NL)	2014
Career Perspectives (WGS, NL)	2017

Overview of completed training activities

Efficient Writing Strategies (WGS, NL)	2018
Supervising BSc and MSc Students (ESD, WUR, NL)	2018

Optional activities

Research proposal	2014
PhD study trip to Switzerland & Germany (FPE, WUR, CH & DE)	2016
PhD study trip to Canada (FPE, WUR, CA)	2018
Weekly group meetings (FPE, WUR, NL)	2014-2018

The research described in this thesis was financially supported by VLAG Sandwich PhD program – the Netherlands and by the Natural Science Foundation of China (Grant No. 21676172), the National Key Research and Development Program of China (Project No. 2016YFE0101200), and the International S&T Cooperation Program (ISTCP) – China.

Cover design by Lu Zhang (a tribute to *The Thinker* by Auguste Rodin)

Printed by ProefschriftMaken

